KoG

BROJ 2
ZAGREB, 1997
CIJENA 35 KN

ISSN 1331-1611

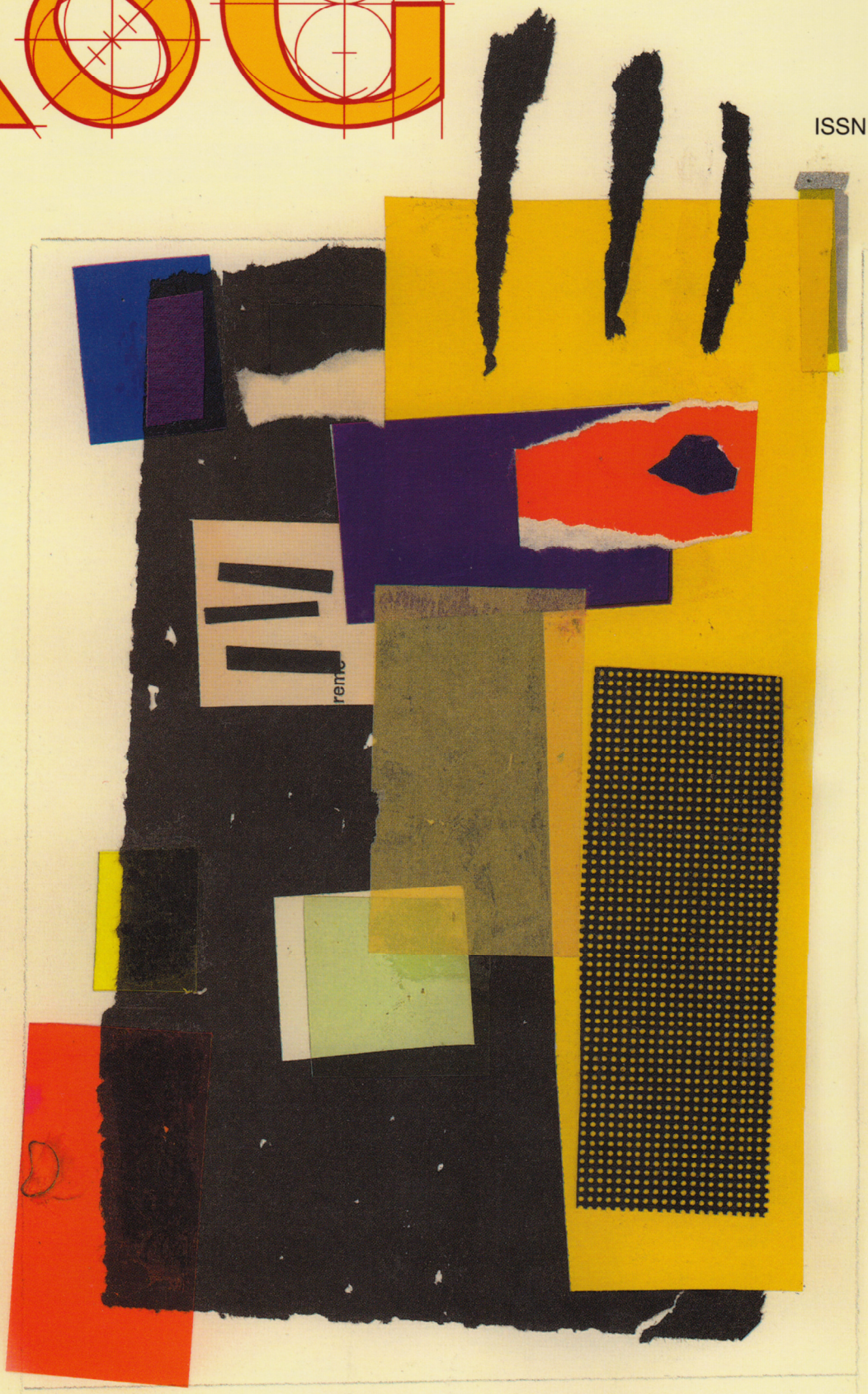

ZNANSTVENO-STRUČNO-INFORMATIVNI ČASOPIS
HRVATSKOG DRUŠTVA ZA KONSTRUKTIVNU GEOMETRIJU I KOMPJUTORSKU GRAFIKU

ISSN 1331-1611

BROJ 2
Zagreb, 1997.

KoG

ZNANSTVENO-STRUČNO-INFORMATIVNI ČASOPIS
HRVATSKOG DRUŠTVA ZA KONSTRUKTIVNU GEOMETRIJU I KOMPJUTORSKU GRAFIKU

SADRŽAJ

UPUTE SURADNICIMA

KoG je časopis koji objavljuje znanstvene i stručne radove te ostale priloge iz područja konstruktivne geometrije i kompjutorske grafike

ZNANSTVENI I STRUČNI ČLANCI

1. **Izvorni znanstveni rad** sadrži neobjavljene rezultate izvornih znanstvenih istraživanja, a znanstvene su informacije složene tako da se točnost analiza i izvoda, na kojima se rezultati temelje, može provjeriti.
2. **Prethodno priopćenje** znanstveni je rad što sadrži jedan ili više novih znanstvenih podataka čija priroda zahtijeva hitno objavljivanje. Ne mora nužno imati dovoljno pojedinosti za ponavljanje i provjeru rezultata.
3. **Pregledni rad** znanstveni je rad što sadrži izvoran, sažet i kritički prikaz jednog područja ili njegova dijela u kojemu autor aktivno djeluje. Mora biti istaknuta uloga autorova izvornog doprinosa u tom području u s obzirom na već publicirane radove te pregled tih radova.
4. **Stručni rad** sadrži korisne priloge iz područja struke koji nisu vezani za izvorna istraživanja autora, a iznesena zapažanja ne moraju biti novost u struci.

Rad, duljine do 30.000 znakova, mora biti neobjavljen i ne smije se istodobno ponuditi drugom časopisu. Autor za svoj rad predlaže kategoriju, a konačnu odluku o svrstavanju donosi Izdavački savjet na temelju zaključaka recenzenata.

Rad može biti napisan na hrvatskom, engleskom ili njemačkom jeziku. Autor predaje tekst na jeziku kojei odabere, te sažetak na hrvatskom i engleskom. Sažetak opsegom ne bi trebao biti veći od 600 znakova. Naslov članka mora biti sažet i informativan. Citiranu literaturu treba poredati po abecednom redu prezimena autora. Radovi iz časopisa citiraju se: redni broj, prezime i inicijal imena autora ili skupine autora, naslov rada, naziv časopisa, volumen, godina u zagradi, broj časopisa u godini, broj početne i završne stranice rada. Knjige se citiraju: redni broj, prezime i inicijal imena autora ili grupe autora, naslov knjige, nakladnik, mjesto izdanja, godina.

Članci trebaju biti dopunjeni kontaktnim podacima o autoru: ime i prezime, stručno zvanje, znanstveni stupanj, naziv poduzeća ili ustanove u kojoj radi, adresa ustanove i kuće, brojevi telefona i telefaksa, e-mail adresa, broj žiro-računa.

O prihvaćanju ili odbijanju rada autor bit će obavješten.

OSTALI PRILOZI

To su stručni osvrti i prikazi raznih sadržaja iz širokog područja geometrije i grafike, vijesti i izvješća o znanstveno-stručnim skupovima, prikazi knjiga, časopisa, studentskih radova, softvera i hardvera koji se objavljuju u rubrikama "Geometrija i grafika" i "Vijesti, izvješća, prikazi".

Rukopisi i svi prilozi predaju se uredništvu.

Za znanstvene i stručne radove potrebna su tri ispisa, a za ostale samo jedan.

Prihvaćene radove autori dostavljaju elektronskom poštom kao ASCII datoteke. Preporučuje se LaTeX format.

Podrobnije upute dobivaju se u uredništvu.

KoG

ISSN 1331-1611

Znanstveno-stručno-informativni časopis Hrvatskog društva za konstruktivnu geometriju i kompjutorsku grafiku

Osnivač i izdavač
Hrvatsko društvo za konstruktivnu geometriju i kompjutorsku grafiku

Izdavački savjet
Miroslav Ambruš-Kiš, Sonja Gorjanc, Miljenko Lapaine, Vlasta Szirovicza

Urednica
Sonja Gorjanc

Lektorica
Branka Makovec

Grafičko oblikovanje
Miroslav Ambruš-Kiš
Grafička priprema
Gordan Vrban

Ilustracije na omotu
Alida Bitunjac, kolaž
Miroslav Ambruš-Kiš, vektorska grafika
HW/SW: PowerMacintosh, Macromedia Freehand 7.04, Adobe Photoshop 4.04

Tisak
"O-tisak", Zagreb

Adresa uredništva
10000 Zagreb, Avenija V. Holjevca 15, Hrvatska
telefon:
+385 (0)1 670-509
telefaks:
+385 (0)1 45-61-206

KoG na Internetu:
e-mail: kog@master.grad.hr
http://www.mzt.hr/mzt/hrv/info/hdk/kogmain.htm

Naklada
250 primjeraka

Časopis izlazi jednom na godinu

Ovaj broj časopisa financiralo je Ministarstvo znanosti i tehnologije Republike Hrvatske.

ISSN 1331-1611

KoG

№ 2
Zagreb, 1997.

SCIENTIFIC AND PROFESSIONAL INFORMATION JOURNAL OF
CROATIAN SOCIETY FOR CONSTRUCTIVE GEOMETRY NAD COMPUTER GRAPHICS

CONTENTS

GUIDE TO THE COLLABORATORS

"KoG" is the journal publishing scientific and professional papers and other contributions from the field of constructive geometry and computer graphics.

SCIENTIFIC AND PROFESSIONAL PAPERS

1. **Original scientific paper** contains unpublished results of the original scientific research, and the scientific information is presented in such a way that it permits the exactness of analysis and derivations the results are based upon to be checked.
2. **Preliminary communication** is a scientific work containing one or more new scientific data, the nature of which requests urgent publishing. It need not necessarily convey sufficient number of details for repetition or checking of results.
3. **Review** is a scientific paper containing original, condensed and critical presentation of a field or its segment in which the author participates actively. The role of the author's original contribution in this field must be pointed out as related to already published works, accompanied by the survey of these works.
4. **Professional paper** contains useful contributions from the professional field which are not bound to the original research of the author, and the observations presented need not be a novelty in the profession.

The paper containing 30.000 characters should be unpublished and it mustn't be offered to some other journal at the same time. The author suggests for his/her paper the category, and the final decision about how it is going to be classified is reached by the Publishing Council on the basis of the conclusions made by reviewers.

The paper can be written in Croatian, English or German. Author hands in the text in the language he/she has chosen, and the abstract in Croatian and English. The abstract should not exceed 600 characters. Paper title should be concise and informative. The reference should be listed in alphabetical order by author's family name. The papers from journals are to be cited as follows: number, author's or group of author's last name, initials, title of reference article , name of journal, volume, the year of publication in parenthesis, number of journal in the year, number of the first and end page of the paper. Books are cited as follows: number, author's last name, author's initials, title of the book, publisher, city, year of publishing.

The articles should be supplemented by the notes to authors: name, last name, title, scientific degree, name of the firm or institution he/she works at, home and institution address, phone and fax numbers, e-mail, number of bank account.

Author will be notified about his paper being either accepted or rejected.

OTHER ATTACHMENTS

These are professional reviews and presentations of various contents from the wider area of geometry and graphics, news and reports about scientific and professional gatherings, presentations of books, journals, student papers, softwares and hardwares published in the departments on "Geometry and Graphics" and "News, reports and presentations".

Manuscripts and all attachments are to be sent to the Editorial. For scientific and professional papers three copies are needed, for all other only one is enough.

Accepted papers are to be sent by authors by electronic mail as ASCII files. LaTeX format is recommanded.

More detailed instructions are available tfom the Editorial.

KoG

ISSN 1331-1611

Scientific and Professional Information Journal of Croatian Socitey for Constructive Geometry and Computer Graphics

Founder and Publisher

Croatian Society for Constructive Geometry and Computer Graphics

Board of Trustees

Miroslav Ambruš-Kiš, Sonja Gorjanc, Miljenko Lapaine, Vlasta Szirovicza

Editor

Sonja Gorjanc

Design

Miroslav Ambruš-Kiš

Layout

Gordan Vrban

Cover page illustrations

Alida Bitunjac, collage

Miroslav Ambruš-Kiš, vector graphics

(HW/SW: PowerMacintosh, Macromedia Freehand 7.04, Adobe Photoshop 4.04)

Print

"O-tisak" d.o.o., Zagreb

Editorial Address

Avenija V. Holjevca 15, 10000 Zagreb

CROATIA

phone: + 385 1 670 509

fax: + 385 1 4561 206

KoG on Internet

e-mail: kog@master.grad.hr

http://www.mzt.hr/mzt/hrv/info/hdk/kogmain.htm

Circullation

250

Published annualy

This issue has been financially supported by Croatian Ministry of Science and Technology

Original scientific paper
Accepted 16.04.1997.

MARIA KMETOVA AND MARTA SZILVASI-NAGY*

Sphere Covering by Rational Quadratic Beziér Patches

Sphere Covering by Rational Quadratic Beziér Patches
ABSTRACT.
A covering of the sphere in the three-dimensional Euclidean space is constructed consisting of three-sided and two-sided regions. Each region is represented as a rational quadratic Beziér patch over a triangular or a rectangular domain, respectively.
Keywords: Beziér patches, rational spline-functions

Prekrivanje kugle racionalnim kvadratičnim Beziérovim plohama
SAŽETAK
Prekrivanje kugle u trodimenzionalnom euklidskom prostoru konstruirano je tako da se sastoji od trostranih i dvostranih područja. Svako područje predstavljeno je po dijelovima racionalnim kvadratičnim Beziérovim plohama nad trokutastom ili pravokutnom domenom.
Ključne riječi: Beziérove plohe, racionalne splajn funkcije

INTRODUCTION

In the practice of geometric modelling a recurrent request is to describe different objects by a given collection of spline-functions. The exact representation of the three-dimensional sphere in the Euclidean space by quadratic rational spline-functions has been the subject of several papers in the CAD-literature. Unfortunately, the first publication on constructing rational Beziér sphere patches [5] contains an error [2], and the paper on the exact representation of a spherical cap by a single rational Beziér patch [1] is not easily available. So we have no information about the type of Beziér patches in that representation.

Our subdivision technique of the sphere is based on the investigation of quadrics given in [4], especially on the following theorem:

The rational quadratic Beziér triangle is a quadric if and only if all three extended boundary curves meet in one point of the quadric.

From this theorem it follows that the sphere can't be subdivided into triangular regions represented by rational quadratic Beziér patches. Therefore, patches of other type are also necessary to fill the gaps between the triangular patches.

An obvious construction of triangular regions satisfying the condition of the theorem is the following. Four given points on the sphere determine a tetrahedron. The planes of the faces around a fixed vertex cut the sphere in three circular arcs bordering an appropriate triangular region (Fig. 1).

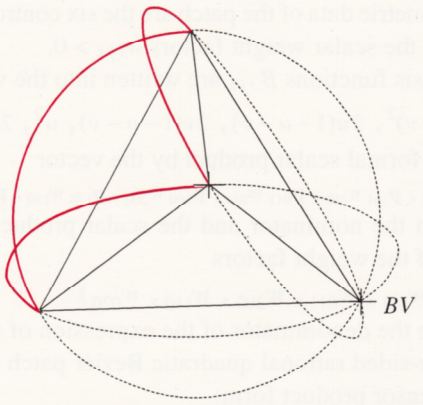

Fig.1: Appropriate triangular region of the sphere.

Four such triangular regions are determined by the tetrahedron. Between each two neighbouring triangles a two-sided gap arises. There are six such two-sided regions. Each of them will be covered by a degenerated four-sided Beziér patch (Fig.2).

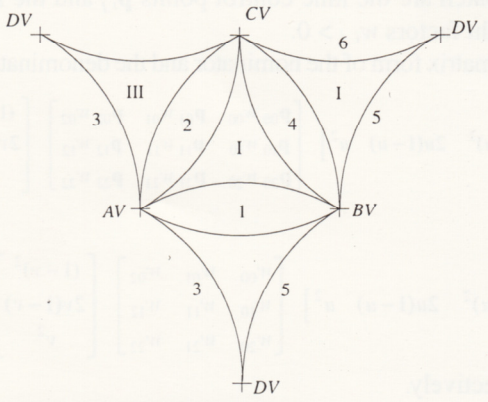

Fig.2: Subdivision of the sphere.

The computations of the geometric data of a two-sided patch have been carrried out by *Mathematica* [6], what is the new result of this paper.

MATHEMATICAL DESCRIPTION OF RATIONAL QUADRATIC PATCHES

The two-parametric vector equation of a rational quadratic Beziér patch over a triangular parameter domain has the form [3]:

* Supported by the Hungarian Nat. Found. for Sci. Research (OTKA) No. T020498

$$\mathbf{r}(u,v) = \sum_{\substack{i,j,k\geq 0 \\ i+j+k=2}} \mathbf{p}_{ijk}\, w_{ijk}\, B_{ijk}(u,v,s) \;/\; \sum_{\substack{i,j,k\geq 0 \\ i+j+k=2}} w_{ijk}\, B_{ijk}(u,v,s)$$

where u, v and s are the barycentric coordinates of a point in the triangular domain with respect to the vertices of the triangle, $u + v + s = 1$ and $0 \leq u,v,s \leq 1$.

$$B_{ijk}(u,v,s) = \frac{2!}{i!\,j!\,k!}\, u^i v^j s^k$$

are the bivariate Bernstein basis functions of degree 2. The geometric data of the patch are the six control points $\mathbf{p}_{ijk}$ and the scalar weight factors $w_{ijk} > 0$.

If the basis functions B_{ijk} are written into the vector

$((1-u-v)^2,\ 2u(1-u-v),\ 2v(1-u-v),\ u^2,\ 2uv,\ v^2)$,

then the formal scalar product by the vector

$(\mathbf{p}_{002}\, w_{002},\ \mathbf{p}_{101}\, w_{101},\ \mathbf{p}_{011}\, w_{011},\ \mathbf{p}_{200}\, w_{200},\ \mathbf{p}_{110}\, w_{110},\ \mathbf{p}_{020}\, w_{020})$

stands in the nominator and the scalar product by the vector of the weight factors

$(w_{002},\ w_{101},\ w_{011},\ w_{200},\ w_{110},\ w_{020})$

stands in the denominator of the expression of $\mathbf{r}(u,v)$.

The four-sided rational quadratic Beziér patch is given by the tensor product form:

$$\mathbf{r}(u,v) = \sum_{i,j=0}^{2} \mathbf{p}_{ij}\, w_{ij}\, B_i(u)\, B_j(v) \;/\; \sum_{i,j=0}^{2} w_{ij}\, B_i(u)\, B_j(v),$$

where $0 \leq u,v \leq 1$ and

$$B_i(u) = \frac{2!}{i!(2-i)!}\, u^i (1-u)^{2-i}, \quad (i = 0,1,2)$$

is the quadratic Bernstein basis. The geometric data of the patch are the nine control points $\mathbf{p}_{ij}$ and the scalar weight factors $w_{ij} > 0$.

The matrix form of the nominator and the denominator are

$$\begin{bmatrix}(1-u)^2 & 2u(1-u) & u^2\end{bmatrix} \begin{bmatrix}\mathbf{p}_{00}w_{00} & \mathbf{p}_{01}w_{01} & \mathbf{p}_{02}w_{02} \\ \mathbf{p}_{10}w_{10} & \mathbf{p}_{11}w_{11} & \mathbf{p}_{12}w_{12} \\ \mathbf{p}_{20}w_{20} & \mathbf{p}_{21}w_{21} & \mathbf{p}_{22}w_{22}\end{bmatrix} \begin{bmatrix}(1-v)^2 \\ 2v(1-v) \\ v^2\end{bmatrix}$$

and

$$\begin{bmatrix}(1-u)^2 & 2u(1-u) & u^2\end{bmatrix} \begin{bmatrix}w_{00} & w_{01} & w_{02} \\ w_{10} & w_{11} & w_{12} \\ w_{20} & w_{21} & w_{22}\end{bmatrix} \begin{bmatrix}(1-v)^2 \\ 2v(1-v) \\ v^2\end{bmatrix},$$

respectively.

SPHERICAL PATCHES

Each boundary curve of a triangular patch is a segment of the circumscribed circle of a regular triangle. Such a circular arc of 60° can be represented as a quadratic rational Beziér curve determined by the control points P_0, P_1 and P_2 and the corresponding weights 1, 1/2 and 1 (Fig.3).

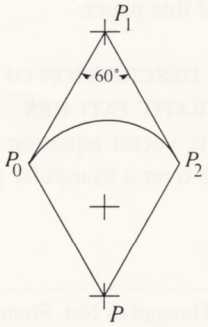

Fig.3: Control points of a circular arc.

Obviously, the point P_1 is the reflected lower vertex P of the triangle on the line of P_0 and P_2. The control points of the 4x3 boundary curves of the spherical patches can be computed from the vertices of the tetrahedron in a similar way by appropriate reflexions of the corresponding vertices. As the boundary curves of a Beziér patch are Beziér curves generated by the boundary control points of the triangular patch, all the geometric data of the triangular patches are determined by the four vertices *AV*, *BV*, *CV* and *DV* of the tetrahedron (Fig.4).

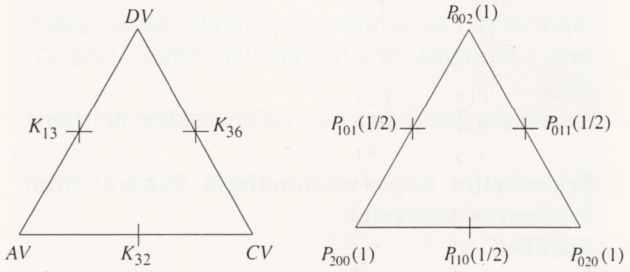

Fig.4: Control points and weights of a triangular patch.

The coordinates of the vertices of the tetrahedron and the control points are listed in Fig.5 in the input form of *Mathematica*.

```
AV={-1,1,-1}; BV={1,-1,-1}; CV={1,1,1}; DV={-1,-1,1};
K11={1,1,-3}; K21={0,0,-3}; K31={-1,-1,-3};
K12={1,3,-1}; K22={0,3,0}; K32={-1,3,1};
K13={-3,1,1}; K23={-3,0,0}; K33={-3,-1,-1};
K14={3,1,-1}; K24={3,0,0}; K34={3,-1,1};
K15={1,-3,1}; K25={0,-3,0}; K35={-1,-3,-1};
K16={1,-1,3}; K26={0,0,3}; K36={-1,1,3};
```

Fig.5. The coordinates of the control points.

The control points $K\,I\,J$, (I = 1,2,3 and J = 1...6) are numbered according to the two-sided patches, where the second index is the patchnumber. The circles building the patch boundaries on the sphere are drawn by *Mathematica* in Fig.6.

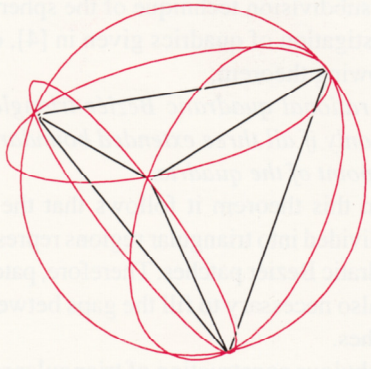

Fig.6: Patch boundaries determined by four points of the sphere.

The usual way of representing a triangular patch by parameter lines is drawing three sets of surface curves according to constant barycentric coordinates in the triangular parameter domain: $u = const$, $v = const$ and $s = 1 - u - v = const$. Unfortunately, *Mathematica* requires constant limits for the parameter values in the command ParametricPlot3D. Therefore, the triangular domain bordered by the lines $u = 0$, $v = 1$ and $u + v = 1$ has to be transformed into a rectangular domain for example by the parameter transformation $u = t - st$ and $v = st$, $(0 \le s,t \le 1)$. In our notation *bfig*3 [*u_*,*v_*], [*k*] (k = 1,..,4) is the two-parametric vector equation of a triangular Beziér patch (Fig.7).

```
Array[bfig3[u_,v_],4];
fu[s_,t_]:=t-s t;
fv[s_,t_]:=s t;
A[RGBColor[r_,g_,b_]]:=CMYKColor[0,r,r,1-r];
A[GrayLevel[x_]]:=GrayLevel[x];
triangs=ParametricPlot3D
   [{bfig3[fu[s,t],fv[s,t]][1],
   bfig3[fu[s,t],fv[s,t]][2],
   bfig3[fu[s,t],fv[s,t]][3],
   bfig3[fu[s,t],fv[s,t]][4]}
//Evaluate,{s,0,1},{t,0,1},PlotPoints->{12,12},
Boxed->False,Axes->None,
ColorOutput->A,Background->GrayLevel[0.8],
ViewPoint->{1,-3,.5}];
```

Fig. 7: Drawing command for the triangular patches.

The four patches drawn by *Mathematica* are shown in Fig. 8 together with the control net of one patch.

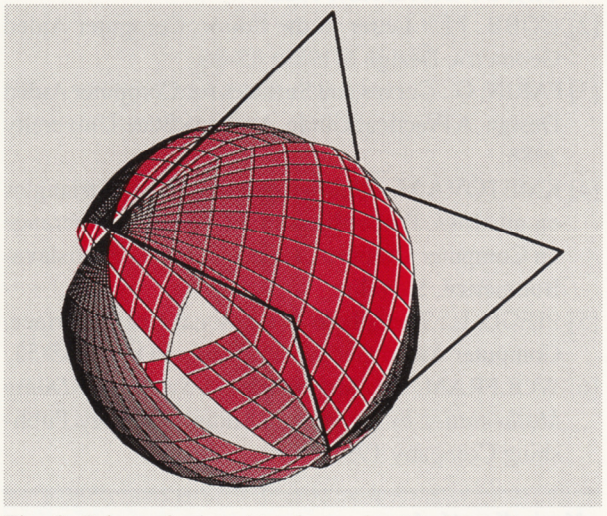

Fig. 8: Triangular patches drawn by *Mathematica*.

The two-sided patches can be considered as degenerated four-sided patches. The geometric data of such a patch are not determined by the two opposite boundary curves coinciding with the boundaries of the neighbouring triangular patches. In Fig.9 the degenerated control net of the 2nd patch and the corresponding Beziér control net over a rectangular parameter domain are shown. The unknown data are the geometric data of the middle longitudinal parameter curve, namely, the control point P_{11} and its weight w, moreover the weights of the points P_{10} and P_{12} coinciding with the vertex CV and AV, respectively. For symmetry reasons these weights are equal, denoted by c.

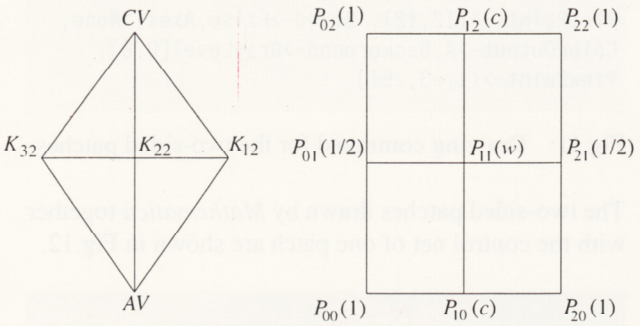

Fig.9: Geometric data of a degenerated two-sided patch.

These unknown data in the vector equation of the rectangular Beziér patch can be determined from the condition that any point of the generated patch must lie on the sphere. After substituting the coordinates of an arbitrary point of the patch into the equation of the sphere (with center point in the origin and radius=3) and reordering the equation, the coefficients of the terms $u^i v^j$ (i = 0..4, v = 0..4) can be collected with *Mathematica*. The condition that each coefficient equals to zero leads to a system of equations for the unknowns. However, the number of equations is greater than the number of unknowns, and the equations are not linear, the solution

$$P_{11} = (0,3,0), \quad w = \sqrt{3}/3, \quad c = \sqrt{3}/2$$

can be found interactively by *Mathematica*. After that it can be verified easily that an arbitrary point of the generated patch by these data lies on the sphere indeed. The control net of a two-sided patch is shown in Fig.10.

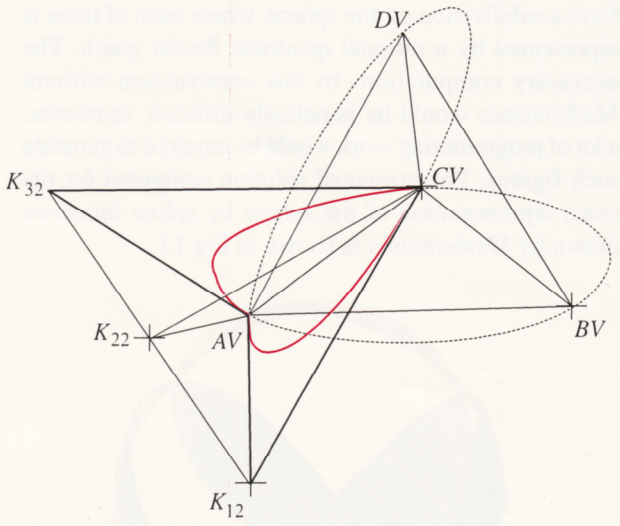

Fig.10: The control net of a two-sided patch.

The drawing command for the six patches is written in Fig.11, where bfig2 [u_,v_] [k], (k = 1,..,6) denotes the two-parametric vector equation of a rational quadratic Beziér patch over a rectangular domain.

```
Array[bfig2[u_,v_],6];
monds=
ParametricPlot3D[{bfig2[u,v][1],bfig2[u,v][2],
   bfig2[u,v][3],bfig2[u,v][4],
   bfig2[u,v][5],bfig2[u,v][6]}
//Evaluate,{u,0,1},{v,0,1},
PlotPoints->{12,12}, Boxed->False,Axes->None,
ColorOutput->A,Background->GrayLevel[0.8],
ViewPoint->{1,-3,.5}]
```

Fig.11: Drawing command for the two-sided patches.

The two-sided patches drawn by *Mathematica* together with the control net of one patch are shown in Fig.12.

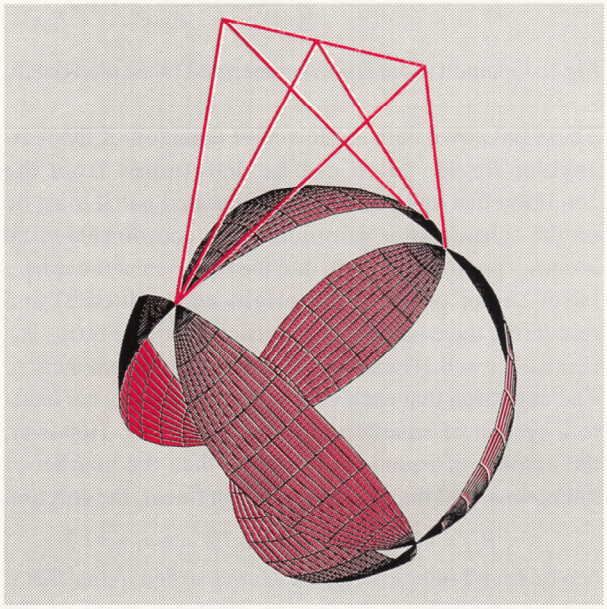

Fig.12: Two-sided patches drawn by *Mathematica*.

Finally, the four triangular and six two-sided patches form a subdivision of the sphere, where each of them is represented by a rational quadratic Beziér patch. The necessary computations to this construction without *Mathematica* would be hopelessly difficult, moreover, a lot of programming work would be required to generate such figures. The presented solution computed for the exact representation of the sphere by spline functions drawn by *Mathematica* is shown in Fig.13.

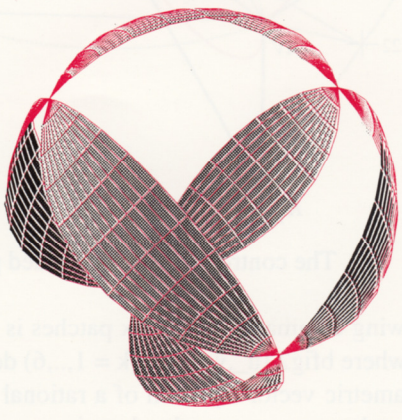

Fig. 13 a

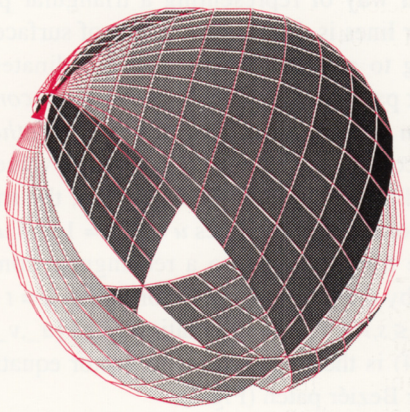

Fig. 13 b

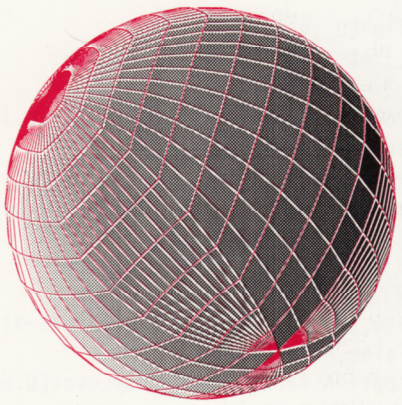

Fig. 13 c

Fig.13: The covering of the sphere.

References

[1] COBB, J.E.: Tiling the sphere with rational Beziér patches,Technical Report UUCS-88-009, Dept. of Computer Science, University of Utah, Salt Lake City, UT 84112, July, 1988.

[2] COBB, J.E.: Letter to the Editor, Computer Aided Geometric Design 6(1989) 85-86.

[3] FARIN, G.: Curves and Surfaces for Computer Aided Design, A Practical Guide, Arozona State University 1988.

[4] KMETÓVÁ M.: Rational quadratic Beziér triangles on quadrics, Proceedings of 12. Spring Conference on Computer Graphics, June 5-7, 1996., Bratislava-Budmerice, Slovakia

[5] PIEGL, L.: The sphere as a rational Beziér surface, Computer Aided Geometric Design 3(1986) 45-52.

[6] WOLFRAM, S.: *Mathematica, A System for Doing Mathematics by Computer*, Addison-Wesley Publishing Company 1991.

Maria Kmetóvá
Department of Mathematics, Faculty of Natural Sciences, University of Education
Farská 19, 949 74 Nitra, Slovakia
kmt@unitra.sk

Marta Szilvasi-Nagy
Department of Geometry, Institute of Mathematics, Technical University of Budapest, H-1521 Hungary
szilvasi@math.bme.hu

Original scientific paper
Accepted 29.04.1997

DANIELA VELICHOVA

Geometric Modelling of Hyperpatches

Geometric Modelling of Hyperpatches
ABSTRACT
The paper deals with the modelling of solids (hyperpatches) on the basis of their creative laws. Creative representation of a solid enables to modell also solids with "curve-like" edges, not only solids with the polyhedral boundary as in the boundary representation method. There is provided also the possibility to control a non-homogeneous distribution of the interior points of a solid created as an interpolated figure. Basic notions such as a solid cell, an isoparametric curve segment and an isoparametric surface patch, or tangent space and density vector in a solid point are described and their relevance to the intrinsic geometric properties of the solid is discussed. Composite solid modelling problems on adjoining of the elementar solid cells are mentioned.
Keywords: solid modelling, creative space, interpolation of hyperpatches

Geometrijsko modeliranje po dijelovima hiperplohama
SAŽETAK
Rad se bavi modeliranjem tijela (solids) na osnovi njihovih zakona stvaranja (creative laws). Kreativno predstavljanje tijela omogućava i modeliranje tijela koja imaju "zakrivljene" stranice, ne samo tijela s poliedarskim stranicama kao što je to slučaj u metodi prezentiranja rubova (boundary representation method). Postoji također i mogućnost upravljanja nehomogenom raspodjelom unutarnjih točaka tijela kreiranog poput interpoliranog lika. Opisani su osnovni pojmovi kao što su ćelija tijela, segment izoparametarske krivulje i dio izoparametarske plohe, ili tangentni prostor i vektor gustoće u točki tijela, a raspravlja se i o njihovoj primjerenosti unutarnjim geometrijskim osobinama tijela. Spomenuti su problemi modeliranja složenog tijela pri dodavanju elementarnih ćelija.
Ključne riječi: modeliranje tijela, kreativni prostor, interpolacija po dijelovima hiperplohama

1. INTRODUCTION

Solid modelling is one of those interesting problems, which are still developing parts of Computer Graphics. Solids can be created due to their creative laws or by description of the incidence structure of their boundary. There exists a lot of literature concerned the second mentioned way of modelling, this topic is given in details in Mantyla [1].

Let us look therefore in details at the modelling of solids on the basis of their creative laws and representations in the Creative space.

Let K be a Creative space, an ordered pair $K = (U,G)$, where U - base is a set of figures in the space (subsets of the extended Euclidean space $\overline{E}_3$) and G- generator is a set of generating principles ($G = GP(\overline{E}_3) \cup L$, while $GP(\overline{E}_3)$ is a group of projective transformations in $\overline{E}_3$ and L is a set of interpolations). More detailed description can be found in Velichovà [3], [6].

Solid T (a three-parametric subset of $\overline{E}_3$) is in K synthetically represented by its creative representation, an ordered pair (U,G), where $U \in U$ (a basic figure) and $G \in G$ (a generating principle) are such, that applying the generating principle G on the basic figure U the created solid T will be obtained. Generating principle G can be a geometric transformation, a class of geometric transformations or any interpolation. The first two types of generating principles provide modelling of solids which are homogeneous, i.e. their interior points are uniformly distributed. This feature of the uniform points' distribution is implicitly assumed in the case of solids defined by their incidence structure describing order and incidence of all elements (vertices, edges, faces) of the boundary of solids as three-dimensional regions in $\overline{E}_3$. In this case we even restrict our considerations on polyhedra only, while using creative representation we can create also more complex shaped solids with "curve-like" edges.

The possibility to describe and to control the feature of the non-uniform distribution of points in a solid is provided in the case of its modelling as an interpolated figure, using its creative representation in which the generating principle is an interpolation. This fact can play a very important role in many technical branches (science of materials, timber industry) but also in the sphere of medical diagnostics and image processing. Industrial design and CAGD of non-homogeneous solids using new efficient computer systems seem to be very perspective.

2. BASIC NOTIONS

Elementary notions and considerations concerned the problem of the solid interpolation can be easily deduced by analogy with the interpolation of curves and surfaces, increasing the dimension of a figure to three.

Analytic representation of a hyperpatch - solid cell C is a vector function

$$\mathbf{r}(u,v,w) = (x(u,v,w),y(u,v,w),z(u,v,w),h(u,v,w))$$

defined on the region $\Omega = [0,1]^3$ (where x, y, z and h are homogeneous coordinate functions at least C^3 continuous on a given region Ω), which is a local homeomorphic mapping of the region Ω on the hyperpatch C (according to Velichová [5]). A notion hyperpatch - cell of a solid analogously corresponds to notion of a curve segment or a surface patch. Composite solid can be obtained as a composition of several elementary cells. A notion isoparametric surface of a solid can be coordinated to a notion isoparametric curve of a surface. There exist three isoparametric systems of surfaces (exactly one of parameters u, v, w is constant) forming a net of surfaces in a solid. Boundary surfaces (faces) correspond to the constant values equal to 0 or 1. Setting two of parameters u, v, w equal to a constant value we can speak about isoparametric curves in a solid, and if the values are equal to 0 or 1 about boundary isoparametric curves (edges). Two isoparametric surfaces from different systems intersect in an isoparametric curve, two isoparametric curves intersect in a point. In a point of a solid all three parameters are constant and we denote them as parametric (curvilinear) coordinates of a solid point. Points with parametric coordinates equal to 0 or 1 only are vertices of a solid. A hyperpatch boundary (see Fig. 1) consists of

6 boundary surface patches -
face surfaces of a hyperpatch
$\mathbf{r}(0,v,w)$, $\mathbf{r}(1,v,w)$, $\mathbf{r}(u,0,w)$, $\mathbf{r}(u,1,w)$, $\mathbf{r}(u,v,0)$, $\mathbf{r}(u,v,1)$

12 boundary curve segments -
edge curves of a hyperpatch
$\mathbf{r}(0,0,w)$, $\mathbf{r}(0,1,w)$, $\mathbf{r}(1,0,w)$, $\mathbf{r}(1,1,w)$,
$\mathbf{r}(0,v,0)$, $\mathbf{r}(0,v,1)$, $\mathbf{r}(1,v,0)$, $\mathbf{r}(1,v,1)$,
$\mathbf{r}(u,0,0)$, $\mathbf{r}(u,0,1)$, $\mathbf{r}(u,1,0)$, $\mathbf{r}(u,1,1)$,

8 corner points - vertices of a hyperpatch
$\mathbf{r}(0,0,0)$, $\mathbf{r}(0,1,0)$, $\mathbf{r}(1,0,0)$, $\mathbf{r}(1,1,0)$,
$\mathbf{r}(0,0,1)$, $\mathbf{r}(0,1,1)$, $\mathbf{r}(1,0,1)$, $\mathbf{r}(1,1,1)$.

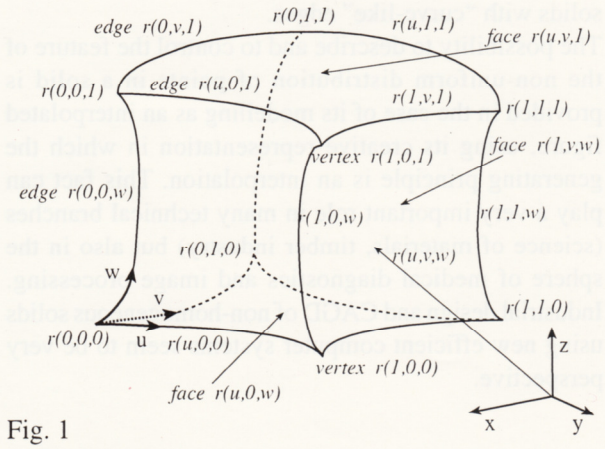

Fig. 1

The analytic representation of a hyperpatch can be obtained easily, from the creative representation, by the multiplication of matrices, which are analytic representations of the creative representation elements. Creative representation of a hyperpatch, an ordered pair (U,G), can have six possible forms according to the different types of the basic figure U and the suitable generating principle G:

(a surface patch, a class of geometric transformations)
(a solid cell, a geometric transformation)
(a net of boundary surface patches, an interpolation)
(a sequence of surface patches, an interpolation)
(a grid of boundary edge curves, an interpolation)
(a grid of points, an interpolation).

In the first two types of the hyperpatch creative representation the analytic representation of a generating principle is a regular square matrix of rank 4 with real numbers as elements (for a geometric transformation) or elements in a form of the real functions of one real variable all defined and at least C^1 continuous at the unit closed interval [0,1] (for a class of geometric transformations). In both cases the basic figure is analytically represented by a vector function, of one variable for a curve segment and of two variables for a surface patch, defined and satisfying certain conditions on the closed regions, as described in Velichová [3], [5]. Hyperpatches determined by these representations are homogeneous, and different types of created solids are described in Velichová [4]. For example, a solid of revolution can be created from a surface patch subdued to a class of revolutions about an axis, or a ruled solid from the same basic figure subdued to a class of translations. In the Fig. 2 there are illustrations of several solids generated by classes of geometric transformations.

Next 3 types of creative representations use as the basic figures ordered sets of points, curve segments or surface patches. These can be analytically represented by their vector equations and form the elements of the matrices - analytic representation of the basic figures - maps of the created hyperpatches, distributed in the appropriate order. Generating principle is in all 3 types an interpolation.

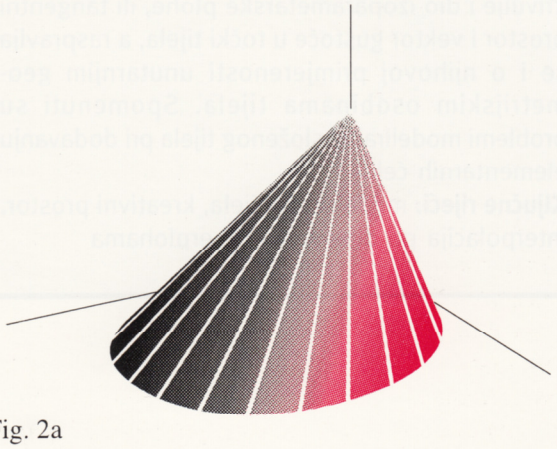

Fig. 2a

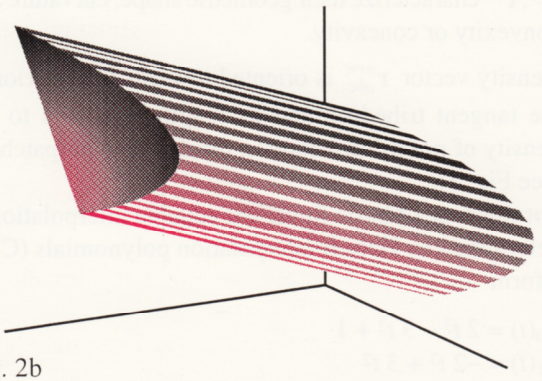

Fig. 2b

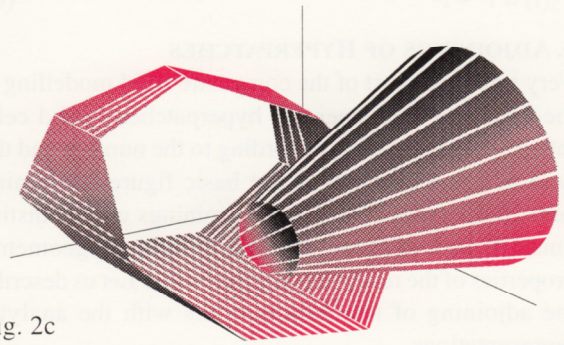

Fig. 2c

3. INTERPOLATION OF SOLIDS

In the following, we will describe the tri-cubic interpolation (cubic interpolation in three different directions) of a hyperpatch. Analytic representation of a tri-cubic solid cell is in a form

$$\mathbf{r}(u,v,w) = \mathbf{a}_{333}u^3v^3w^3 + \mathbf{a}_{332}u^3v^3w^2 + \ldots + \mathbf{a}_{100}u + \mathbf{a}_{000} =$$

$$= \sum_{i=0}^{3}\sum_{j=0}^{3}\sum_{k=0}^{3}\mathbf{a}_{ijk}\,u^i v^j w^k$$

$$= \sum_{i=0}^{3}\sum_{j=0}^{3}\sum_{k=0}^{3}F_i(u)\,F_j(v)\,F_k(w)\,\mathbf{b}_{ijk}$$

for $(u,v,w) \in [0,1]^3$, where $F_i(u)$, $F_j(v)$, $F_k(w)$ are cubic interpolation polynomials.

The set up of algebraic coefficients $\mathbf{a}_{ijk}$ (64 vectors) does not reveal clearly geometric features of the interpolated hyperpatch, while the set up of geometric coefficients $\mathbf{b}_{ijk}$ defines directly geometric properties of a hyperpatch and these even form a basic figure in the hyperpatch creative representation. From the analytic point of view geometric coefficients $\mathbf{b}_{ijk}$ form a three-dimensional matrix of the type 4×4×4, the map of a hyperpatch. The elements of this map are analytic representations of the hyperpatch basic figure elements, it means quadruples of homogeneous coordinates of the hyperpatch points (finite points in $\overline{E}_3$), tangent vectors of the hyperpatch edges, twist vectors of the hyperpatch faces, and vectors defining the distribution of points inside the hyperpatch - density vectors (points in $\overline{E}_3$ at infinity).

Let the basic figure of a hyperpatch be an ordered grid of 64 finite points in $\overline{E}_3$. According to the type of the used interpolation polynomials we can obtain a tri-cubic interpolation hyperpatch containing all elements of its basic figure (polynomials (A)), or such, that contains only 8 points of the given basic grid (Bernstein cubic polynomials (B)). In the first type, the basic grid of points defines also the curvature of edges and faces, and density of the hyperpatch, i.e. distribution of points inside. Analogy of a Beziér patch, approximation Beziér cubic hyperpatch (cell) defined by a grid of 4×4×4 points consists of faces, which are Beziér cubic approximation patches. Edges are Beziér cubic curve segments passing through the 8 corner points. Density of points' distribution inside the cell is an approximation of the order and position of points inside the basic figure grid and it is defined implicitly in the basic figure of the hyperpatch.

Interpolation polynomials are for $t = u, v, w$ in a form

$$\begin{aligned} F_0(t) &= -4.5\,t^3 + 9\,t^2 - 5.5\,t + 1 \\ F_1(t) &= 13.5\,t^3 - 22.5\,t^2 + 9\,t \\ F_2(t) &= -13.5\,t^3 + 18\,t^2 - 4.5\,t \\ F_3(t) &= 4.5\,t^3 - 4.5\,t^2 + t \end{aligned} \qquad (A)$$

$$\begin{aligned} F_0(t) &= (1-t)^3 \\ F_1(t) &= 3\,t\,(1-t)^2 \\ F_2(t) &= 3\,t^2\,(1-t) \\ F_3(t) &= t^3 \end{aligned} \qquad (B)$$

Map of a hyperpatch can be considered as an ordered quadruple of the square matrices $B_k = (P_{ijk})$, $i, j, k = 0,1,2,3$ of the type 4×4. Analytic representation of a hyperpatch is then in a form

$$\mathbf{r}(u,v,w) = \sum_{k=0}^{3} F_k(w)\left(\sum_{i=0}^{3}\sum_{j=0}^{3}F_i(u)\,B_k\,F_j(v)\right),$$

$$(u,v,w) \in [0,1]^3.$$

Let us now consider another basic figure of a hyperpatch, while the elements of this ordered set of points are not only finite points, but also points in $\overline{E}_3$ at infinity - vectors. These describe geometric properties of the created hyperpatch explicitly. The map of such basic figure can be also considered as an ordered quadruple of the square matrices of the rank 4 - arrays B_k, for $k = 0,1,2,3$. Each array is a basic figure of an iso-parametric patch and contains also density vectors of the points' distribution in the hyperpatch. Let us establish the following designations (in the Fig.3 illustrated for the curvilinear coordinate values $u = v = w = 0$):

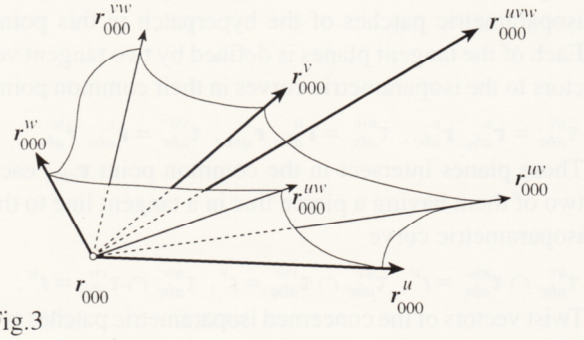

Fig.3

$\mathbf{r}(u,v,w) = \mathbf{r}_{uvw}$ solid point

$\dfrac{\partial \mathbf{r}(u,v,w)}{\partial u} = \mathbf{r}^{u}_{uvw}$ tangent vector to the isoparametric curve

$\dfrac{\partial^2 \mathbf{r}(u,v,w)}{\partial u \partial v} = \mathbf{r}^{uv}_{uvw}$ twist vector to the isoparametric patch

$\dfrac{\partial^3 \mathbf{r}(u,v,w)}{\partial u \partial v \partial w} = \mathbf{r}^{uvw}_{uvw}$ density vector

Separate arrays are then in a form

$$B_0 = \begin{pmatrix} \mathbf{r}_{000} & \mathbf{r}_{010} & \mathbf{r}^{v}_{000} & \mathbf{r}^{v}_{010} \\ \mathbf{r}_{100} & \mathbf{r}_{110} & \mathbf{r}^{v}_{100} & \mathbf{r}^{v}_{110} \\ \mathbf{r}^{u}_{000} & \mathbf{r}^{u}_{010} & \mathbf{r}^{uv}_{000} & \mathbf{r}^{uv}_{010} \\ \mathbf{r}^{u}_{100} & \mathbf{r}^{u}_{110} & \mathbf{r}^{uv}_{100} & \mathbf{r}^{uv}_{110} \end{pmatrix}$$

$$B_1 = \begin{pmatrix} \mathbf{r}_{001} & \mathbf{r}_{011} & \mathbf{r}^{v}_{001} & \mathbf{r}^{v}_{011} \\ \mathbf{r}_{101} & \mathbf{r}_{111} & \mathbf{r}^{v}_{101} & \mathbf{r}^{v}_{111} \\ \mathbf{r}^{u}_{001} & \mathbf{r}^{u}_{011} & \mathbf{r}^{uv}_{001} & \mathbf{r}^{uv}_{011} \\ \mathbf{r}^{u}_{101} & \mathbf{r}^{u}_{111} & \mathbf{r}^{uv}_{101} & \mathbf{r}^{uv}_{111} \end{pmatrix}$$

$$B_2 = \begin{pmatrix} \mathbf{r}^{w}_{000} & \mathbf{r}^{w}_{010} & \mathbf{r}^{vw}_{000} & \mathbf{r}^{vw}_{010} \\ \mathbf{r}^{w}_{100} & \mathbf{r}^{w}_{110} & \mathbf{r}^{vw}_{100} & \mathbf{r}^{vw}_{110} \\ \mathbf{r}^{uw}_{000} & \mathbf{r}^{uw}_{010} & \mathbf{r}^{uvw}_{000} & \mathbf{r}^{uvw}_{010} \\ \mathbf{r}^{uw}_{100} & \mathbf{r}^{uw}_{110} & \mathbf{r}^{uvw}_{100} & \mathbf{r}^{uvw}_{110} \end{pmatrix}$$

$$B_3 = \begin{pmatrix} \mathbf{r}^{w}_{001} & \mathbf{r}^{w}_{011} & \mathbf{r}^{vw}_{001} & \mathbf{r}^{vw}_{011} \\ \mathbf{r}^{w}_{101} & \mathbf{r}^{w}_{111} & \mathbf{r}^{vw}_{101} & \mathbf{r}^{vw}_{111} \\ \mathbf{r}^{uw}_{001} & \mathbf{r}^{uw}_{011} & \mathbf{r}^{uvw}_{001} & \mathbf{r}^{uvw}_{011} \\ \mathbf{r}^{uw}_{101} & \mathbf{r}^{uw}_{111} & \mathbf{r}^{uvw}_{101} & \mathbf{r}^{uvw}_{111} \end{pmatrix}$$

Geometric coefficients of an analytic representation of the interpolated hyperpatch are in this case: 8 quadruples of the hyperpatch vertices coordinates, 24 tangent vectors to the hyperpatch edges, 24 twist vectors of the hyperpatch faces and 8 density vectors in the hyperpatch vertices. In this way we describe geometrically not only the boundary of the hyperpatch as a three-dimensional region in the extended Euclidean space $\overline{E}_3$, but also the intrinsic distribution of the region's points.

At any point $\mathbf{r}_{abc}$ of a hyperpatch there is defined a tangent trihedron Γ_{abc} formed by 3 tangent planes to the isoparametric patches of the hyperpatch in this point. Each of the tangent planes is defined by two tangent vectors to the isoparametric curves in their common point,

$\tau^{uv}_{abc} = \mathbf{r}^{u}_{abc}\ \mathbf{r}^{v}_{abc}$, $\tau^{uw}_{abc} = \mathbf{r}^{u}_{abc}\ \mathbf{r}^{w}_{abc}$, $\tau^{vw}_{abc} = \mathbf{r}^{v}_{abc}\ \mathbf{r}^{w}_{abc}$.

These planes intersect in the common point $\mathbf{r}_{abc}$, each two of them having a pierce line in a tangent line to the isoparametric curve

$\tau^{uv}_{abc} \cap \tau^{uw}_{abc} = t^{u}$, $\tau^{uv}_{abc} \cap \tau^{vw}_{abc} = t^{v}$, $\tau^{uw}_{abc} \cap \tau^{vw}_{abc} = t^{w}$.

Twist vectors of the concerned isoparametric patches $\mathbf{r}^{uv}$, $\mathbf{r}^{uw}$, $\mathbf{r}^{vw}$ characterize their geometric shape, curvature and convexity or concavity.

Density vector $\mathbf{r}^{uvw}_{abc}$ is oriented towards the interior of the tangent trihedron and its length is related to the density of points' distribution inside the hyperpatch (see Fig. 3).

For this type of basic figure the suitable interpolation is determined by Hermit interpolation polynomials (C) in a form

$$F_0(t) = 2t^3 - 3t^2 + 1$$
$$F_1(t) = -2t^3 + 3t^2$$
$$F_2(t) = t^3 - 2t^2 + t$$
$$F_3(t) = t^3 - t^2 \qquad (C)$$

4. ADJOININGS OF HYPERPATCHES

Very important part of the composite solid modelling is the adjoining of elementary hyperpatches - solid cells into a composite solid. According to the number and the type of equal elements in the basic figures of joining cells, three types of different adjoinings can be distinguished, each of them determining different geometric properties of the resulted composite solid. Let us describe the adjoining of two hyperpatches with the analytic representations

$\mathbf{p}(u,v,w)$, $\mathbf{q}(u,v,w)$, $(u,v,w) \in \Omega$,

while the analytic representation of the resulting solid will be denoted as $\mathbf{r}(u,v,w)$.

A. *Continuous adjoining* - G^0 continuity

The two joining cells have a common boundary face patch, it means, in the maps of the joining cells there exist 16 equal (or collinear) elements: 4 quadruples of coordinate vectors of the adjoining boundary patches' vertices, 8 tangent vectors to the edges of the adjoining boundary patches in the corner points and 4 twist vectors of the adjoining boundary patches in these vertices (Fig. 4).

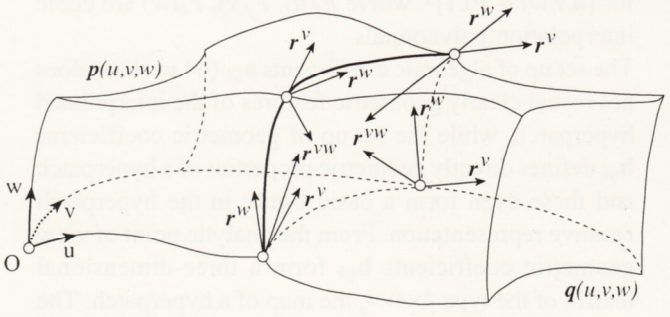

Fig. 4

The composite solid is a continuous region in the extended Euclidean space $\overline{E}_3$ and contains no wholes or bubbles. The adjoining face patches are equal and fit perfectly together, coincide. Isoparametric curve segments which are not parts of the adjoining faces need not be smooth. There can be created new edges in the boundary curve segments of the joining faces and new vertices in their corner points.

$\mathbf{p}(1,v,w) = \mathbf{q}(0,v,w) = \mathbf{r}(0.5,v,w)$

The presented equation expresses in the compound form 16 equations, which determine the collinearity of the vectors representing coinciding faces of the adjoining hyperpatches.

B. *Smooth adjoining* - G^1 continuity

Except of the common adjoining face patch, two joining cells must satisfy also the condition of the collinear tangent vectors to all adjoining isoparametric curve segments in the points of the common isoparametric patch. This means, that the adjoining of all isoparametric curve segments not inciting with the common isoparametric patch and 4 adjoining boundary patches is smooth. These conditions can be expressed by the following three compound equations

$$\mathbf{r}^{u}_{0.5vw} = \alpha . \mathbf{p}^{u}_{1vw} = \beta . \mathbf{q}^{u}_{0vw}$$

$$\mathbf{r}^{uw}_{0.5vw} = \gamma . \mathbf{p}^{uw}_{1vw} = \delta . \mathbf{q}^{uw}_{0vw}$$

$$\mathbf{r}^{uv}_{0.5vw} = \varepsilon . \mathbf{p}^{uv}_{1vw} = \varphi . \mathbf{q}^{uv}_{0vw}$$

where $\alpha, \beta, \gamma, \delta, \varepsilon, \varphi$ are non zero real numbers.

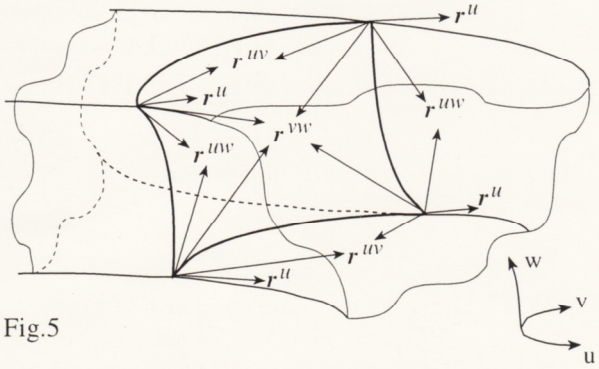

Fig.5

To the former 16 equal (collinear) elements necessary for G^0 continuity we must add 4 tangent vectors to the adjoining edges and 8 twist vectors of the smoothly adjoining boundary patches, two of them in the each of the 4 common vertices. The maps of the joining cells will consist of 28 equal (or collinear) elements (Fig. 5).

C. *Homogeneous adjoining* - G^2 continuity

In addition to the equality of all previous geometric parameters of the adjoining cells for G^0 and G^1 continuity, the continuous distribution of the cell's points will be assured as well, requiring the collinearity of density vectors in the common vertices; the maps of the joining cells will have equal (or collinear) 32 elements.

5. APPLICATION POSSIBILITIES

Global properties of the solid models - volume, surface area, moment of inertia, center of gravity, and so on, can be calculated by the evaluating the triple integral

$$\Phi = \int_{Solid} f(\mathbf{r}) dV$$

where Φ is the property required, $f(\mathbf{r})$ is a vector function describing Φ and integration is over the entire volume of the solid.

For a composite solid S created by adjoining of a finite number of cells C_i

$$S = \bigcup_{i=1}^{n} C_i$$

any integral taken over the solid decomposes into the sum of integrals

$$\int_S f(\mathbf{r})\, dV = \sum_{i=1}^{n} \int_{C_i} f(\mathbf{r})\, dV$$

where the cells C_i have disjoint interiors. The methods of evaluating triple integrals on computers are discussed in details by Mortenson [2].

The volume of a solid cell represented analytically by a vector function

$\mathbf{r}(u,v,w) = (\mathbf{x}(u,v,w), \mathbf{y}(u,v,w), \mathbf{z}(u,v,w), \mathbf{h}(u,v,w))$

defined and at least C^3 continuous on the region $\Omega = [0,1]^3$, is the value of the triple integral

$$V = \iiint_{\Omega} (\mathbf{r}^u \mathbf{r}^v \mathbf{r}^w)\, du\, dv\, dw$$

where $(\mathbf{r}^u \mathbf{r}^v \mathbf{r}^w)$ is the triple scalar product of the partial derivatives of the analytic representation - vector function $\mathbf{r}(u,v,w)$ with respect to the variables u, v, w.

Outlined problematic concerned interpolation of solids is a new but very interesting and perspective sphere of a further developement in geometric modelling of figures in E_3. It will undoubtedly serve as a source of a wide field for study of the three-dimensional figures in complexity, it means not excluding their interior density - the distribution of their intrinsic points, which is up till now a sphere ignored by Geometry.

There had been developed a system of easy separate programmes (in QB45 and TPASCAL programming lan-guages) providing calculations and visualizations of solids on the base of the mentioned theory which are used at the Department of Mathematics, Slovak Technical University in Bratislava. Some of them are used regularly in the pedagogical process.

REFERENCES

[1] MANTYLA, M.: *An Introduction to Solid Modeling*, Computer Science Press, USA, 1988

[2] MORTENSON, M.: *Geometric Modeling*, John Wiley & Sons, New York, USA, 1985

[3] VELICHOVÁ, D.: Creative Geometry, Proceedings of the 6th ICECGDG, Tokyo, Japan, 1994, pp. 302-304

[4] VELICHOVÁ, D.: Geometric Figures Modelling in a Timespace, Proceedings of the SCCG'93, Budmerice, Slovakia, 1993, pp.178 -180

[5] VELICHOVÁ, D.: Geometry of Solid Interpolation, Proceedings of the 12th SCCG, Bratislava - Budmerice, Slovakia, 1996, pp. 165 - 173

[6] VELICHOVÁ, D.: Interpolation of Solids, Proceedings of the 7th ICECGDG, Cracow, Poland, 1996, pp. 161 - 165

RNDr. Daniela VELICHOVÁ, CSc.
Department of Mathematics, Mechanical Engineering Faculty, Slovak Technical University
Námestie Slobody 17, 812 31 Bratislava, Slovakia
tel:+4217 3596 394, fax:+4217 749
email: velichov@dekan.sjf.stuba.sk

Original scientific paper
Accepted 07. 07. 1997.

GLORIA BITTERFELD

Sinthesis of Grassmann Chain Mechanisms in the Plane Using the *Ausdehnungslehre* and *Mathematica*

Sinthesis of Grassmann Chain Mechanisms in the Plane Using the *Ausdehnungslehre* and *Mathematica*

ABSTRACT

The Grassmannian mathematical system, well known as the Ausdehnungslehre (Linear Extension Theory) together with the symbolic computation program Mathematica is used to synthesise a class of planer mechanisms, named Grassmann mechanisms. The objective of investigating Grassmann mechanisms is to be able to compute easily the design parameters of the mechanism from given trajectory points.
Mechanisms in this class have moving links rotating on pivots and intersecting tracks. The paper reports on the simplest type of synthesis result of Grassmann Chain mechanisms using four given precision points for each mechanism apart to determine the design parameters of the mechanism of the class whose trajectory passes through those points.

Sinteza mehanizama Grassmanovog lanca u ravnini uz primjenu *Ausdehnungslehre* i *Mathematice*

SAŽETAK

Grassmannov matematički sustav, poznat kao *Ausdehnungslehre* zajedno sa programom za simboličko računanje *Mathematica* koristi se za sintetiziranje klase ravninskih mehanizama, nazvanih Grassmannovim mehanizmima. Cilj istraživanja Grassmannovih mehanizama je omogućavanje lakšeg izračunavanja dizajna parametara mehanizma iz zadanih točaka putanje.
Mehanizmi u toj klasi imaju pomične veze koje rotiraju na pivotima i sjekuće staze. Članak izvještava o rezultatu najjednostavnijeg tipa sinteze mehanizama Grassmannovog lanca uz primjenu četiri zadane točke preciznosti za svaki dio mehanizma da bi se odredilli parametri dizajna mehanizma iz klase čije trajektorije prolaze kroz te točke.

1. INTRODUCTION

Mechanisms are less versatile than robots, but less expensive, and if a straightforward method for automatic mechanism synthesis could be developed, more manufacturing processes could be automated inexpensively. The concept of the *Ausdehungslehre* was first expounded in 1844 by Hermann Grassmann and forms a language which has a geometric interpretation as a "prescription to construct" [1]. The *Ausdehnungslehre* is a superset of the Victor Calculus, and hence has significant applications to engineering, particularly when implemented with a symbolic computational program like *Mathematica* [2]. This paper implements a synthesis of Grassmann Chain mechanisms constructed of two chains of mechanisms with moving links rotating on pivots and intersecting tracks. That is to start with a required motion and to determine the parameters of a mechanism to give this motion. A numerical example is presented.
To our knowledge there has been no previous work on synthesis of these of mechanisms, or on the use of the *Ausdehnungslehre* to develop theories in this area.

2. THE *AUSDEHNUNGSLEHRE* AND GEOMETRIC DUALITY

One of the important facets of Grassmannís theory is its geometrical interpretation. The progressive ($\wedge$) and the regressive ($\overline{\wedge}$) products may be interpreted geometrically as follows: the progressive product or *wedge* operator may be read as constructing higher order elements from lower order elements and the regressive products or *wedge-bar* operator as intersecting elements to form lower order ones [3]. The regressive product operation is based on the fundamental formula called The Rule of the Middle Factor [4].
Geometric duality in the plane can be represented as in Table 1 below [3]:

Progresive Product	Regresive Product
$L \equiv P_1 \wedge P_2$	$P \equiv L_1 \overline{\wedge} L_2$
$\pi \equiv P_1 \wedge P_2 \wedge P_3$	$1 \equiv L_1 \overline{\wedge} L_2 \overline{\wedge} L_3$
$\pi \equiv L \wedge P$	$1 \equiv P \overline{\wedge} L$

Table 1: Geometric Duality

Where: **P** denotes a point
L denotes a line
π denotes a plane
1 denotes the unit scalar

The equivalence relation ≡ is used to affirm that these relations are true algebraically up to a scalar multiple. For some cases three lines do not intersect at a point.

3. Synthesis of Grassmann Chain Mechanisms - General Case

The simple class of planar mechanisms discussed in this paper is that which involves just fixed pivots and sliders, and which have a single degree of freedom.
Given any number of precision points for each mechanism of the chain it is required to find the chain mechanism which will describe the trajectories for each mechanism apart through those points. Their input is considered to be a point rotating with uniform angular velocity in a circle.

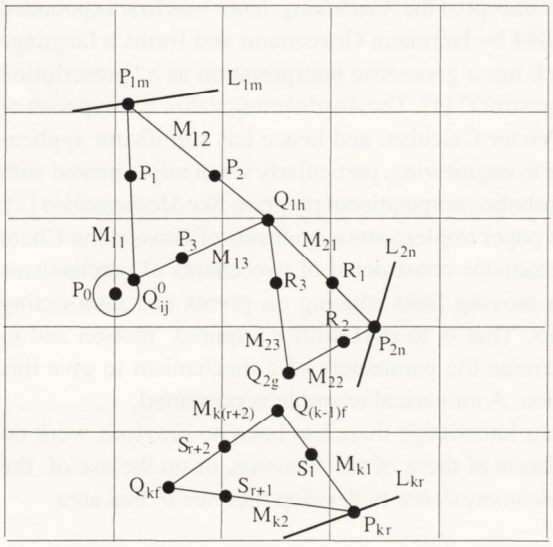

Figure 1: The Construction Scheme of Grassmann Chain Mechanism in the General Case

Regarding to the Figure 1 Grassmann Chain Mechanism notation is as follows:
Note that the first indices refer to the number of the link mechanism.

	First Link **Mechanism**	Second Link ..... **Mechanism**	k^{th} Link **Mechanism**
N° of tracks (order)	m	n	r
N° of pivots	m+2	n+2	r+2
Tracks	$\mathbf{L}_{11},...,\mathbf{L}_{1m}$	$\mathbf{L}_{21}, ..., \mathbf{L}_{2n}$	$\mathbf{L}_{k1}, ..., \mathbf{L}_{kr}$
Pivots	$\mathbf{P}_1, ..., \mathbf{P}_{m+2}$	$\mathbf{R}_1, ..., \mathbf{R}_{n+2}$	$\mathbf{S}_1, ..., \mathbf{S}_{r+2}$
Sliding points	$\mathbf{P}_{11}, ..., \mathbf{P}_{1m}$	$\mathbf{P}_{21}, ..., \mathbf{P}_{2n}$	$\mathbf{P}_{k1}, ..., \mathbf{P}_{kr}$
N° of precision points	h	g	f
Precision points	$\mathbf{Q}_{11}, ..., \mathbf{Q}_{1h}$	$\mathbf{Q}_{21}, ..., \mathbf{Q}_{2g}$	$\mathbf{Q}_{k1}, ..., \mathbf{Q}_{kf}$
N° of mobile links	m+2	n+2	r+2
Mobile links	$\mathbf{M}_{11}, ..., \mathbf{M}_{1(m+2)}$	$\mathbf{M}_{21}, ..., \mathbf{M}_{2(n+2)}$	$\mathbf{M}_{k1}, ..., \mathbf{M}_{k(r+2)}$

Table 2: The Notation of Grassmann Chain Mechanism

$\mathbf{P}_0$ — represents the center of the input circle
$\mathbf{Q}^0_{ij}$ — represents the intersection point on the circle made by the last mobile link passing through the last pivot of the first link mechanism corresponding to the precision point $\mathbf{Q}_{ij}$ of the link mechanism
$\mathbf{Q}_{(k-1)i}$ — represents the i^{th} precision point of the second last link mechanism of the chain mechanism

The proposed Chain Mechanism has only two chains mechanisms with one track and three pivots each.

3.1. The Synthesis of the First Link Mechanism of the Chain

The proposed synthesis process has two stages as follows [5]:

3.1.1. Stage 1 for the First Link Mechanism: Location of the Last Pivot and the Center of the Circle

The first stage is the synthesis of the center of the circle $\mathbf{P}_0$ and the last pivot $\mathbf{P}_3$. This part of the synthesis requires only four precision points as shown in Table 3. It is easy to observe, that the number of unknowns of this stage does not depend on the number of tracks and the other pivots of the mechanism and depends only on the unknown coordinates of the center of the circle $\mathbf{P}_0$ and the pivot $\mathbf{P}_3$.

Definition of the points $\mathbf{P}_0$ and $\mathbf{P}_3$	**N° of unknowns of the first stage**
$\mathbf{P}_0 = \Theta + x_0\,\mathbf{i} + y_0\,\mathbf{j}$	x_0 , y_0
$\mathbf{P}_3 = \Theta + x_3\,\mathbf{i} + y_3\,\mathbf{j}$	x_3 , y_3

Table 3: The Number of Unknowns of the First Stage of the Synthesis

If the mechanism is to be of 1 degree of freedom the problem is to find the center of the unit circle, the pivots and the position of the tracks.
With reference to Figure 1 select 4 precision points $\mathbf{Q}_{1h}$, where h=1, 2, 3, 4 and join with coresponding points $\mathbf{Q}^0_{ij}$ on the circle and pass through pivot $\mathbf{P}_3$.

$$\mathbf{Q}_{1h} \wedge \mathbf{P}_3 \wedge \mathbf{Q}^0{}_{ij} = 0 \quad i=1 \text{ and } j=1, 2, 3, 4 \qquad (1)$$

Solve these equations for the coordinates of $\mathbf{P}_0$ (the center of the circle) and $\mathbf{P}_3$ (the last pivot of the first mechanism). The result allows two sets of solutions, so we may have two possibilities for $\mathbf{P}_0$ and $\mathbf{P}_3$.
Assume the selected order of the four given precision points $\mathbf{Q}_{11}\mathbf{Q}_{12}\mathbf{Q}_{13}\mathbf{Q}_{14}$ and select the corresponding rotating points at equal intervals on the circle circumference. We have an infinite number of possibilities for the selection of the position of the

rotating points on the circle circumference. For each particular selection of the rotating points, the solution of the points $\mathbf{P}_0$ and $\mathbf{P}_3$ is changed. Therefore, there is an infinite number of solutions for the points $\mathbf{P}_0$ and $\mathbf{P}_3$. These solutions are related to the position of the respective rotating points. The selection of the rotating points gives the time of movement from one precision point to the another.

Suppose that those rotating points have the positions as follows:

$\mathbf{Q}^0_{11} = \Theta + [x_0 + R\,Cos(0)]\,\mathbf{i} + [y_0 + R\,Sin(0)]\,\mathbf{j}$;
$\mathbf{Q}^0_{12} = \Theta + [x_0 + R\,Cos(Pi/2)]\,\mathbf{i} + [y_0 + R\,Sin(Pi/2)]\,\mathbf{j}$;
$\mathbf{Q}^0_{13} = \Theta + [x_0 + R\,Cos(Pi)]\,\mathbf{i} + [y_0 + R\,Sin(Pi)]\,\mathbf{j}$;
$\mathbf{Q}^0_{14} = \Theta + [x_0 + R\,Cos(3Pi/2)]\,\mathbf{i} + [y_0 + R\,Sin(3Pi/2)]\,\mathbf{j}$;

It is important to notice that we have two solutions for $\mathbf{P}_0$ and $\mathbf{P}_3$. For each permutation of the four precision points the positions of the points $\mathbf{P}_0$ and $\mathbf{P}_3$ will be changed as is shown in Table 3. There is a correspondence between the precision points ($\mathbf{Q}_{1h}$) and the rotating points ($\mathbf{Q}^0_{ij}$) and for any changes in this correspondence, the solution for the center of the circle $\mathbf{P}_0$ and the pivot $\mathbf{P}_3$ will be changed.

The number of possibilities for the position of $\mathbf{P}_0$ and $\mathbf{P}_3$ is related to the number of precision points and the fact that there are two solutions in each case. If the number of the precision points is greater than four then, to the first four selected precision points add the other precision points and the number of possibilities of the position of $\mathbf{P}_0$ and $\mathbf{P}_3$ will be increase.

With reference to Table 4 for 4 precision points there will be 48 (2 × 24) changes, for precision points there will be 240 (2×120) changes and for 6 precision points there will be 720 (2×360) changes.

3. 1. 2. Stage 2 for the First Mechanism: Location of Pivots and Tracks

The second stage is the synthesis of the tracks and all other pivots. The number of tracks determines the number of pivots of the second stage. If m represents the number of tracks then, m+1 represents the number of pivots of the second stage of synthesis.

Table 5, 6 and 7 show the number of pivots and the orientation of the tracks required by stage 2 of the synthesis as a function of the number of precision points.

Table 4: Number of Possibilities for the Position of $\mathbf{P}_0$ and $\mathbf{P}_3$. Related to the Permutation of the Precision Points

N° of precision points	Permutations of the precision points out of four	N° of solutions for $\mathbf{P}_0$ and $\mathbf{P}_3$
4	4_{P4}	48
5	5_{P4}	240
6	6_{P4}	720

Table 5: Number of Precision Points Related to the Number of Pivots and the Tracks Oriented Anywhere in the Plane

N° of tracks and their positions	**Definition of the tracks $\mathbf{L}_{1m}$**	**N° of pivots of the second stage**	**Definition of the pivots P**	**N° of unknown parameters**	**N° of precision points h**
One track anywhere in the plane	$\mathbf{L}_{11} = (\Theta + xa\mathbf{i}) \wedge (\Theta + yb\,\mathbf{j})$	2	$\mathbf{P}_1 = \Theta + x_1\mathbf{i} + y_1\mathbf{j}$ $\mathbf{P}_2 = \Theta + x_2\mathbf{i} + y_2\mathbf{j}$	x_1, y_1 x_2, y_2 xa, yb	6
Two tracks anywhere in the plane	$\mathbf{L}_{11} = (\Theta + xa_1\mathbf{i}) \wedge (\Theta + yb_1\mathbf{j})$ $\mathbf{L}_{12} = (\Theta + xa_2\mathbf{i}) \wedge (\Theta + yb_2\mathbf{j})$	3	$\mathbf{P}_1 = \Theta + x_1\mathbf{i} + y_1\mathbf{j}$ $\mathbf{P}_2 = \Theta + x_2\mathbf{i} + y_2\mathbf{j}$ $\mathbf{P}_3 = \Theta + x_3\mathbf{i} + y_3\mathbf{j}$	x_1, y_1 x_2, y_2 x_3, y_3 xa_1, yb_1 xa_2, yb_2	10
Three tracks anywhere in the plane	$\mathbf{L}_{11} = (\Theta + xa_1\mathbf{i}) \wedge (\Theta + yb_1\mathbf{j})$ $\mathbf{L}_{12} = (\Theta + xa_2\mathbf{i}) \wedge (\Theta + yb_2\mathbf{j})$ $\mathbf{L}_{13} = (\Theta + xa_3\mathbf{i}) \wedge (\Theta + yb_3\mathbf{j})$	4	$\mathbf{P}_1 = \Theta + x_1\mathbf{i} + y_1\mathbf{j}$ $\mathbf{P}_2 = \Theta + x_2\mathbf{i} + y_2\mathbf{j}$ $\mathbf{P}_3 = \Theta + x_3\mathbf{i} + y_3\mathbf{j}$ $\mathbf{P}_4 = \Theta + x_4\mathbf{i} + y_4\mathbf{j}$	x_1, y_1 x_2, y_2 x_3, y_3 x_4, y_4 xa_1, yb_1 xa_2, yb_2 xa_3, yb_3	14
m		m+1		(2m+1)*2	(2m+1)*2

Table 6 shows the mechanism parameters if the track $\mathbf{L}_{1m}$ is parallel to one of the axes. This table could be considered as a particular case of Table 5.
If there are more than two tracks their orientation in the plane could vary. For example, the position of two tracks in the plane could be: both anywhere in the plan - Table 5, both parallel to one of the axes - Table 6, or one track parallel to an axis and one track anywhere in the plane - Table 7.

With reference to the Figure 1 the second stage is the synthesis the pivots $\mathbf{P}_1$, $\mathbf{P}_2$ and the position of the tracks $\mathbf{L}_{1m}$. Assume that the mobile link from the rotating points $\mathbf{Q}^0_{ij}$ will pass through the pivot $\mathbf{P}_1$, then will intersect the first track $\mathbf{L}_{11}$ in a sliding point $\mathbf{P}_{11}$.
Proceeding around the loop shows that the final equation comes from the requirement that the points $\mathbf{P}_{1m}$, $\mathbf{P}_{m+1}$ and $\mathbf{Q}_{1h}$ be collinear, that is

$$\mathbf{P}_{1m} \wedge \mathbf{P}_{m+1} \wedge \mathbf{Q}_{1h} = 0 \qquad (2)$$

where h=1, 2, 3, 4, ... , is the number of precision points and m represents the number of tracks.
Table 8 shows the final equations for the general case of m tracks starting with one and two tracks.

Table 6: Number of Precision Points Related to the Number of Pivots and Tracks Oriented Parallel to One the Axes in the Plane

N° of tracks and their positions	Definition of the tracks $\mathbf{L}_{1m}$	N° of pivots of the second stage	Definition of the pivots P	N° of unknown parameters	N° of precision points h
One track parallel to one of the axes	$\mathbf{L}_{11} = (\Theta + yb\mathbf{j}) \wedge \mathbf{i}$	2	$\mathbf{P}_1 = \Theta + x_1\mathbf{i} + y_1\mathbf{j}$ $\mathbf{P}_2 = \Theta + x_2\mathbf{i} + y_2\mathbf{j}$	x_1, y_1 x_2, y_2 yb	5
Two tracks parallel to one of the axes	$\mathbf{L}_{11} = (\Theta + yb_1\mathbf{j}) \wedge \mathbf{i}$ $\mathbf{L}_{12} = (\Theta + yb_2\mathbf{j}) \wedge \mathbf{i}$	3	$\mathbf{P}_1 = \Theta + x_1\mathbf{i} + y_1\mathbf{j}$ $\mathbf{P}_2 = \Theta + x_2\mathbf{i} + y_2\mathbf{j}$ $\mathbf{P}_3 = \Theta + x_3\mathbf{i} + y_3\mathbf{j}$	x_1, y_1 x_2, y_2 x_3, y_3 yb_1 yb_2	8
Three tracks parallel to one of the axes	$\mathbf{L}_{11} = (\Theta + yb_1\mathbf{j}) \wedge \mathbf{i}$ $\mathbf{L}_{12} = (\Theta + yb_2\mathbf{j}) \wedge \mathbf{i}$ $\mathbf{L}_{13} = (\Theta + yb_3\mathbf{j}) \wedge \mathbf{i}$	4	$\mathbf{P}_1 = \Theta + x_1\mathbf{i} + y_1\mathbf{j}$ $\mathbf{P}_2 = \Theta + x_2\mathbf{i} + y_2\mathbf{j}$ $\mathbf{P}_3 = \Theta + x_3\mathbf{i} + y_3\mathbf{j}$ $\mathbf{P}_4 = \Theta + x_4\mathbf{i} + y_4\mathbf{j}$	x_1, y_1 x_2, y_2 x_3, y_3 x_4, y_4 yb_1 yb_2 yb_3	11
m		m+1		3m+2	3m+2

Table 7: Number of Precision Points Related to the Number of Pivots and Tracks Oriented One Parallel to One of the Axes and One Anywhere in the Plane

N° of tracks and their positions	Definition of the tracks $\mathbf{L}_{11}$ and $\mathbf{L}_{12}$	N° of pivots of the second stage	Definition of the pivots P	N° of unknown parameters	N° of precision points h
Two tracks in the plane: one parallel to one of the axes and one anywhere in the plane	$\mathbf{L}_{11} = (\Theta + yb_1\mathbf{j}) \wedge \mathbf{i}$ $\mathbf{L}_{12} = (\Theta + xa_2\mathbf{i}) \wedge (\Theta + yb_2\mathbf{j})$	3	$\mathbf{P}_1 = \Theta + x_1\mathbf{i} + y_1\mathbf{j}$ $\mathbf{P}_2 = \Theta + x_2\mathbf{i} + y_2\mathbf{j}$ $\mathbf{P}_3 = \Theta + x_3\mathbf{i} + y_3\mathbf{j}$	x_1, y_1 x_2, y_2 x_3, y_3 yb_1 xa_2, yb_2	9

N° of tracks	Final Equation
one track	$F[1] = ((Q^0_{ij} \wedge P_1) \barwedge L_{11}) \wedge P_2 \wedge Q_{1h} = P_{11} \wedge P_2 \wedge Q_{1h}$
two tracks	$F[2] = ((((Q^0_{ij} \wedge P_1) \barwedge L_{11}) \wedge P_2) \barwedge L_{12}) \wedge P_3 \wedge Q_{1h} = P_{12} \wedge P_3 \wedge Q_{1h}$
m tracks	$F[m] = P_{1m} \wedge P_{m+1} \wedge Q_{1h}$

Table 8: Final Equations for m Tracks

Note: If the second stage of synthesis has more than four unknown more than four precision points are required. The supplementary precision points firstly must satisfy the condition (1) to find their corresponding rotating points and secondly the condition (2) to find the mechanism parameters required by the second stage.

3. 2. The Determination of the Unknown Parameters in Grassman Chain Mechanism - General Case

With determination of the unknown parameters method of Grassman Chain Mechanisms is an extension of the synthesis method for Grassmann Mechanisms.

Grassmann Chain Mechanisms may be constructed by two, three or any number of mechanisms joined in a chain. Each mechanism has an independent number of tracks and pivots (e. g. the first mechanism could have one track and tree pivots, the second mechanism could have two tracks and four pivots and the third mechanism could have again one track and three pivots).

The construction scheme for Grassmann Chain Mechanisms is shown in the Figure 1.

This part is called determination of unknown parameters, because the method used involves precision lines in addition to precision points. Precision lines are lines which the trajectory must touch or through which it must pass. In the examples, they will be represented as variable points with one of the coordinates fixed.

The determination of the unknown parameters of the second mechanism has also two stages: the first stage of this method calculates the location of the last pivot and second stage calculates the location of the pivots and tracks.

3. 2. 1. Stage 1 for the Second Link Mechanism: Location of the Last Pivot

With reference to the Figure 1 the first stage is the determination of the last pivot $\mathbf{R}_3(\mathbf{R}_{n+2})$.

The Grassmannian expression for the first stage is:

$$\mathbf{Q}_{1h} \wedge \mathbf{R}_{n+2} \wedge \mathbf{Q}_{2g} = \mathbf{0} \qquad (3)$$

where h=1,2 is the number of the precision point of the first link mechanism and g =1, 2, 3, 4, ..., is the number of the precision point of the second link mechanism.

Solve these equations for the coordinates of the pivot $\mathbf{R}_3(\mathbf{R}_{n+2})$.

This part of synthesis requires only two precision points as shown in Table 9.

Definition of the pivot R_{n+2}	N° of unknowns of the first stage
$\mathbf{R}_{n+2} = \Theta + x_{n+2}\mathbf{i} + y_{n+2}\mathbf{j}$	x_{n+2} , y_{n+2}

Table 9: Number of Unknowns of the First Stage

For the same reason as discussed in section 3.1.1. the number of unknowns to be solved in the first stage of the second link mechanism synthesis does not depend on the number of tracks and the other pivots of the mechanism.

To determine unknown parameters of the second mechanism it is necessary to have two precision points and four precision lines.

The method of the first stage:

The stage has only two unknowns. Assume the selected order of the two precision points ($\mathbf{Q}_{21}$ and $\mathbf{Q}_{22}$) and select the corresponding precision points from the first mechanism ($\mathbf{Q}_{11}$ and $\mathbf{Q}_{12}$). Apply equation (3) and solve for the co-ordinates of the pivot $\mathbf{R}_3(\mathbf{R}_{n+2})$.

Suppose there are given four precision lines:

$\mathbf{L}_{p1} = (\Theta + a\mathbf{j}) \wedge x_{Lp1}\mathbf{i}$, $\mathbf{L}_{p2} = (\Theta + b\mathbf{j}) \wedge x_{Lp2}\mathbf{i}$,

$\mathbf{L}_{p3} = (\Theta + c\mathbf{j}) \wedge x_{Lp3}\mathbf{i}$ and $\mathbf{L}_{p4} = (\Theta + d\mathbf{j}) \wedge x_{Lp4}\mathbf{i}$,

where: x_{Lp1}, x_{Lp2}, x_{Lp3} and x_{Lp4} are the x co-ordinates where the trajectory must pass or touch the precision lines.

Assume that the trajectory will pass or touch the precision lines in at least one point. Write this point each precision line with x co-ordinate unknown

$\mathbf{Q}_{Lp1} = \Theta + x_{Lp1}\mathbf{i} + a\mathbf{j}$, $\mathbf{Q}_{Lp2} = \Theta + x_{Lp2} + b\mathbf{j}$,

$\mathbf{Q}_{Lp3} = \Theta + x_{Lp3}\mathbf{i} + c\mathbf{j}$ and $\mathbf{Q}_{Lp4} = \Theta + x_{Lp4} + d\mathbf{j}$.

Apply the condition that the mobile link to the corresponding points from the previous trajectory ($\mathbf{Q}_{13}$, $\mathbf{Q}_{14}$, $\mathbf{Q}_{15}$ and $\mathbf{Q}_{16}$) passes through the last pivot $\mathbf{R}_3(\mathbf{R}_{n+2})$, and solve for their unknown co-ordinates.

$$\begin{aligned} \mathbf{Q}_{13} \wedge \mathbf{R}_3 \wedge \mathbf{Q}_{Lp1} &= \mathbf{0} \\ \mathbf{Q}_{14} \wedge \mathbf{R}_3 \wedge \mathbf{Q}_{Lp2} &= \mathbf{0} \\ \mathbf{Q}_{15} \wedge \mathbf{R}_3 \wedge \mathbf{Q}_{Lp3} &= \mathbf{0} \\ \mathbf{Q}_{16} \wedge \mathbf{R}_3 \wedge \mathbf{Q}_{Lp4} &= \mathbf{0} \end{aligned} \qquad (4)$$

Solve these equations for the x co-ordinates of the precision lines and find the precision points on the respective precision lines, $\mathbf{Q}_{23}$, $\mathbf{Q}_{24}$, $\mathbf{Q}_{25}$ and $\mathbf{Q}_{26}$.

The selection order of the precision points or the precision lines of the second link mechanism with the respective precision points of the first link mechanism determines the trajectory shape and the Chain Mechanism assembly. For each permutation of the precision points or the precision lines the position of the pivot $\mathbf{R}_3(\mathbf{R}_{n+2})$ will be changed as is shown in the Table 10.

3. 2. 2. Stage 2 for the Second Link Mechanism: Location of Pivots and Tracks

The second stage is the determination of the tracks and all other pivots. The number of tracks determines the number of pivots.

The method of the second stage:

With reference to Figure 1 the second stage is the determination of the pivots $\mathbf{R}_1, \ldots, \mathbf{R}_{n+1}$ and the position of the tracks $\mathbf{L}_{21}, \ldots, \mathbf{L}_{2n}$.

Assume that all mobile links from the precision points of the first mechanism $\mathbf{Q}_{1h}$ will pass through the pivot $\mathbf{R}_1$ and then insersect the track $\mathbf{L}_{2n}$ in a sliding point $\mathbf{P}_{2n}$.

The final equation comes from the requirement that the points $\mathbf{P}_{2n}$, $\mathbf{R}_{n+1}$ and $\mathbf{Q}_{2g}$ be collinear that is

$$\mathbf{P}_{2n} \wedge \mathbf{R}_{n+1} \wedge \mathbf{Q}_{2g} = \mathbf{0}$$

where g = 1, 2, 3, 4,..., is the number of the precision point of the second link mechanism and n = 1, 2, 3, 4,... is the number of the track of the second link mechanism. Table 11. shows the final equation for the general case of n tracks starting with one and two tracks.

Table 11: Final Equation for n Tracks

4. Example Using Four Precision Points for Each Mechanism of the Chain Mechanism

Referring to the Table 5 to synthesis the first mechanism it is necessary to have six precision points. As the result of that for the second mechanism it is necessary to have also two precision points and four precision lines. As the problem gave only four precision points for the first mechanisms and two precision points and two precision lines for the second mechanism it will be assume any two of the unknowns for each mechanism.

4.1. The First Link Mechanism

The first mechanism has the following precision points: $\mathbf{Q}_{11} = \Theta + 7\mathbf{i} - \mathbf{j}$, $\mathbf{Q}_{12} = \Theta + \mathbf{i}$, $\mathbf{Q}_{13} = \Theta + 2\mathbf{i} - 2\mathbf{j}$ and $\mathbf{Q}_{14} = \Theta + 5\mathbf{i} - 3\mathbf{j}$.

Assume the position of the track $\mathbf{L}_{11} = (\Theta + 3\mathbf{j}) \wedge \mathbf{i}$.

Referring to the synthesis method presented in the paragraph 3.1. the first mechanism has the following solutions:

$\mathbf{P}_0 = \Theta + 1.25\mathbf{i} - 1.25\mathbf{j}$, $\mathbf{P}_3 = \Theta + 3.25\mathbf{i} - 2.25\mathbf{j}$,

$\mathbf{P}_1 = \Theta + 2.52301\mathbf{i} - 0.427847\mathbf{j}$ and

$\mathbf{P}_2 = \Theta + 4.96599\mathbf{i} - 0.517007\mathbf{j}$.

The first mechanism will plot the trajectory as is show in the figure below.

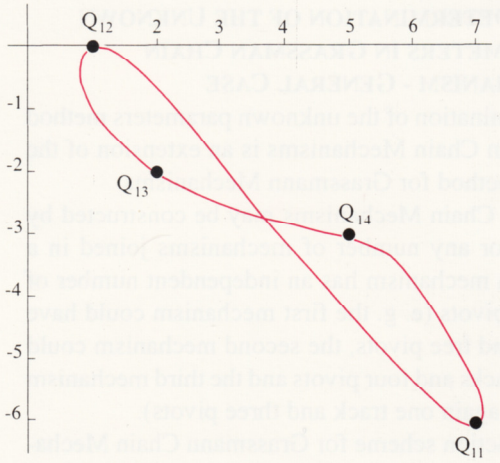

Figure 2: The Trajectory of the First Link Mechanism

4. 2. The Second Link Mechanism

The second mechanism has the following precision points: $\mathbf{Q}_{21} = \Theta + 9\mathbf{i} - 4\mathbf{j}$, $\mathbf{Q}_{22} = \Theta + 7\mathbf{j}$ and the following precision lines:

$\mathbf{L}_{p1} = \Theta + x_{Lp1}\mathbf{i} - 6\mathbf{j}$ and $\mathbf{L}_{p2} = \Theta + x_{Lp2}\mathbf{i} - 5\mathbf{j}$.

Assume the position of the track $\mathbf{L}_{21} = (\Theta + 10\mathbf{j}) \wedge \mathbf{i}$.

Stage 1: Select the precision points $\mathbf{Q}_{21}$ and $\mathbf{Q}_{22}$. For each of the precision points the mobile link must join them and their corresponding precision points on the previous trajectory ($\mathbf{Q}_{11}$ and $\mathbf{Q}_{12}$) and pass through the

Table 10: Number of Changes in the Position of $\mathbf{R}_3$ ($\mathbf{R}_{n+2}$) Related to the Permutation of the Precision Points

N° of precision points	Permutation of the precision points out of two	Changes of the position of $\mathbf{R}_{n+2}$
6	${}^6P_2$	30

Number of tracks	Final Equation
one track	$F[1] = ((\mathbf{Q}_{1i} \wedge \mathbf{R}_1) \barwedge \mathbf{L}_{21}) \wedge \mathbf{R}_2 \wedge \mathbf{Q}_{2i} = \mathbf{P}_{2n} \wedge \mathbf{R}_2 \wedge \mathbf{Q}_{2i}$
two tracks	$F[2] = ((((\mathbf{Q}_{1i} \wedge \mathbf{R}_1) \barwedge \mathbf{L}_{21}) \wedge \mathbf{R}_2) \barwedge \mathbf{L}_{22}) \wedge \mathbf{R}_3 \wedge \mathbf{Q}_{2i} = \mathbf{P}_{22} \wedge \mathbf{R}_3 \wedge \mathbf{Q}_{2i}$
n - tracks	$F[n] = \mathbf{P}_{2n} \wedge \mathbf{R}_{n+1} \wedge \mathbf{Q}_{2i=0}$

last pivot $\mathbf{R}_3$. Apply the equation (3) and the problem gives the solution for $\mathbf{R}_3$.

$\mathbf{Q}_{11} \wedge \mathbf{R}_3 \wedge \mathbf{Q}_{21} = \mathbf{0}$

$\mathbf{Q}_{12} \wedge \mathbf{R}_3 \wedge \mathbf{Q}_{22} = \mathbf{0}$

The problem has one solution for $\mathbf{R}_3$: $\mathbf{R}_3 = \Theta - \mathbf{i} - 14\mathbf{j}$. Select any point on each precision line and write this point with x co-ordinate unknown. Then apply the Grassmannian equation (4) and solve for their unknown co-ordinates.

In this example the Grassmannian equations are:

$\mathbf{Q}_{13} \wedge \mathbf{R}_3 \wedge \mathbf{Q}_{Lp1} = \mathbf{0}$

$\mathbf{Q}_{14} \wedge \mathbf{R}_3 \wedge \mathbf{Q}_{Lp2} = \mathbf{0}$

The problem gives the solutions for the points $\mathbf{Q}_{Lp1}$ and $\mathbf{Q}_{Lp2}$. These points may now be consider precision points and named: $\mathbf{Q}_{23} = \Theta + \mathbf{i} - 6\mathbf{j}$, and $\mathbf{Q}_{24} = \Theta + 3.90909\mathbf{i} - 5\mathbf{j}$.

Stage 2: Calculates the co-ordinates of the pivots $\mathbf{R}_1$ and $\mathbf{R}_2$ by applying the equation F[1] from the Table 11.

$((\mathbf{Q}_{11} \wedge \mathbf{R}_1) \barwedge \mathbf{L}_{21}) \wedge \mathbf{R}_2 \wedge \mathbf{Q}_{21} = \mathbf{P}_{21} \wedge \mathbf{R}_2 \wedge \mathbf{Q}_{21}$

$((\mathbf{Q}_{12} \wedge \mathbf{R}_1) \barwedge \mathbf{L}_{21}) \wedge \mathbf{R}_2 \wedge \mathbf{Q}_{22} = \mathbf{P}_{22} \wedge \mathbf{R}_2 \wedge \mathbf{Q}_{22}$

$((\mathbf{Q}_{13} \wedge \mathbf{R}_1) \barwedge \mathbf{L}_{21}) \wedge \mathbf{R}_2 \wedge \mathbf{Q}_{23} = \mathbf{P}_{23} \wedge \mathbf{R}_2 \wedge \mathbf{Q}_{23}$

$((\mathbf{Q}_{14} \wedge \mathbf{R}_1) \barwedge \mathbf{L}_{21}) \wedge \mathbf{R}_2 \wedge \mathbf{Q}_{24} = \mathbf{P}_{24} \wedge \mathbf{R}_2 \wedge \mathbf{Q}_{24}$

The solution for the pivots $\mathbf{R}_1$ and $\mathbf{R}_2$ is:

$\mathbf{R}_1 = \Theta - 4.47433\mathbf{i} - 3.83747\mathbf{j}$ and

$\mathbf{R}_2 = \Theta + 10.7921\mathbf{i} - 4.55935\mathbf{j}$.

The second mechanism will plot the trajectory as is shown in the figure below.

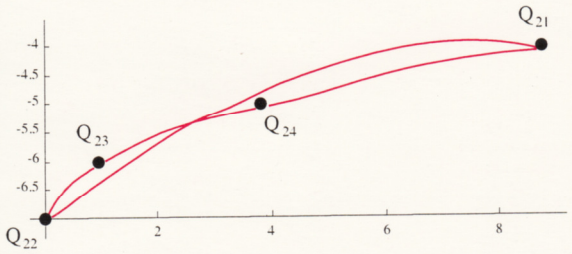

Figure 3: Trajectory of the Second Link Mechanism

5. CONCLUSIONS

The paper has shown a method of synthesis of a class of mechanisms constructed by moving links, rotating on fixed points and intersecting fixed lines using a Grassmannian mathematical formulation and the symbolic computational programme Mathenatica.

REFERENCES

[1] GRASSMANN, H.: *Die Ausdehnungslehre: Vollstandig und in strenger Form bearbeitet,* Berlin, 1862.

[2] WOLFRAM, S.: *Mathematica, a System for doing Mathematics by Computer,* Wolfram Research Inc, Illinois, 1992.

[3] BROWNE, J. M.: The Exterior Calculus and its Application to Engineering, Ph. D Thesis, University of Melbourne, 1979.

[4] WHITEHEAD, A. N.: *A Treatise o Universal Algebra,* Cambridge, 1898.

[5] BITTERFELD, G., BROWNE, J. M., STEINER, J. M.: Application of Grassmann Algebra to Geometry Using Mathematica, AEMC94 Conference, 1994.

Dr. Gloria Bitterfeld
12 Brooks St., South-Oakleigh, 3167
Victoria, Australia
Fax: 61 3 9532 7969
e-mail:stavrou@swin.edu.au

Original scientific paper
Accepted 10. 09. 1997.

ZVONKO ČERIN

Triangles from Central Points

Triangles from Central Points
ABSTRACT
The paper deals with the problem of determining which central points X of the triangle ABC have the property that segments AX, BX, and CX are the sides of a triangle. We shall prove that only thirteen out of hundred and one central points from Kimberling's list have this property. Moreover, the convex hull of ten among these points always consists only of the points having the above mentioned properties.

Trokuti iz središnjih točaka
SAŽETAK
U članku se promatra problem pronalaženja centralnih točaka X trokuta ABC sa svojstvom da su dužine AX, BX i CX stranice nekog trokuta. Pokazuje se da samo trinaest od sto i jedne centralne točke Kimberling-ove liste imaju to svojstvo. Nadalje, konveksna ljuska deset od tih točaka se uvijek sastoji samo od točaka s istim svojstvom.

1. INTRODUCTION

One of the basic problems in triangle geometry is to decide when three given segments are sides of a triangle. The opening chapter of the book *Recent Advances in Geometric Inequalities* by Mitrinović, Pečarić, and Volenec [5] gives an extensive survey of results on this question.

The present article is looking for ways of associating to a triangle ABC a point P of the plane such that segments AP, BP, and CP are always sides of a triangle.

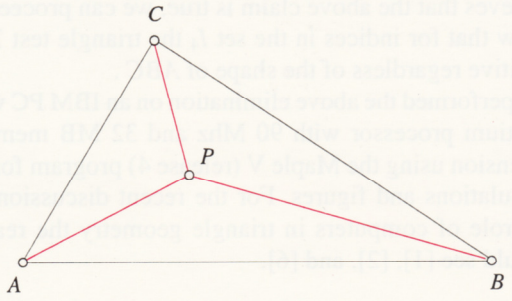

Fig. 1:
When segments AP, BP, and CP are sides of a triangle?

The circumcenter O and the centroid G are easy examples of such points P. Indeed, segments AO, BO, and CO having equal length are sides of an equilateral triangle while the segments AG, BG, and CG being two thirds of medians are sides of a triangle (see [5, p. 20]).

Since O and G are just two of centers or central points of a triangle ABC listed in Table 1 of [3], we can state a problem that we completely answer in this paper.

Problem.
For what natural numbers $\mathbf{i}$ *less than 102 will the central point* X_i *of the triangle ABC from the Kimberling's list have the property that* AX_i, BX_i, *and* CX_i *are sides of a triangle?*

Our main result is the following theorem.

Theorem.
From 101 central points X_i *of the triangle ABC from Kimberling's Table 1, only values 2, 3, 8, 9, 10, 20, 21, 22, 40, 63, 71, 72, and 75 of the index* $\mathbf{i}$ *have the property that* AX_i, BX_i, *and* CX_i *are sides of a triangle regardless of the shape of ABC. For the central point* X_{101} *the only exception are isosceles triangles.*

Let T denote a function that maps each triple (a, b, c) of real numbers to a number
$2a^2b^2 + 2a^2c^2 + 2b^2c^2 - a^4 - b^4 - c^4$.
Since
$T(a,b,c) = (a+b+c)(b+c-a)(a-b+c)(a+b-c)$,
it is clear that positive real numbers a, b, and c are sides of a triangle if and only if $T(a, b, c) > 0$. Let T_i be a short notation for $T(AX_i, BX_i, CX_i)$, where X_i is the i-th central point of ABC and $i = 1,...,101$.

2. PLACEMENT OF ABC

We shall position the triangle ABC in the following fashion with respect to the rectangular coordinate system in order to simplify our calculations. The vertex A is the origin with coordinates (0,0), the vertex B is on the x-axis and has coordinates $(r\,h, 0)$, and the vertex C has coordinates $(g\,r\,u\,/\,k, 2\,f\,g\,r\,/\,k)$, where
$h = f + g$, $k = f\,g - 1$, $u = f^2 - 1$, $v = g^2 - 1$,
$\varphi = f^2 + 1$, $\psi = g^2 + 1$, $\Phi = f^4 + 1$ and $\Psi = g^4 + 1$.
The three parameters r, f, and g are the inradius and the cotangents of half of angles at vertices A and B. Without loss of generality, we can assume that both f and g are larger than 1 (i. e., that angles A and B are acute).

Nice features of this placement are that all central points from Table 1 in [3] have rational functions in f, g, and r as coordinates and that we can easily switch from f, g, and r to side lengths a, b, and c and back with substitutions

$$a = \frac{r f (g^2+1)}{k},\quad b = \frac{r g (f^2+1)}{k},\quad c = r h,$$

$$f = \frac{(b+c)^2 - a^2}{\sqrt{T(a,b,c)}},\quad g = \frac{(a+c)^2 - b^2}{\sqrt{T(a,b,c)}},\quad r = \frac{\sqrt{T(a,b,c)}}{2(a+b+c)}.$$

Moreover, since we use the Cartesian coordinate system, computation of distances of points and all other formulas and techniques of analytic geometry are available and well-known to widest audience. A price to pay for these conveniences is that symmetry has been lost and some expressions are complicated and awkward to print.

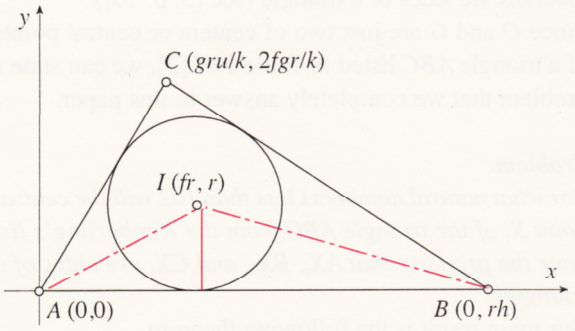

Fig. 2: Parameters are the intriadius and the cotangens of half of angles at vertices A and B.

The third advantage of the above position of the base triangle is that we can easily find coordinates of a point with given trilinears. More precisely, if a point P with coordinates x and y has projections P_a, P_b, and P_c onto the sidelines BC, CA, and AB and $\lambda = PP_a/PP_b$ and $\mu = PP_b/PP_c$, then

$$x = \frac{g\,h(\varphi\mu + u)\,r}{f\,\psi\,\lambda\,\mu + g\,\varphi\,\mu + h\,k}, \quad y = \frac{2\,f\,g\,h\,r}{f\,\psi\,\lambda\,\mu + g\,\varphi\,\mu + h\,k}.$$

This formulas will greatly simplify our exposition because there will be no need to give explicitly coordinates of points but only its first trilinear coordinate. For example, we write $X_6[a]$ to indicate that the symmedian point X_6 has trilinears equal $a:b:c$. Then we use the above formulas with $\lambda = a/b$ and $\mu = b/c$ to get the coordinates

$$\left(\frac{(f\,u\,v + 2g\,\Phi)\,g\,h\,r}{2(f^2\,\Psi + f\,g\,u\,v + g^2\,\Phi)}, \frac{f\,g\,h^2 k\,r}{f^2\,\Psi + f\,g\,u\,v + g^2\,\Phi}\right)$$

of X_6 in our coordinate system.

3. Curve determined by the function T

Let P be a point in the plane of the triangle ABC with coordinates p and q. We can easily find that

$t_{ABC} = T(AP, BP, CP)$ is

$3k^4\,(p^2 + q^2)^2 - 4k^3\,r(p^2 + q^2)\,(k_1 p + k_2 q) -$
$- 2k^2\,r^2\,(k_3 p^2 - k_4 p\,q - k_5 q^2) +$
$+ f^2\,r^3\,k_6\,k_7\,(4kvp - 8gkq - r\,k_6\,k_7),$

where

$k_1 = f\,v + 2g\,u, \quad k_2 = 2f\,g,$

$k_3 = f^2\,\Psi - 2g^2\,\Phi - 2f\,g\,u\,v - 2f^2\,g^2, \quad k_4 = 8f^2\,g\,v,$

$k_5 = f^2\,\Psi + 2f\,g^3\,v + 2g^2\,\Phi - 10f^2\,g^2 - 2f\,g\,u,$

$k_6 = f\,v - 2g$ and $k_7 = g\,h + k.$

It follows that $t_{ABC} = 0$ is the equation of an algebraic curve of order four which represents the boundary of two regions in the plane of ABC. The first region includes the vertices A, B, and C and has the property that a point P belongs to it if and only if segments AP, BP, and CP are not sides of a triangle. The second region which we denote by T_{ABC} is the complement of the first and has the property that a point P belongs to it if and only if segments AP, BP, and CP are sides of a triangle. Hence, the second region gives the solution to the first question in the introduction. The boundary of T_{ABC} (i. e., the curve $T_{ABC} = 0$) is drawn in Figure 3.

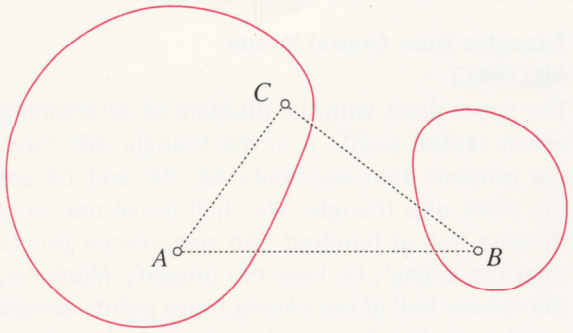

Fig. 3: Graph of the curve $t_{ABC} = 0$ that is the boundary of the region consisting of all points P such that segments AP, BP and CP are sides of a triangle.

Our problem is thus equivalent with the problem of determining which central points from the Kimberling's Table 1 are in the region T_{ABC} for every triangle ABC.

4. Elimination of 87 central points

An easy task is to eliminate 87 central points X_i by exhibiting a triangle for which $T_i \le 0$. In fact, only three triangles with $r = 1$ and (f, g) equal to

$$t_1 = (2,5), \qquad t_2 = (2,20), \qquad t_3 = \left(\frac{101}{100}, \frac{102}{100}\right)$$

will suffice. Indeed, $T_i \le 0$ for the triangle t_j and $i \in I_j$, where $j = 1, 2, 3$,

$I_0 = \{1,...,101\}$,

$I_2 = \{18, 26, 35, 45, 50, 69, 73, 76, 77, 78, 87\}$,

$I_3 = \{29, 48, 49, 64, 66, 67, 70, 74, 84, 92, 93, 98\}$,

$I_4 = \{2, 3, 8, 9, 10, 20, 21, 22, 40, 71, 72, 75, 101\}$, and

$I_1 = I_0 - I_2 - I_3 - I_4$.

The above statement is simple to state but the reader should be aware that there is a lot of work behind it because we must know coordinates of each central point from Kimberling's list. Under the assumption that one believes that the above claim is true, we can proceed to show that for indices in the set I_4 the triangle test T_i is positive regardless of the shape of ABC.

We performed the above elimination on an IBM PC with Pentium processor with 90 Mhz and 32 MB memory extension using the Maple V (release 4) program for all calculations and figures. For the recent discussion on the role of computers in triangle geometry the reader should see [1], [2], and [6].

5. X_2 - Centroid

$X_2[1/a]$ is the intersection of medians which join vertices with midpoints of opposite sides. Hence,

$$T_2 = \frac{16}{9}\,\frac{r^4 g^2 f^2 h^2}{k^2}$$

is always positive.

6. X_3 - CIRCUMCENTER

$X_3[\cos A]$ is the intersection of perpendicular bisectors of sides. It follows that

$$T_3 = \frac{3}{256}\,\frac{r^4(f^2+1)^4(g^2+1)^4}{k^4}$$

is always positive.

7. X_8 - NAGEL POINT

$X_8[(b+c-a)/a]$ is the intersection of lines AA_{ea}, BB_{eb}, and CC_{ec}, where A_{ea}, B_{eb}, and C_{ec} are projections of excenters A_e, B_e, and C_e onto sidelines BC, CA, and AB, respectively. One can easily find

$$T_8 = \frac{16\,r^4(h^2(k^2-k+1)-3k^3)}{k^2}$$

Since $h^2 \geq 4(k+1)$ and $k^2 - k + 1 > 0$, we get that the third factor of T_8 is larger than $k^3 + 4$. Hence, $T_8 > 0$.

8. X_9 - MITTENPUNKT

$X_9[b+c-a]$ is the point of concurrence of the symmedians of the excentral triangle $A_eB_eC_e$. Recall that symmedians are obtained by reflecting the medians about the corresponding interior angle bisectors.
In the standard way we discover that

$$T_9 = \frac{r^4 S_9}{16\,k^4(h^2+k^2+k)^4}, \text{ where}$$

$$S_9 = \sum_0^6 p_i\,k^{6-i}(k+1)^{6-i}h^{2i},\quad p_i = \sum_0^4 q_{ij}\,k^{4-j}, \text{ and}$$

$$[q_{ij}] = \begin{bmatrix} 0 & 0 & -16 & 0 & 0 \\ 0 & -8 & -32 & -32 & 0 \\ 3 & -24 & -8 & -96 & -16 \\ 12 & -20 & 32 & 8 & -64 \\ 18 & 4 & 26 & 168 & -8 \\ 12 & 12 & -12 & 100 & 16 \\ 3 & 4 & -14 & 4 & 3 \end{bmatrix}.$$

It is not clear how one can argue that the polynomial S_9 is always positive. But, the following miraculous method will accomplish this goal.
Write S_9 in terms of f and g. We get a polynomial U_9 with 97 terms. Since both f and g are larger than 1, we shall replace them with $1 + f$ and $1 + g$, where new variables are positive. This substitution will give us a new polynomial V_9 with 279 terms only 9 of which have negative coefficients. If all coefficients were positive, we would be done. In order to get rid of these 9 troublesome terms, we must perform two more substitutions that reflect cases $f \geq g$ and $g \geq f$. Hence, if we replace f with $g + u'$ for $u' \geq 0$, from V_9 we shall get a polynomial P_9 in g and u' with 353 terms and all coefficients positive. Similarly, if we substitute g with $f + v'$ for $v' \geq 0$, from V_9 we shall get a polynomial Q_9 in f and v' also with 353 terms and all coefficients positive. This concludes our proof that $T_9 > 0$.

9. X_{10} - SPIEKER CENTER

$X_{10}[(b+c)/a]$ is the incenter of the medial triangle $A_mB_mC_m$ whose vertices are midpoints of sides. It follows that

$$T_{10} = \frac{r^4 S_{10}}{16\,k^4}, \text{ where}$$

$$S_{10} = (k+3)(3k+1)(k-1)^2h^4 - 2k^2(4k^3-7k^2-38k-31)h^2 - k^4(4k+7)(4k+3).$$

In order to prove that $T_{10} > 0$ we apply the method of proof for X_9. Polynomials U_{10}, V_{10}, and P_{10}, are of medium size having 29, 71, and 77 terms.

10. X_{21} - SCHIFFLER POINT

$X_{21}[(b+c-a)/(b+c)]$ is the point of concurrence of Euler lines of triangles BCX_1, CAX_1, and ABX_1, where X_1 is the incenter of ABC. Recall that the line joining the centroid and the circumcenter of a scalene triangle ABC is called the *Euler line of* ABC.
It follows that

$$T_{21} = \frac{16r^4(k+1)^2(f^2h^2-k^2)^2(g^2h^2-k^2)^2(h^2+k^2+4k)}{k^3(3h^2+3k^2+8k)^4}$$

so T_{21} is clearly always positive.

11. X_{63} - ISOGONAL CONJUGATE OF THE CRUCIAL POINT

$X_{63}[b^2+c^2-a^2]$ is the point of intersection of the line joining X_1 (incenter) with X_{21} (Schiffler point) and the line joining X_8 (Nagel point) with X_{20} (De Longchamps point - reflection of the orthocenter at the circumcenter).
In the usual way we find that

$$T_{63} = \frac{32r^4 S_{63}}{k^3(h^2+k^2+4k)^4},$$

where S_{63} is a polynomial of degree 10 in h with coefficients polynomials in k of degree at most 11. The polynomial U_{63} has 72 terms while V_{63} has 162 terms and all coefficients positive. Hence, $T_{63} > 0$.

12. CENTRAL POINT X_{71}

$X_{71}[a(b+c)(b^2+c^2-a^2)]$ is the point of intersection of the line joining X_4 (orthocenter) with X_9 (Mittenpunkt) and the line joining X_6 (Grebe-Lemoine or symmedian point) with X_{31} (2nd Power point). As above, we find that

$$T_{71} = \frac{r^4 S_{71}}{16\,k^4(h^4+k^4+4h^2k^2+7h^2k+3k^3+2k^2)^4},$$

where S_{71} is a polynomial of degree 20 in h with coefficients polynomials in k of degree at most 22. The polynomial U_{71} has 265 terms while V_{71} has 615 terms and only 8 negative coefficients. The polynomials P_{71} and Q_{71} both have 821 terms and all coefficients positive. Hence, $T_{71} > 0$.

13. CENTRAL POINT X_{72}

$X_{72}[(b+c)(b^2+c^2-a^2)]$ is the point of intersection of the line joining X_1 (incenter) with X_6 (Grebe-Lemoine point) and the line joining X_4 (orthocenter) with X_8

(Nagel point). By standard procedure we find that

$$T_{72} = \frac{r^4 S_{72}}{k^2 (f^2+1)^2 (g^2+1)^2}, \text{ where}$$

$$S_{72} = (k^2 + 28k + 4)\, h^6 + k\,(k^3 - 4k^2 - 65k - 80)\, h^4 + \\ + 2k\,(2k^4 - 6k^3 - 55k^2 - 104k - 64)\, h^2 + \\ + k^4\,(5k + 8)\,(4k^2 + 11k + 8).$$

The polynomial U_{72} has 38 terms while V_{72} has 78 terms and all coefficients positive. Hence, $T_{72} > 0$.

14. X_{75} - ISOGONAL CONJUGATE OF THE 2ND POWER POINT

$X_{75}[1/a^2]$ is the point of intersection of the line joining X_7 (Gergonne point) with X_8 (Nagel point) and the line joining X_{10} (Spieker center) with X_{76} (3rd Brocard point - isogonal conjugate of the 3rd Power point). By usual method we find that

$$T_{75} = \frac{r^4 f^2 g^2 h^2 S_{75}}{k^2 (h^2k^2 + 3h^2k + k^3 + h^2 + k^2)^4},$$

where S_{75} is a polynomial of degree 10 in h with coefficients polynomials in k of degree at most 13. The polynomial U_{75} has 109 terms while V_{75} has 268 terms and only 15 negative coefficients. The polynomials P_{75} and Q_{75} both have 319 terms and all coefficients positive. Hence, $T_{75} > 0$.

15. CENTRAL POINT X_{101}

$X_{101}[a/(b-c)]$ is the point on the circumcircle in which intersect the line joining X_{71} with X_{74} (isogonal conjugate of the intersection of Euler line with line at infinity) and the line joining X_{10} (Spieker center) with X_{98} (Tarry point). In the usual way we find that

$$T_{101} = \frac{r^4 m_1 m_2 m_3 (f-g)^2 (fk-h)^2 (gk-h)^2}{16k^4 (h^4 + k^4 - h^2k^2 - 4h^2k + 2k^3 - 3h^2 + k^2)^2}$$

where

$$m_1 = 3f^2g^2 + f^3g + 2f^2 + g^2 + fg,$$

$$m_2 = 3f^2g^2 + fg^3 + f^2 + 2g^2 + fg,$$

$$m_3 = (1+3k)h^2 + (1+k)k^2.$$

From this it is obvious that $T_{101} > 0$ in all cases except when ABC is isosceles.

16. X_{40} - CIRCUMCENTER OF THE EXTRIANGLE

$X_{40}[(b+c)\,((b-c)^2 + a(b+c) - a^2) - a^3]$ is the point of concurrence of the perpendiculars from the excenters to the respective sides. Then

$$T_{40} = \frac{r^4 S_{40}}{16k^4}, \text{ where}$$

$$S_{40} = 3h^8 + (4k^2 - 24k - 8)\, h^6 - \\ - (14k^4 + 24k^3 - 56k^2 - 32k + 16)\, h^4 + \\ + 4k^2\,(k+2)\,(k^3 + 12k^2 + 2k - 4)\, h^2 + \\ + k^4\,(k^2 - 4k - 4)\,(3k^2 + 4k + 4).$$

The polynomial U_{40} has 41 terms while V_{40} has 71 terms and only 8 negative coefficients. Consider V_{40} as a polynomial of degree 8 in g. It is amazing that coefficients of g^5, g^4, and g^3 are polynomials in f with all coefficients positive. Even greater miracle is that quadratic trinomials associated to the first three terms (corresponding to powers 8, 7, and 6 with g^6 factored out) and the last three terms (quadratic part of V_{40}) both have positive leading coefficients and negative discriminants. We conclude that $T_{40} > 0$.

17. X_{20} - DE LONGCHAMPS POINT

When we apply the above method of proof to De Longchamps point X_{20} or to Exeter point X_{22} it does not work so that we must do something else. The idea is to position the triangle ABC so that the circumcenter O is the origin, the vertex C is $[r, 0]$ where r denotes the circumradius, and positions of the vertices A and B are determined by parameters f and g which are tangents of half of angles that OA and OB make with the x-axis OC. Without loss of generality we can assume that $f > 0$ and $g > 0$. With this placement the triangle test T_{20} is an expression that will clearly always be positive.

The coordinates of A and B are

$$\left(\frac{r(1-f^2)}{1+f^2}, \frac{2rf}{1+f^2}\right) \text{ and } \left(\frac{r(1-g^2)}{1+g^2}, \frac{2rg}{1+g^2}\right).$$

It follows that X_{20} has coordinates

$$\left(\frac{r(k^2+4k-h^2)}{(fh-k)(gh-k)}, \frac{-2rh(k+2)}{(fh-k)(gh-k)}\right),$$

while

$$T_{20} = \frac{64r^4((h^2+3)(k+3)^2 + f^2g^2)}{(fh-k)^2(gh-k)^2}.$$

18. X_{22} - EXETER POINT

$X_{22}[b^4 + c^4 - a^4]$ is the point of concurrence of lines A_gA_t, B_gB_t, and C_gC_t, where A_g is the intersection different from A of the median line AA_m with the circumcircle and A_t is the intersection of tangents to the circumcircle at B and C and with B_g, C_g, B_t and C_t defined analogously.

In order to prove that $T_{22} > 0$ we use the same placement of the base triangle ABC as in the proof for X_{20}.

Since the equation of the circumcircle is $x^2 + y^2 = r^2$, one can find coordinates of A_g, B_g, and C_g by solving quadratic equations. The coordinates of A_t, B_t, and C_t are

$$(r, rg), \qquad (r, rf), \qquad \left(\frac{-rk}{k+2}, \frac{rh}{k+2}\right).$$

It follows that X_{22} has coordinates

$$\left(\frac{r(k^2+4k-h^2)}{h^2+k^2-4k-8}, \frac{-2rh(k+2)}{h^2+k^2-4k-8}\right), \text{ while}$$

$$T_{22} = \frac{64r^4 S_{22}}{(h^2+k^2-4k-8)^4}, \text{ where}$$

$$S_{22} = (k+3)^2 h^6 + 2(k+1)\,(k^3 + k^2 - 16k - 34)\, h^4 + \\ + (k^4 - 4k^3 + 112k + 224)\,(k+1)^2 h^2 + \\ + 16\,(k^3 - 12k - 20)\,(k+1)^3.$$

If we consider S_{22} as a polynomial in f and g we get a

polynomial W_{22} with 27 terms. When we replace f with $g + u$ in W_{22} we obtain a polynomial of order 8 in u whose coefficients are polynomials in g with all coefficients positive. Hence, W_{22} is positive when $f \geq g$. In a similar way we see that it is also positive when $g \geq f$. Hence, $T_{22} > 0$.

19. NEW TRIANGULAR TRIPLES

We can now compute distances AX_i, BX_i, and CX_i for last twelve central points from our theorem to get the following corollary.

Most interesting points, lines, circles, curves,... associated with the triangle ABC are expressions that involve symmetric functions of lengths a, b, and c of sides BC, CA, AB that we denote as follows.

$s = a + b + c$, $t = bc + ca + ab$, $m = abc$,
$s_a = -a + b + c$, $s_b = a - b + c$, $s_c = a + b - c$,
$m_a = bc$, $m_b = ca$, $m_c = ab$,
$d_a = b - c$, $d_b = c - a$, $d_c = a - b$,
$z_a = b + c$, $z_b = c + a$, $z_c = a + b$.

For each $k \geq 2$, s_{ka}, s_{kb}, and s_{kc} are derived from s_a, s_b and s_c with the substitution $a = a^k$, $b = b^k$, $c = c^k$. In a similar fashion we can define analogous expressions using letters m, d, t and z.

For an expression f, let $[f]$ denote a triple $(f, \varphi(f), \psi(f))$, where $\varphi(f)$ and $\psi(f)$ are cyclic permutations of f. For example, if $f = \sin A$ and $g = b + c$, then
$[f] = (\sin A, \sin B, \sin C)$ and $[g] = (b + c, c + a, a + b)$.
Let us call a triple $[a]$ of real numbers *triangular* provided a, b, and c are sides of a triangle.

COROLLARY

If the triple $[a]$ *is triangular, then the triples*

$$\left[\sqrt{a(a z_a + 2d_a^2 - a^2)}\right], \left[\sqrt{2a^2 z_{2a} - d_a^4 - a^4}\right],$$

$$\left[\sqrt{z_a(z_{2a} - m_a) + a(2z_{2a} - m_a) - a^3}\right],$$

$$\left[\sqrt{a^6 - 3a^2 d_{2a}^2 + 2d_{2a}^2 z_{2a}}\right],$$

$$\left[\sqrt{a m_a z_a + a^2(2z_{2a} - m_a) - a^4 - d_a^2 z_{2a}}\right],$$

$$\left[\sqrt{d_{2a}^2 z_{2a}^2 - 2a^2 d_{2a}^2 z_{2a} + 2a^6 z_{2a} - a^8}\right],$$

$$\left[\sqrt{m_a(a^4 - 2a^2 d_a^2 + d_{2a}^2)}\right],$$

$$\left[\sqrt{m_a(a^2 d_{2a}^2 + a^4 z_a^2 - a^6 - d_a^2 d_{2a}^2)}\right],$$

$$\left[m_a(a^5 z_a^3 + a^6(2z_{2a} - m_a) - a^8 - a^7 z_a - a^4 z_a^2(z_{2a} - 3m_a) + a^3 d_a^3 d_{2a} + a^2 d_{2a}^2 m_a - a d_a d_{2a}^3 - d_a^2 d_{2a}^2)^{\frac{1}{2}}\right],$$

$$\left[(3a d_a^2 m_a z_a + a^2 d_a^2(3m_a + z_{2a}) + a^3 m_a z_a + a^4(m_a + z_{2a}) - a^6 - d_a^4 z_a^2)^{\frac{1}{2}}\right],$$

$$\left[a\sqrt{z_a^2(z_{2a} - m_a) - am}\right], \text{ and (with } ABC \text{ not isosceles) } \left[m_a | d_a |\right] \text{ are also triangular.}$$

20. NAGEL POINT - SECOND PROOF

In this and the following sections we shall give alternative proofs for all fourteen central points using more traditional methods of proof. Of course, again we shall suppress most details because they are awkward to print.

We first find that $AX_8^2 = a(a s_a + 2d_a^2)/s$. It follows that

$$T_8 = \frac{T(a,b,c)(s^3 - 24m)}{s^3} \text{ is positive since } s^3 \geq 27m.$$

21. MITTENPUNKT - SECOND PROOF

Since $AX_9^2 = (a^2(s_{2a} + z_{2a}) - d_a^4)/(s_2 - 2t)^2$, we obtain $T_9 = S_9 / q^4$, where S_9 is a polynomial
$(4R^2 - r^2)(12R^2 + 16rR + r^2)\sigma^4 -$
$- 2q^3 r(4R^2 - 8rR + r^2)\sigma^2 - q^6 r^2$, and $q = r + 4R$.

Here, σ is the semi-perimeter, r is the inradius, and R is the circumradius. In order to derive this representation for S_9 we first write numerator and denominator of $T([AX_9])$ in terms of elementary symmetric polynomials s, t, and m and then use the fact [5, p.7] that lengths of sides a, b, and c are roots of the polynomial
$x^3 - 2\sigma x^2 + (\sigma^2 + q r)x - 4R\sigma$.

The conclusion that $S_9 > 0$ is argued as follows. Let

$$l_{\pm} = 2R^2 + 10R - r^2 \pm 2(R - 2r)\sqrt{R^2 - 2Rr}.$$

It is well-known (see [5, p. 2]) that $l_- \leq \sigma^2 \leq l_+$. Hence, it suffices to show that the polynomial S_9 is positive on the segment $[l_-, l_+]$. In other words, it suffices to show that for every number p in the interior of the segment $[l_-, l_+]$, replacing σ^4 and σ^2 with p^2 and p in S_9 we obtain positive value.

Any point p from this segment different from l_- and l_+ can be represented as $(l_- + k l_+)/(k + 1)$ for some positive real number k. When we compute S_9 at p or at l_- and l_+ and substitute $R = 2r + \varepsilon$, where $\varepsilon \geq 0$ (recall that $R \geq 2r$), we obtain $\lambda(M - N)$, where expressions λ, M, and N are all positive. But, on can check that $M^2 - N^2$ is positive so that our claim follows.

22. SPIEKER CENTER AND DE LONGCHAMPS POINT – SECOND PROOF

Since $AX_{10}^2 = (a s_{2a} + s(z_{2a} - m_a))/(4s)$, we have $T_{10} = S_{10} / 16$, where S_{10} denotes the polynomial
$3\sigma^4 - 2r(4q - 35r)\sigma^2 - r^2(4q - r)(4q + 3r)$.

We continue as in the above proof to show that $S_{10} > 0$ for every triangle.

The identical approach applies to the central points X_{20} (De Longchamps point), X_{22} (Exeter point), X_{40}, X_{63}, X_{71}, X_{72}, and X_{75}.

23. SCHIFFLER POINT – SECOND PROOF

This time
$AX_{21}^2 =$
$m z_a^2(a^2(s_{2a} - m_a) + a m_a z_a + s_b s_c z_{2a})/(s(s^3 - 4st + 5m)^2)$,

so that the sign of T_{21} depends only on the sign of $8r\,\sigma\,(r+R)$ which is clearly positive.

24. CENTRAL POINT X_{101} – SECOND PROOF

Since $AX_{101}{}^2 = m_a{}^2\, d_a{}^2\, (s_4 + m\, s - a^3\, z_a - b^3\, z_b - c^3\, z_c)$, we immediately get

$$T_{101} = \frac{d_a^2\,(a\,s_a + m_a)\,d_b^2\,(a\,s_b + m_b)\,d_c^2\,(a\,s_c + m_c)}{(s^4 - 5\,s^2 t + 4t^2 + 6\,m\,s)^2}$$

is always positive unless ABC is isosceles.

25. CONVEX HULL OF THE POLYNOMIAL GROUP

The results in the previous sections might be quite inadequate to some readers because it is clear from the Section 3 that the region T_{ABC} in the plane of the triangle ABC consisting of all points P such that segments AP, BP, and $C\,P$ are sides of a triangle is rather large while we have only found thirteen points that always belong to this region. In this section we shall improve our results by showing that the same technique applies to prove that the convex hull of the central points X_2, X_3, X_8, X_9, X_{20}, X_{21}, X_{63}, X_{71}, X_{72}, and X_{75} always belongs to the region T_{ABC}. Notice that these are precisely the points for which our argument involving polynomials with all coefficients positive worked.

Theorem

For any triangle ABC the convex hull of central points X_2, X_3, X_8, X_9, X_{20}, X_{21}, X_{63}, X_{71}, X_{72}, and X_{75} consists only of points P with the property that the segments AP, BP, and CP are sides of a triangle.

Proof.

We shall only give outlines for the proof that the segment GO joining the centroid G with the circumcenter O and the triangle GON with vertices G, O, and the Nagel point N both lie in the region T_{ABC}. In a similar fashion one can show that any segment and any triangle on any two and on any three of the ten central points listed in the statement of the theorem have the same property. Of course, it is impossible to give all details of our proofs because in some cases we get polynomials with hundreds of terms so that without computers this approach is a hard task. Since most readers might make a standard mistake in thinking that everything about triangles belongs to elementary mathematics (whatever this might mean), it would be interesting to the author to see their "elementary" proofs of our results.

A point P in the interior of the segment GO has coordinates $[p, q]$, where

$p = r\,(3h\,k\,x + 2f\,v + 4g\,u)\,/\,(6k(x+1))$,

$q = r\,(8f\,g + 3(h^2 - k^2)\,x)\,/\,(12k(x+1))$ and x is a positive real number.

When we substitute these values into the polynomial t_{ABC} we obtain $r^4\,S_{GO}\,/\,(6912\,(x+1)^4)$, where

$S_{GO} = \sum_{i=0}^{4} k_i\,x^i$ and each coefficient k_i is a polynomial in f and g. The replacement of f with $1+f$ and g with $1+g$ in k_i for $i=0,\ldots,4$ leads to polynomials with all coefficients positive which completes our proof for this very simple case. For most other segments with ends among ten points from the statement we must also perform substitutions $f = g + u'$ and $g = f + v'$ (with u', $v' \geq 0$) in order to get polynomials with all coefficients positive.

Let us now consider the triangle GON. An arbitrary point P in its interior has coordinates $[p, q]$, where

$p = r\,(6\,(f\,\psi - 2g)\,x\,y + 2(f\,v + 2g\,u)\,x + 3h\,k\,y + 2f\,v + 4g\,u)\,/\,(6k\,(x+1)(y+1))$,

$q = r\,(24x\,y + 8f\,g\,x + 3(h^2 - k^2)\,y + 8f\,g)\,/\,/\,(12k\,(x+1)(y+1))$,

and x and y are positive real numbers. When we substitute these values into the polynomial t_{ABC} we obtain $r^4\,S_{GON}\,/\,(6912\,(x+1)^4\,(y+1)^4)$, where S_{GON} is a polynomial of order 8 in x and y and whose coefficients k_i $(i=0,\ldots,24)$ are polynomials in f and g. The replacement of f with $1+f$ and g with $1+g$ in k_i for $i=0,\ldots,24$ leads to polynomials with almost all coefficients positive. However, after we perform substitutions $f = g + u'$ and $g = f + v'$ (with u', $v' \geq 0$) we obtain polynomials with all coefficients positive which completes our proof. For other triangles the same strategy always applies but with far more complicated polynomials (with several hundreds of terms and very large coefficients).

REFERENCES

[1] DAVIS, J. P.: The rise, fall, and possible transfiguration of triangle geometry: A mini-history, American Mathematical Monthly 102 (1995), 205–214.

[2] GALE, D.: From Euclid to Descartes to Mathematica to oblivion?, Math. Intellingencer 14 (1992), 68–69.

[3] KIMBERLING, C.: Central points and central lines in the plane of a triangle, Mathematics Magazine, 67 (1994), 163–187.

[4] KIMBERLING, C.: Point-to-line distances in the plane of a triangle, Rocky Mountain Journal of Math, 24 (1994), 1009–1026.

[5] MITRINOVIĆ, D. S., PEČARIĆ, J. E., VOLENEC, V.: *Recent Advances in Geometric Inequalities*, Kluwer Academic Publishers, Dordrecht, 1989.

[6] OLDKNOW, A.: Computer aided research into triangle geometry, Math. Gaz. 80 (1996), 263–274.

Dr. sc. Zvonko Čerin,
Kopernikova 7,
10 020 Zagreb, CROATIA, Europe
email: CERIN@CROMATH.MATH.HR

Originelle wissenschaftliche Arbeit
Angenomen 08. 10.1997

IVANKA BABIĆ, BRANKO KUČINIĆ

Hyperbolische Perspektive I

Dieser Artikel ist dem Herrn Prof. Akademiker Dr. sc. S. Bilinski gewidmet, weil er in unseren Kreisen die Forschungen über das Projizieren im hyperbo-lischen H^3 - Raum inizierte und weil er unsen Professor war.

Hyperbolic Perspective I
ABSTRACT
In the hyperbolic space the central projection is considered, adjusted to the perspective, by defining the image plane and centre of projection, and the reference plane perpendicular to the image plane. This is the analogy of the so called piercing point method in the Euclidean space supplemented by indefinitely distant elements. The analogue of the method of Monge in H3-space realised on M-model enables necessary constructive procedures. The position and metric relations associated with the reference plane are also worked out thoroughly. Thus, the whole procedure is prepared to be applied.
Basic differences from the perspective of Euclidean space are: h-horizon is hyperbola, there is avoidable hyperbola instead of avoidable line, and the pencils of parallel lines in the plane (1 can be projected into the elliptic, parabolic and hyperbolic pencils (Theorem 3).
Keywords:
hyperbolic space, H-model, central projection, perspective, piercing point method

Hiperbolička perspektiva I
SAŽETAK
U hiperboličkom prostoru razmatra se centralno projiciranje, prilagođeno za perspektivu, tako da se definira ravnina slike i centar projiciranja, te osnovna ravnina okomita na ravninu slike. Ovo je analogija tzv. metode probodišta u euklidskom prostoru nadopunjenom neizmjerno dalekim elementima. Analogon Mongeove metode u H^3-prostoru ostvaren na M-modelu omogućuje potrebne konstruktivne postupke. Razrađeni su položajni i metrički odnosi vezani uz osnovnu ravninu. Time je čitav postupak pripremljen za primjenu.
Osnovne razlike od perspektive euklidskog prostora su: *h* - horizont je hiperbola, postoji *izbježna hiperbola* umjesto izbježnog pravca, a pramenovi paralelnih pravaca ravnine P_1 mogu se preslikati u eliptičke, paraboličke ili hiperboličke pramenove (Teorem 3).
Ključne riječi:
hiperbolički prostor, M-model, centralna projekcija, perspektiva, metoda probodišta

In dieser Arbeit wird das Problem der Konstruktion einer Perspektive im M-Modell des hyperbolischen H^3- Raumes erforscht. Das Grundziel der Arbeit ist die Perspektivbilder von der Reel-objekten zu konstruiren, die auch selbst reelle Bilder sind. Die Methode, wodurch das erreicht wird, ist die Durchschnittmethode. Damit die Zentralprojektion zur Perspektive wird, soll man die Elemente für die Konstruktion des perspektivischen Bildes auf einer Bildebene so organiesieren, daß die Eindeutigkeit erreicht wird. Eine Perspektive ensteht dabei wie im euklidischen Raum durch Projektion eines Objekts aus einem Punkt auf eine Bildebene. Dabei werden die Ergebnisse über die Zentralprojektion aus [8] und [9], über die darstellende Geometrie im hyperbolischen H^3 - Raum aus [1], [3] , [4] und über das M-Modell aus [2] benützt.
Es sei im H^3 -Raum ein Paar zueinander senkrechten – Ebenen Π_1 und Π_2 und ein eigentlicher Punkt O als Projektionszentrum ($O \notin \Pi_1$, $O \notin \Pi_2$) angegeben. Π_1 und Π_2 werden als Grundriß bzw. Aufrißebene für die Mongeer Methode gemäß [1] , [3] , [4] verwendet. Weiters bezeichen wir Π_1 auch als Grundebene und Π_2 ist die Bildebene für die Zentralprojektion. Damit wird die Zentralprojektion eines Raumteiles auf die Bildebene bzw. Aufrißebene Π_2 eindeutig definiert, die analog zur Durchschnittmethode im euklidischen Raum ist [7].
Die Projektionsstrahlen, die die Bildebene in den eigentlichen Punkten durchstoßen, bilden das Innere des Parallelkegels Φ, dessen Spitze das Projektionszentrum O, der sogennanten Augpunkt, der Perspektive ist. Der Abstand d des Zentrums O von der Bildebene Π_2 ist die Paralleldistanz (Abb.1.: im Profil die Ebene Γ). Das bedeutet, daß nur von solchen Objekten die sich innerhalb des Parallelkegels Φ befinden , ein reelles Bild existiert. Wegen der Eindeutigkeit soll die Seite des Parallelkegels Φ, die gegensätzlich der Ebene Π_2 in

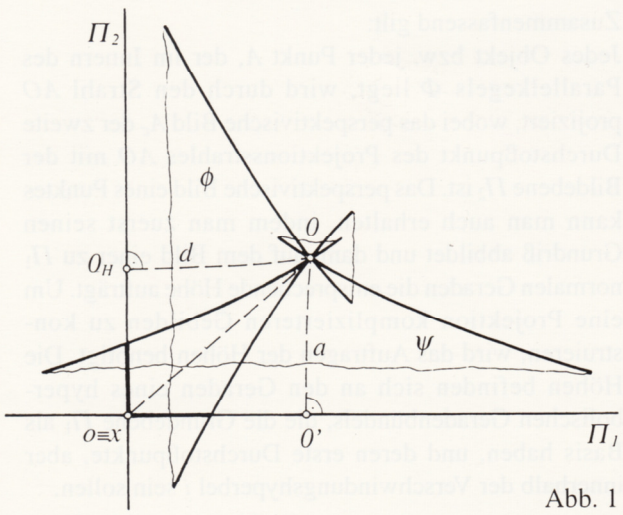

Abb. 1

bezug O ist, vernachläßigt werden. Analog zum euklidischen bezeichnet man den Parallelkegel Φ als *Verschwindungskegel*, weil seine ganze Oberfläche auf die Grenzpunkte der Bildebene Π_2 projiziert wird.

Analog gibt es einen Parallelkegel Y aller Parallelen zu P_1 mit der Spitze O und der Distanz a zu P_1. Die Erzeugende von Y projizieren die Grenzpunkte der Grundebene P_1. Auch hier soll die Seite des Parallelkegels Y, die gegensätzlich der Ebene P_1 in bezug O ist, vernachläßigt werden. Für die weitere Unteruchungen ist es wichtig die Schnittkurve des Parallelkegels Y mit der P_2-Ebene zu bestimmen.

Definition

Die Schnittkurve des Parallelkegels Ψ und der Bildebene Π_2 nennt man die h - Horizont.

Das ist die Menge der Punkte der P_2-Ebene, die die perspektivischen Bilder von den Grenzpunkten der Ebene P_1 sind. Diese Schnittkurve ist offensichtlich ein Hyperbelast h, wobei der andere Ast dieser Hyperbel reell sein kann oder nicht. Sie hat jedoch keinerlei Bedeutung, da die andere Seite des Parallelkegels Y vernachläßigt wird.

Die wichtige Rolle hat uch die Schnittkurve des Verschwindungskegels Φ mit der Π_1-Ebene. Man kann beweisen, daß diese Kurve auch eine Hyperbel ist.

Definition

Die Schnittkurve des Verschwindungskegels Φ und der Grundebene Π_1 nennt man die Verschwindungshyperbel und bezeichnet man mit i.

Die Verschwindungshyperbel i ist die Menge von den Punkten der P_1-Ebene, deren perspektivischen Bilder die Grenzpunkte der Bildebene P_2 sind.

Die Grundfläche von Objekten mit reellen perspektiwischen Bilder müssen im Innern der Verschwindungshyperbel i liegen.

Der reelle Schnitt der Parallelkegel Φ und Ψ mit der gemeinsamen Spitze O besteht aus zwei Erzeugenden durch O, die parallel zur x-Achse sind (Abb. 1).

Zusammenfassend gilt:

Jedes Objekt bzw. jeder Punkt A, der im Innern des Parallelkegels Φ liegt, wird durch den Strahl AO projiziert, wobei das perspektivische Bild A_c der zweite Durchstoßpunkt des Projektionsstrahles AO mit der Bildebene Π_2 ist. Das perspektivische Bild eines Punktes kann man auch erhalten, indem man zuerst seinen Grundriß abbildet und dann auf dem Bild einer zu Π_1 normalen Geraden die entsprechende Höhe aufträgt. Um eine Projektion komplizierteren Gebilden zu konstruieren, wird das Auftragen der Höhen benötigt. Die Höhen befinden sich an den Geraden eines hyperbolischen Geradenbündels, die die Grundebene Π_1 als Basis haben, und deren erste Durchstoßpunkte, aber innerhalb der Verschwindungshyperbel i sein sollen.

Im M-Modell [2] wird das hyperbolische H^3-Raum in der Möbius-Ebene auf folgende Weise interpretiert:

Die Kreise und die Geraden der Möbius-Ebene sind die Randbilder der Ebenen des H^3- Raumes.

Die Paare verschiedener Punkte der Möbius-Ebene sind die Bilder der Grenzpunkte der Geraden des H^3-Raumes.

Ein geordnetes Punktetripel der Möbius-Ebene bestimmt das Bild eines Punktes auf der Trägergeraden des H^3 -Raumes, wobei die erste zwei Punkte die Bilder der Grenzpunkte dieser Trägergeraden sind.

Die Inzidenz ist im gewöhnlichen Sinne: eine Gerade gehört der Ebene an, wenn ihre Grenzpunkte mit dem Randbild der Ebene inzident sind.

Wir betrachten das Analogon der Mongeer Methode des orthogonalen Projizierens auf ein Paar zueinander senkrechten Ebenen Π_1 und Π_2 im M-Modell [1] , [3], [4]. Eine so realisierte konstruktive Bearbeitung des H^3-Raumes läßt die Konstruktionen mit dem euklidischen Lineal und dem Zirkel zu.

Die Bildebene Π_2, die Grundebene Π_1, die senkrecht zur Π_2-Ebene ist, und der Augpunkt O, wurden auf dem Bild 1a. im M-Modell dargestellt. Die Schnittgerade der Grundebene Π_1 und der Bildebene Π_2 ist die Spurgerade $o{\equiv}x$ von der Ebene Π_1. Die von den Normalen auf Π_1 und Π_2 durch O aufgespannte Ebene Γ schneidet die Ebene Π_1 längs der Geraden g_1 und die Ebene Π_2 längs der Geraden g_c . g_1 ist senkrecht zur Spurgeraden $o{\equiv}x$ durch den Grundriß $\overline{O}'$ des Augpunktes O. g_c ist senkrecht auch zur Spurgeraden $o{\equiv}x$ durch den Aufriß $O''{\equiv}O_H$, den sogennanten Hauptpunkt.

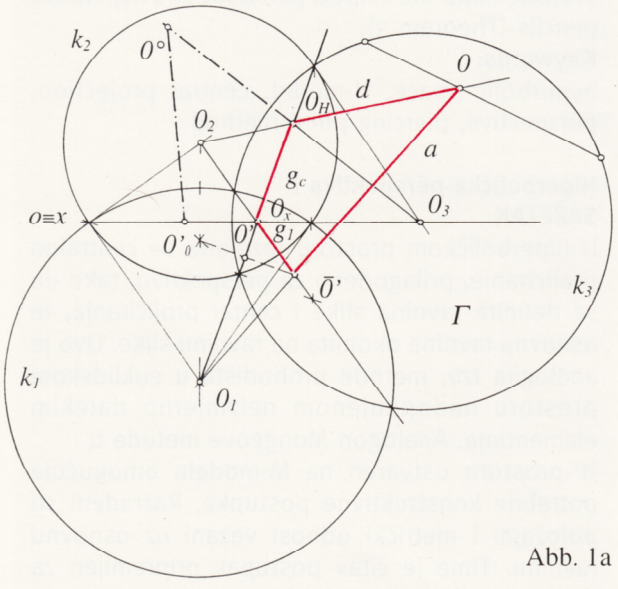

Abb. 1a

Nach der Rotation der Grundebene Π_1 um die Spurgerade $o{\equiv}x$ in die Bildebene Π_2 nach dem dargestellten Verfahren in [3], liegen die Punkte O' und O_H auf derselben Geraden $g_c \equiv g_1$ der Bildebene. Wahre Länge der Distanzen d und a sind auf dem umgeklappten Lamberter Viereck $O\ O_H\ O_x O'$ in die Bildebene Π_2 zu sehen, dabei gilt:

$$d_o = O_o O_H \quad a_o = O_o O_o' \text{ (Abb.1a).}$$

Die Verschwindungshyperbel i wird so konstruiert, daß man die ersten Durchstoßpunkte der Kegelserzeugende Φ nach der Konstruktionen in [3] bestimmt. Da es sich um einen Verschwindungskegel handelt, deckt sich der Aufriß seiner Basis mit k_2 (Abb.2). Die Achse dieses Kegels ist zu Π_1 überparallel und seine vier Erzeugende sind zu Π_1 parallel (mit der Distanz a). Die Grenzpunkte der zweien zur x-Achse parallel Erzeugenden sind gleichzeitig die reellen zwei Grenzpunkte des Kegelschnitts i, der noch zwei verschiedene Grenzpunkte hat. Daraus geht hervor, daß diese Kurve 2. Ordnung gemäß [5] eine Hyperbel ist.

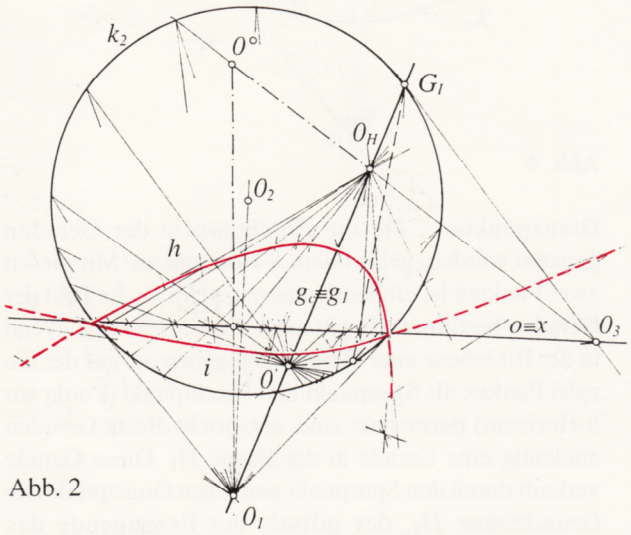

Abb. 2

In der Bildebene wird der h-Horizont so bestimmt, daß die zweiten Durchstoßpunkte der Kegelserzeugende Ψ auf Grund [3] konstruiert werden (Abb.2). In diesem Fall ist der Grundriß der Kegelbasis Ψ mit der Bildebene Π_2 gedeckt.

GERADEN DER GRUNDEBENE Π_1

In der Grundebene Π_1, die gleichzeitig die Grundrißebene ist, sollen die Geraden hervorgehoben werden, die zur Spurgeraden $o \equiv x$ senkrecht sind und die Mengen der Geraden, die überparallel zur Spurgeraden $o \equiv x$ sind. (Abb.3).

Die Geraden, die zur Spurgeraden $o \equiv x$ senkrecht sind, bilden ein hyperbolisches Geradenbüschel, deren Geraden die p-Geraden gennant werden und den Fallinien in der Ebene analog sind [3]. Das Perspektivbild jeder von diesen Geraden bekommt man so, daß durch diese p-Geraden und den Augpunkt O eine Hilfsebene gelegt wird. Jede solche Ebene ist zur Bildebene Π_2 senkrecht und das ist eine sogennante zweitprojizierende Ebene. Ihre Schnittgerade mit der Ebene Π_2 ist der zweite Spurgerade dieser Ebene, die das Perspektivbild der p-Geraden enthält. Alle diese Ebenen bilden ein Ebenenbüschel, dessen Träger die Gerade OO_1 ist, die durch den Augpunkt O und den Scheitelpunkt O_1 des p-Geradenbüschels verläuft. Alle zweite Spurgeraden dieser Ebenen bilden ein eliptisches Geradenbüschel in der Bildebene Π_2, dessen Scheitelpunkt der Punkt O_H ist (wegen $OO_H \perp \Pi_2$). Jeder von diesen zweiten Spurgeraden schneidet die Spurgerade $o \equiv x$ in einem Punkt, der der Durchstoßpunkt der zugehörigen p-Geraden mit der Bildebene Π_2 ist. Dem nach kann das perspektivische Bild jeder von den p-Geraden so bestimmt werden, daß durch ihren Durchstoßpunkt, zum Beispiel $P \in o \equiv x$, und durch den Punkt O_H die p_c- Gerade aufgestellt wird. Der Schnittpunkt P_{Ih} auf diese Weise gewonnenen p_c-Geraden mit der h-Horizont ist das Perspektivbild einer von den Grenzpunkten der p-Geraden. Der Schnittpunkt K der p_c-Geraden mit dem Randbild der Bildebene Π_2 ist der Durchstoßpunkt dieser p-Geraden mit der Verschwindungskegel Φ. Das perspektivische Bild des Teiles der p-Geraden vom Punkt K außerhalb des Parallelkegels Φ ist uneigentlich (ideell)

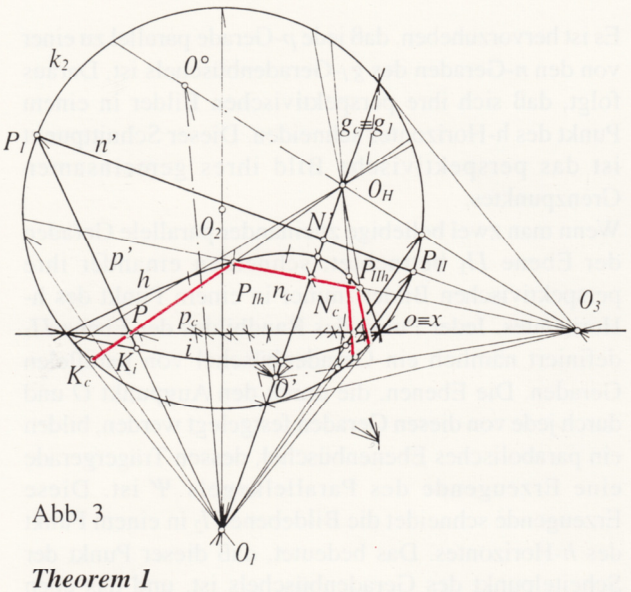

Abb. 3

Theorem 1

Das perspektivische Bild des Büschels der überparallelen p-Geraden der Ebene Π_1 ist ein eliptisches Geradenbüschel, dessen Scheitelpunkt der Punkt O_H ist.

Jede p-Gerade definiert, nach angeführten Theoremen in [3] und [1], ein Büschel der n-Geraden, dessen Geraden zur Spurgeraden $o \equiv x$ überparallel sind. Es ist wichtig in der Ebene Π_1 jenes Geradenbüschel der n-Geraden hervorzuheben, dessen Trägergerade, die durch den Punkt O' verlaufende p-Gerade, sogennante g_1-Gerade, ist. In diesem Fall ist die g_1-Gerade auch die gemeinsame Senkrechte des Büschels der n-Geraden, was nach den bewiesenen Tatsachen in [1] gilt. Der Scheitelpunkt dieses Büschels ist der uneigentliche (ideelle) Punkt O_3 (Abb.3). In diesem Fall bilden die festgelegten Ebenen durch den Augpunkt O und jede von den n-Geraden ein Ebenenbüschel, dessen Trägergerade die Gerade OO_3 ist. Die zweiten Spurgeraden dieser Ebenen, in dennen die perspektivischen Bilder der n-Geraden liegen, sind zueinander überparallel. Sie bestimmen ein Geradenbüschel mit dem Scheitel O_3 und mit der gemeinsamen Senkrechten g_c. Also, um das perspektivische Bild einer von den n-Geraden bestimmen zu können, genügt es, das Bild nur eines Punktes dieser

n-Geraden zu konstruieren. Das kann das Bild einer von ihren Grenzpunkten sein, der mit der *h*-Horizont inzident ist, oder der Schnittpunkt *N* der Geraden *n* und g_1. Der Punkt N_c liegt dann auf der Gerade g_c, weil der Projektionsstrahl *NO* in der Ebene Γ liegt und die Bildebene Π_2 auf der g_c-Geraden durchstößt. Bei deiser Abbildung werdwn einige n-Geraden aus dem Geradenbüschel O_3 in den uneigentlichen n_c-Geraden abgebildet.

Theorem 2

Das perspektivische Bild eines Büschels von überparallelen n-Geraden, dessen Trägergerade eine p-Geraden in Π_1 ist, ist ein hyperbolisches Geradenbüschel von n_c-Geraden mit dem Scheitel, der ein uneigentlicher Punkt der Spurgerade o≡x ist.

Es ist hervorzuheben, daß jede *p*-Gerade parallel zu einer von den *n*-Geraden des g_1-Geradenbüschels ist. Daraus folgt, daß sich ihre perspektivischen Bilder in einem Punkt des h-Horizontes schneiden. Dieser Schnittpunkt ist das perspektivische Bild ihres gemeinsamen Grenzpunktes.

Wenn man zwei beliebige zueinander parallele Geraden der Ebene Π_1 betrachtet, schneiden einander ihre perspektivischen Bilder immer in einem Punkt des h-Horizontes. Jeder Punkt des Randbildes der Ebene Π_1 definiert nämlich ein Geradenbüschel von parallelen Geraden. Die Ebenen, die durch den Augpunkt *O* und durch jede von diesen Geraden festgelegt werden, bilden ein parabolisches Ebenenbüschel, dessen Trägergerade eine Erzeugende des Parallelkegels Ψ ist. Diese Erzeugendė schneidet die Bildebene Π_2 in einem Punkt des *h*-Horizontes. Das bedeutet, daß dieser Punkt der Scheitelpunkt des Geradenbüschels ist, und das eben jeniges, das das perspektivische Bild des betrachteten parabolischen Geradenbüschels ist. In der Ebene Π_1 gibt es zwei parabolische Geradenbüschel, deren Geraden zur Spurgerade *o*≡*x* parallel sind. Diese zwei parabolischen Geradenbüschel werden wieder auf zwei parabolische Geradenbüschel der Bildebene Π_2 abgebildet, wobei deren Scheitelpunkte dieselben Grenzpunkte der Spurgeraden *o*≡*x* sind.

Theorem 3

Die perspektivischen Bilder der parabolischen Geradenbüschel der Ebene Π_1 sind die Geradenbüschel der Bildebene Π_2, deren Scheitelpunkte die Punkte des h-Horizontes sind. Abhängig davon, ob der Punkt des h-Horizontes ein eigentlicher, unendlich ferner oder uneigentlicher Punkt ist, ist das Geradenbüschel eliptisch, parabolisch oder hyperbolisch.

Um eine Gerade der Ebene Π_1 abzubilden, verwenden wir zwei spezielle Punkte: *den Spurpunkt* d.h. der Durchstoßpunkt der Geraden mit der Bildebene Π_2, der mit seinem perspektivischen Bild zusammenfällt, und einen von den Grenzpunkten der Geraden (Abb.4).

Jede Gerade der Π_1 - Ebene hat den Spurpunkt in der Schnittgeraden *o*≡*x* , und das perspektivische Bild ihren

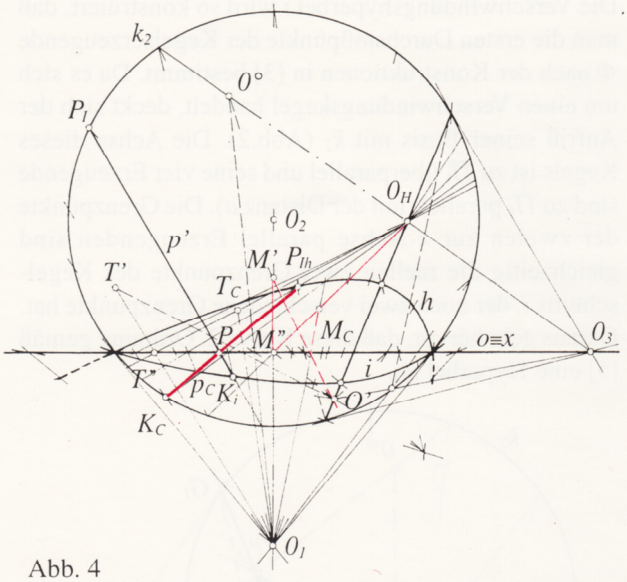

Abb. 4

Grenzpunkten , die *die Fluchtpunkte* der Geraden genannt werden, gehört dem *h*-Horizont an. Mit diesen zwei Punkten ist eindeutig das perspektivische Bild der Geraden bestimmt. Es gilt auch die Umkehrung. Wenn in der Bildebene eine Gerade angegeben ist, auf der die zwei Punkte: als Spurpunkt und Fluchtpunkt (Punkt am *h*-Horizont) bezeichnet sind, entspricht dieser Geraden eindeutig eine Gerade in der Ebene Π_1. Diese Gerade verläuft durch den Spurpunkt und jenen Grenzpunkt der Grundebene Π_1, der mittels der Erzeugende des Parallelkegels Ψ bestimmt wird. Dabei ist der Durchstoßpunkt dieser Erzeugende mit der Bildebene der Fluchtpunkt d.h. der Punkt, der mit dem *h*-Horizont inzident ist. Auf Grund dieser Überlegungen folgt:

Theorem 4

Jeder Geraden der Grundebene Π_1 entspricht in der Bildebene ein geordnetes Punktepaar (P, P_{1h})- der Spurpunkt und der Fluchtpunkt. Der Spurpunkt kann dabei eigentlicher, unendlich ferner Punkt oder uneigentlicher Punkt sein. Umgekhert, jedem geordneten Punktepaar (R, R_{1h}) in der Bildebene kann man genau nur eine Gerade der Ebene Π_1 zuordnen , wenn der Punkt R auf der Spurgerade o≡x liegt, und der Punkt R_{1h} zum h-Horizont gehört, oder wenn die beiden Punkte R und R_{1h} zum h-Horizont gehören.

PUNKTE IN DER GRUNDEBENE Π_1

Die Punkte der Grundebene Π_1 werden als Schnittpunkte zweier Geraden der Grundebene erfaßt. Speziell verlaufen durch jeden Punkt eine *p*- und eine *n*-Gerade. Die Bilder dieser Geraden können entweder wie im vorigen Abschnitt durch die Bilder zweier spezieller Punkte (Spurpunkt, Fluchtpunkt) oder durch das zum euklidischen analoge Durchschnittsverfahren [7], [3] bestimmt werden. Das perspektivische Bild *Tc* des Punktes *T* kann man noch als der zweite Durchstoßpunkt des Projektionsstrahles *TO* mit der Bildebene Π_2 gemäß [3] konstruieren (Abb.4).

FIGUREN IN DER GRUNDEBENE Π_1

Auf Grund der oben erwähnten Tatsachen ist es einfach das perspektivische Bild einer beliebigen Figur der Π_1-Ebene zu bestimmen.

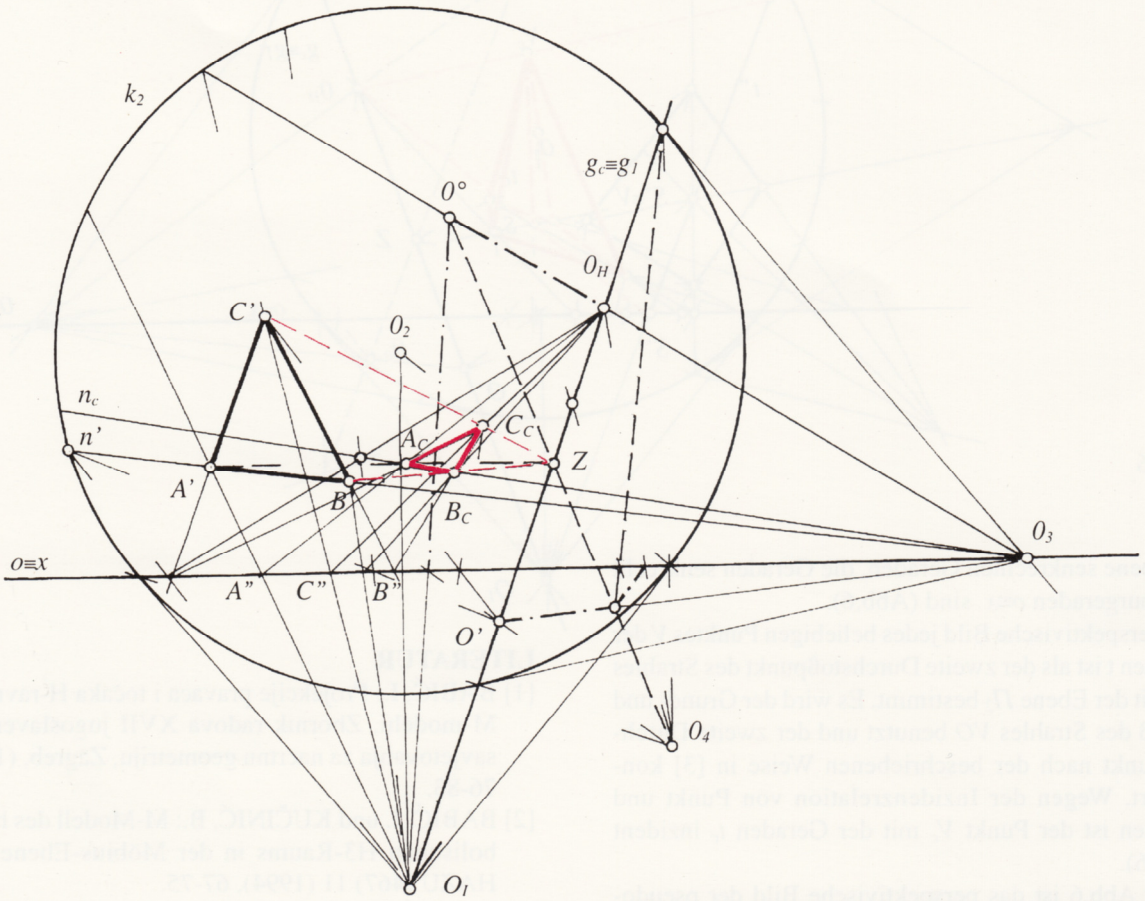

Abb. 5

In Abb.5 wird das Dreieck ABC dargestellt. Die Seite AB dieses Dreieckes ist zur Spurgerade $o \equiv x$ überparallel, das heißt, auf der n-Geraden liegende Seite. Der Grundriß des Dreieckes ist in "wahrer Gestalt" dargestellt und sein Aufriß ist die Strecke, die auf der $o \equiv x$ Achse liegt. In diesem Fall wurden die p- und n- Geraden und auch ihre Eigenschaften benutzt. Durch jeden Punkt des Dreieckes $A'B'C'$ ist eine p-Gerade gelegt, während die Seite AB schon auf der n-Geraden liegt. Auf Grund der Theoremen 1 und 2 ist das perspektivische Bild A_cB_c der Seite AB konstruiert. Der Punkt C_c ist durch das Durchschnittverfahren wie in Abb.4 bestimmt. Weiter verwenden wir, daß einander die Geraden $A'C'$ und A_cC_c im Punkt der Spurgerade $o \equiv x$ schneiden, was auch für andere zugeordnete Geradenpaare gilt. Diese Tatsache ist evident, da durch den Spurpunkt der Geraden auch ihr Grundriß und das perspektivische Bild verlaufen (Theorem 4).

Da sich zugeordnete Geraden in den Punkten längs einer Achse schneiden, existiert eine H-perspektiven Kollineation in der Bildebene. Nach dem Grundtheorem der H-perspektiven Kollineation [4] , bedingt die Existenz der Achse auch die Existenz des H-Zentrums.

Das Zentrum der H-perspektiven Kollineation in der Bildebene ist der Punkt Z, in dem der durch den Augpunkt O senkrecht zur Symetrieebene des Winkels (Π_1, Π_2) aufgestellte Strahl z die Bildebene Π_2 durchstößt. Dieser Strahl z ist die Trägergerade eines Ebenenbüschels, der die Bildebene in dem Geradenbüschel mit dem Scheitel Z schneidet. Da der Projektionsstrahl z auch in der Ebene Γ liegt, schneidet er die Gerade g_c im Punkt Z, also $Z \in g_c$. Die Schnittgerade jeder Ebene des Ebenenbüschels mit der Bildebene enthält die umgeklappte Lage des Punktes der Π_1-Ebene und auch sein perspektivisches Bild, das heißt zum Beispiel das Paar (A', A_c), und verläuft in jedem Fall durch den Punkt Z. Das bedeutet, daß der Punkt Z das Zentrum der H-perspektiven Kollineation in der Bildebene ist. Daraus geht hervor, daß die Figuren der Π_1-Ebene nach der Rotation in die Bildebene und ihre perspektivischen Bilder H-perspektiv kollinear zugeordnet sind. Die Achse der H-perspektiven Kollineation ist der Spurgerade $o \equiv x$ und das H-Zentrum ist der Punkt Z.

GERADEN SENKRECHT ZUR GRUNDEBENE Π_1
H-HÖHEN DER OBJEKTE

Die Geraden, die zur Grundebene Π_1 senkrecht sind, sind gleichzeitig zur Bildebene Π_2 überparallel. Jede Ebene, die durch die Gerade $t \perp \Pi_1$ und den Augpunkt O festgelegt ist, ist senkrecht zur Ebene Π_1. Sie schneidet die Bildebene Π_2 in der Geraden $t_c \perp o \equiv x$ (laut [3]). Daraus folgt , daß die parspektivischen Bilder von zur

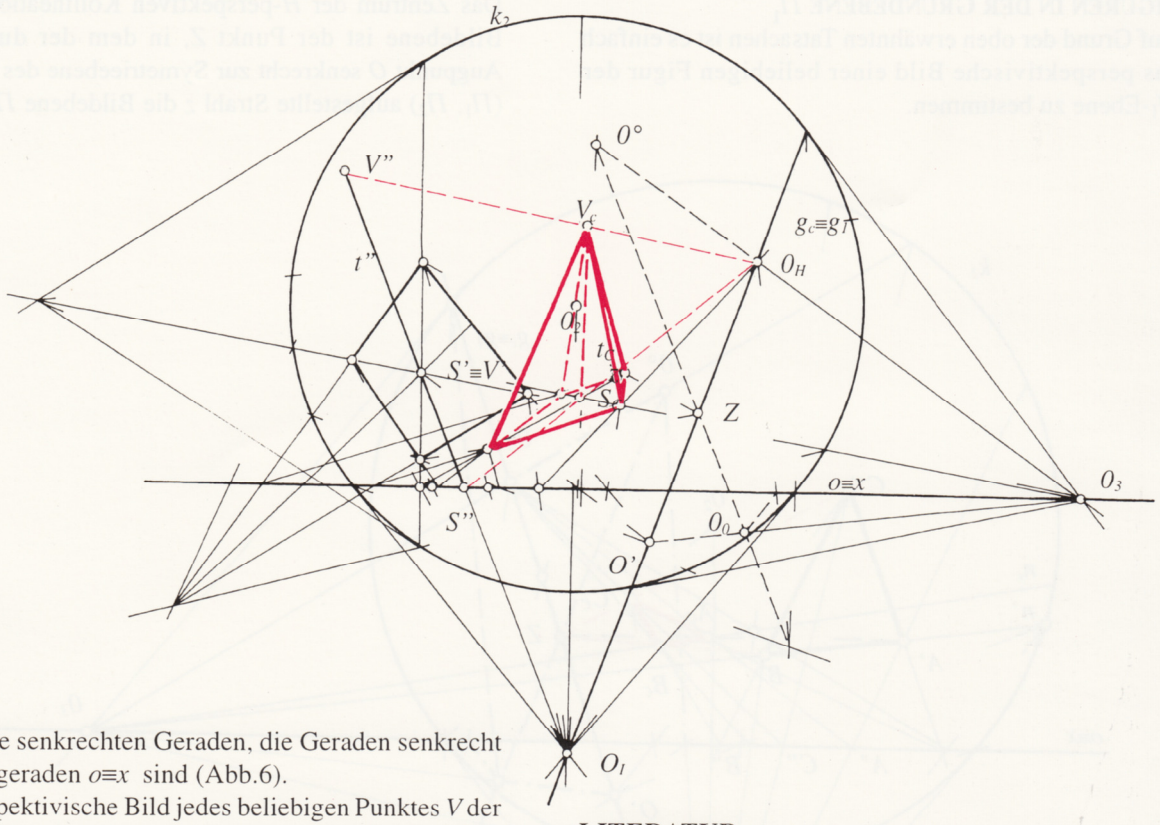

Abb. 6

Π_1-Ebene senkrechten Geraden, die Geraden senkrecht zur Spurgeraden $o \equiv x$ sind (Abb.6).

Das perspektivische Bild jedes beliebigen Punktes V der Geraden t ist als der zweite Durchstoßpunkt des Strahles VO mit der Ebene Π_2 bestimmt. Es wird der Grund- und Aufriß des Strahles VO benutzt und der zweite Durchstoßpunkt nach der beschriebenen Weise in [3] konstruiert. Wegen der Inzidenzrelation von Punkt und Geraden ist der Punkt V_c mit der Geraden t_c inzident (Abb.6).

In der Abb.6 ist das perspektivische Bild der pseudoquadratischen gerechten Pyramide, deren Basis in der Π_1-Ebene liegt, nach dem folgenden Verfahren aufgebaut: Zuerst ist der Grundriß des Pseudoquadrates konstruiert. Seine Diagonalen sind zueinander senkrecht und gleich lang. (Die gegenüberliegenden Seiten sind überparallel.) Der Aufriß des Pseudoquadrates ist die auf der Spurgeraden $o \equiv x$ liegende Strecke. Sein perspektivisches Bild wurde nach dem obenerwähnten Verfahren konstruiert, wobei auch die H-perspektive Kollineation in der Bildebene benutzt wurde.

Die Achse t der Pyramide ist die Senkrechte zur Basisebene Π_1 durch den Schnittpunkt der Diagonalen des Pseudoquadrats. Das perspektivische Bild t_c der Achse t ist zu $o \equiv x$ senkrecht und nach vorhererwähnten Weise konstruiert.

Das perspektivische Bild $V_c \in t_c$ der Pyramidenspitze V ist mittels Durchschnittsverfahren bestimmt.

Auf gleiche Weise kann das perspektivische Bild jedes Objekts konstruiert werden.

LITERATUR

[1] BABIĆ, I.: Projekcije pravaca i točaka H-ravnine u M-modelu, Zbornik radova XVII jugoslavenskog savjetovanja za nacrtnu geometriju, Zagreb, (1990), 76-83.

[2] BABIĆ, I. und KUČINIĆ, B.: M-Modell des hyperbolischen H3-Raums in der Möbius-Ebene, Rad HAZU (467) 11 (1994), 67-75.

[3] BABIĆ, I.: Darstellende Geometrie im hyperbolischen H^3-Raum I. Teil, Rad HAZU (470) 12 (1995), 167-186.

[4] BABIĆ, I.: Darstellende Geometrie im hyperbolischen H^3-Raum II. Teil, Rad HAZU (472) 13 (1997), 13-26.

[5] KLEIN, F.: *Vorlesungen über nicht-euklidische Geometrie*, Verlag von Julius Springer, Berlin, 1928.

[6] KRUPPA, E.: Darstellende Geometrie im projektiven Raum mit elliptischer oder hyperbolischer Maßbestimmung, Sitzungsber. Österr. Akad. Wiss. math.-nat. KL. Abt IIa, 171 (1962), 75-92.

[7] NIČE, V.: *Perspektiva*, Školska knjiga, Zagreb, 1961.

[8] ŠNAJDER, Z.: Spur-und Fluchtpunktsmethode bei Zentralprojektion im hyperbolischen Raum, Matem. vesnik, 2 (17),Beograd, (1965), 127-136.

[9] ŠNAJDER, Z.: Die Zentral-und Zentralgrundriss projektionsmethode im dreidimensionalen hyperbolischen Raum-Lagenaufgaben, Matem.vesnik, 6 (21), Beograd, (1969), 355-364.

Dr. sc. Ivanka Babić
Građevinski fakultet Sveučilišta u Zagrebu,
10 000 Zagreb, Kačićeva 26,
tel/fax: +385(01) 66 00 642
e-mail: ibabic@juraj.gradnz. grad.hr

Dr. sc. Branko Kučinić
Građevinski fakultet Sveučilišta u Zagrebu,
10 000 Zagreb, Kačićeva 26,
tel/fax: +385(01) 66 00 642
e-mail: bkucinic @juraj.gradnz. grad.hr

Original scientific paper
Accepted 10.10.1997.

JELENA BEBAN - BRKIĆ

On the Focal Curve of Conic Pencils in I_2

On the Focal Curve of Conic Pencils in I_2
ABSTRACT
Within the classification of conic pencils in the isotropic plane, which has been carried out using methods of analytical geometry and linear algebra, it is specially interesting to observe the curve of isotropic focuses, which is shown to be a 3rd order curve. The properties of this very curve, for the discussed, most common subtype of conic pencils, are determined. It is shown that, referring to the selection of the fundamental points, it is possible to determine its shape, and to classify it according to the Newton's principle.
The discussed cases of conic pencils with its focal curves are illustrated with the figures programmed and drawn by *Mathematica*®.
Keywords: isotropic plane, fundamental points, pencil of conic sections, matrix of quadratic form, eigenvalues, focal curve, Newton's classification

O krivulji fokusa pramena konika u I_2
SAŽETAK
Pri klasifikaciji pramenova konika u izotropnoj ravnini, provedenoj metodama analitičke geometrije i linearne algebre, posebno je interesantno promatrati krivulju izotropnih fokusa za koju se pokazuje da je krivulja 3. reda. Određena su svojstva krivulje fokusa za promatrani, najopćenitiji, podtip pramena. Pokazano je da već prema odabiru temeljnih točaka možemo odrediti njen oblik i klasifikaciju prema Newtonovom principu.
Promatrani slučajevi su prikazani crtežima izrađenim pomoću programa *Mathematica*®.
Ključne riječi: izotropna ravnina, temeljne točke, pramen konika, matrica kvadratne forme, svojstvene vrijednosti, krivulja fokusa, Newtonova klasifikacija

INTRODUCTION

The pencil of conic sections (pencil of conics) is determined by two arbitrarily chosen conics of the pencil ([4], [12], [17]). These two conics have four common points that we call fundamental points of the pencil and mark them A, B, C, and D. Depending on the reality, position and multiplicity of fundamental points, various types of conic pencils can be distinguished. The classification in the projective and affine plane with respect to the position and multiplicity of fundamental points can be found for example in [4], [6].

The isotropic plane $I_2(R)$ is a real affine plane A_2 metrizied with real line $f \subset A_2$ and the point F incidental with it (see [13], [14]). The ordered pair $\{f,F\}$, $F \in f$, is called absolute figure of the plane $I_2(R)$.

Because of $I_2 \subset A_2 \subset P_2$, where P_2 is a real projective plane, all affine and projective properties of the conic pencils and of other geometric configurations in I_2 can be used.

In $I_2 \subset P_2$ the projective, homogeneous, $(x_0 : x_1 : x_2)$ and the accompanying affine coordinates $x = x_1/x_0$, $y = y_2/y_0$ are used. The absolute line f is defined by $x_0 = 0$, and the absolute point F by F (0:0:1). For the fundamental group of transformations one takes the mappings of the form

$$\bar{x} = c_1 + x$$
$$\bar{y} = c_2 + c_3 x + y, \quad \text{where } c_1, c_2, c_3 \in R,$$

which make the three-parametric *Motion group G_3 of isotropic plane* [13].

With the geometry of isotropic plane one can get acquainted through the works of N. M. Makarowa [11], B. Pavković [13], H. Sachs [14], K. Strubecker [18], and others. The conics of isotropic plane were first considered by N. M. Makarowa and K. Strubecker. The conic pencils of the most general type in I_2 have been worked by V. Ščurić-Čudovan [19] by means of synthetic method.

The classification of conic pencils in I_2 can be made with respect to the reality and multiplicity of fundamental points and regarding their position, as well as the position of fundamental straight lines according to the absolute figure $\{f,F\}$. For a more comprehensive classification, the curve of the centres and the curve of isotropic focuses (focal curve) are observed for each type of the conics' pencil. It is specially interesting to observe the focal curve which is going to be proved to be a 3rd order curve. Therefore this very curve is to be discussed in the present paper. An analysis of the most general subtype of conic pencils in I_2 will be made, and the classification of its cases will be carried out, using methods of analytical geometry and linear algebra. The properties of the focal curve for each discussed case are determined and, it is shown that, referring to the choice of the fundamental points, it is possible to determine its shape, and to classify it according to the Newton's principle [16].

The discussed cases of conic pencils with its focal curves are illustrated with the figures programmed and drawn by *Mathematica*®

1. PENCIL OF CONICS

Fundamental points

Let the fundamental points A, B, C, and D be real, mutually different, providing that three of them do not lie on the same straight line. As it is the most general case, the pencils generated by such a selection of points, are called type **I**.

Fundamental lines

The fundamental points are joined by three singular, in three pairs of straight lines degenerated conics. Two arbitrarily chosen pairs, out of this three pairs of straight lines, are called fundamental straight lines.

Let the fundamental straight lines u, v, p and q be given in the equations

$u...\quad a_u x + b_u y + c_u = 0, \qquad u:=CD,$
$v...\quad a_v x + b_v y + c_v = 0, \qquad v:=AB,$
$p...\quad a_p x + b_p y + c_p = 0, \qquad p:=AD,$
$q...\quad a_q x + b_q y + c_q = 0. \qquad q:=BC.$

Main points

Three points of the intersection $K=AB\cap CD$, $L=AD\cap BC$, $M=AC\cap BD$, are called main points.

These are the centres of the singular conics of the pencil. The points K, L, M form a triangle that is self-polar for the conics of the pencil (see [12], [17]).

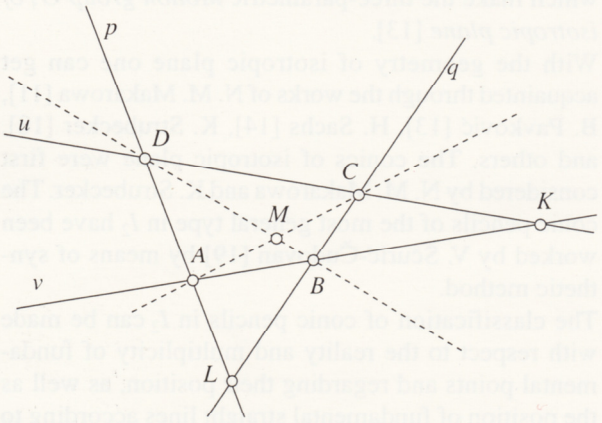

Fig.1: The most general position of the fundamental points, the accompanying fundamental lines and main points.

Fundamental conics

As fundamental conics two arbitrarily conics of the pencil can be chosen. We shall choose the two singular, in two pairs of fundamental straight lines degenerated conics.

Let the fundamental conics of a pencil be given in the equations

$F(x,y) \equiv a_1x^2 + 2b_1xy + c_1y^2 + 2d_1x + 2e_1y + f_1 = 0$, and
$G(x,y) \equiv a_2x^2 + 2b_2xy + c_2y^2 + 2d_2x + 2e_2y + f_2 = 0$,

where at least one of the numbers a_1, b_1, c_1, as well as one of the numbers a_2, b_2, c_2, is different from zero [3].

Their equations can be written in the form

$F(x,y) \equiv u\ v = 0,$
$G(x,y) \equiv p\ q = 0,$

where u, v, p, and q are the fundamental straight lines. The coefficients of the fundamental conics described by means of the coefficients of fundamental straight lines are

$a_1=a_ua_v, \quad 2b_1=a_ub_v+a_vb_u, \quad c_1=b_ub_v,$
$2d_1=a_uc_v+a_vc_u, \quad 2e_1=b_uc_v+b_vc_u, \quad f_1=c_uc_v,$
$a_2=a_pa_q, \quad 2b_2=a_pb_q+a_qb_p, \quad c_2=b_pb_q,$
$2d_2=a_pc_q+a_qc_p, \quad 2e_2=b_pc_q+b_qc_p, \quad f_2=c_pc_q.$

Pencil of Conics

The pencil of conic sections, defined by the fundamental conics $F(x,y) = 0$ and $G(x,y) = 0$, is given in the form

$H(x,y) \equiv \alpha F(x,y) + \beta G(x,y) = 0,$

and by introducing the parameter $\lambda=\beta/\alpha$, $\alpha \neq 0$, we have

$H(x,y) \equiv F(x,y)+\lambda G(x,y) = 0, \quad \lambda \in R.$

The pencil $H(x,y) = 0$ can be written in the form

$$H(x,y) \equiv ax^2+2bxy+cy^2+2dx+2ey+f = 0, \qquad (1.1)$$

where we have marked

$a = a_1 + \lambda a_2 = a_ua_v + \lambda a_pa_q,$
$2b = 2(b_1 + \lambda b_2) = a_ub_v + a_vb_u + \lambda(a_pb_q+a_qb_p),$
$c = c_1 + \lambda c_2 = b_ub_v + \lambda b_pb_q,$
$2d = 2(d_1+ \lambda d_2) = a_uc_v+a_vc_u + \lambda (a_pc_q+a_qc_p),$
$2e = 2(e_1 + \lambda e_2) = b_uc_v+b_vc_u + \lambda (b_pc_q+b_qc_p),$
$f = f_1 + \lambda f_2 = c_uc_v + \lambda c_pc_q.$

For each $\lambda \in R$, the set of zeros of the polynomial $H(x,y) = F(x,y) + \lambda G(x,y)$ presents one of the second order curves if at least one of the numbers a, b, c is different from zero.

Focal curve

The notion of absolute plane points is connected with the notion of the focuses of second order curves. It is known that in the affine plane metrizied through absolute points (I_1, I_2), the tangents drawn from absolute points onto the second order curve intersect in the focuses of the curve (see [16], [17]).

In the isotropic plane in which there is only one absolute point F ($I_1 = I_2 = F$, $F\in R$) the focuses are defined as real contact points of tangents drawn from the absolute point onto the second order curve. The geometric loci of the contact points of all tangents drawn from the absolute point onto the curves of conic pencil is the curve of isotropic focuses that we call focal curve.

2. CURVES OF THE CONIC PENCILS

The type of the curve within the pencil (1.1) depends on the eigenvalues μ_1, μ_2 of the matrix

$$\sigma = \begin{bmatrix} a & b \\ b & c \end{bmatrix}$$

of the quadratic form $ax^2 + 2bxy + cy^2$ within the

polynomial $H = H(x,y)$ ([7], [8]).
The eigenvalues μ_1, μ_2 are obtained as the solutions of the equation

$$\mu^2 - (a + c)\,\mu + a\,c - b^2 = 0,$$

where

$$a + c = tr\,\sigma = \mu_1 + \mu_2,$$

and

$$ac - b^2 = det\,\sigma = \mu_1\,\mu_2.$$

It is known that the set of the second order polynomial zeros represent the curve of elliptical, parabolic or hyperbolic type depending on whether $det\sigma$ is greater, equal or less than zero ([3], [4], [8]).
We are observing the case when $det\,\sigma = 0$. Thereby the answer will be obtained of when and how many conics of the parabolic type are conveyed within the pencil.

$$det\,\sigma = \mu_1\mu_2 = ac - b^2 = \\ = (a_1 + \lambda a_2)(c_1 + \lambda c_2,) - (b_1 + \lambda b_2)^2,$$

that is

$$det\,\sigma = m\,\lambda^2 + n\,\lambda + p, \qquad (2.1)$$

where we have put

$$m = a_2\,c_2 - b_2^2 = a_p a_q\,b_p b_q - (a_p b_q + a_q b_p)/2,$$
$$n = a_1\,c_2 + a_2\,c_1 - 2b_1 b_2 = a_u a_v\,b_p b_q + \\ + a_p a_q\,b_u b_v - (a_u b_v + a_v b_u)(a_p b_q + a_q b_p), \qquad (2.2)$$
$$p = a_1\,c_1 - b_1^2 = a_u a_v\,b_u b_v - (a_u b_v + a_v b_u)^2/4.$$

Discriminante of a polynomial (2.1) is to be marked with D.
It can be derived that the determinant of the matrix σ will be equal zero in the following cases [10]:

i) for each $\lambda \in R$,
if $m=0$, $n=0$, $p=0$;
ii) for neither $\lambda \in R$,
if $m=0$, $n=0$, $p \neq 0$ or $m \neq 0$ i $D<0$;
iii) for $\lambda = -p/n$,
if $m=0$, $n \neq 0$; (2.3)
iv) for $\lambda = -n/2m$,
if $m \neq 0$ and $D=0$
v) for $\lambda_{1,2} = (-n \pm \sqrt{D})/2m$,
if $m \neq 0$ and $D>0$.

It can be seen from (2.3) that within the conic pencil all, two, one or none of the curves can be of parabolic type. In the most general case (2.3, v), two conics of parabolic type will exist that will separate the curves of hyperbolic from those of elliptical type.

3. List and Description of the Pencils of the Type I

Considering the pencils of conic sections of type **I**, the obtained results, according the position of the fundamental points, are given in the following proposition.

Proposition 1.
In the isotropic plane $I_2(R)$ referring to the group G_3 of isotropic motions there are 8 different subtypes of conic pencils determined with four real and mutually different points.

Proof. The proof is given in [2].

List and Description of the Pencils of the Type I

I.1. Fundamental points (A, B, C, D) are real finite points and no connecting straight line of fundamental points is an isotropic line, i. e. a line through the absolute point F.
I.1.1. Main points (K, L, M) are in the finiteness. Thereare two subcases.
I.1.2. One main point is on the absolute line f.
I.1.3. Two main points are on the absolute line f.

I.2. The fundamental points (A, B, C, D) are real finite points and one connecting straight line of the fundamental points is an isotropic line.
I.2.1. The main points (K, L, M) are in the finiteness There are two subcases.
I.2.2. One main point is on the absolute line f.
I.2.3. Two main points are on the absolute line f.

I.3. The fundamental points (A, B, C, D) are real finite points and two connecting straight lines of the fundamental points are isotropic lines.
I.3.1. One main point is on the absolute line f and it coincides with the absolute point F.
I.3.2. Two main points are on the absolute line f and one of them coincides with the absolute point F.

I.4. Two fundamental points are finite points and two on the absolute line f. The two fundamental points on the absolute line f do not coincide with the absolute point F.

I.5. Two fundamental points are finite points and two on the line f. The two fundamental points on the absolute line f do not coincide with the absolute point F. Connecting straight line of the fundamental finite points is an isotropic line.

I.6. Two fundamental points are finite points and two on the absolute line f. One of the two fundamental points on the absolute line f coincides with the point F.

I.7. Three fundamental points are finite points, and one is on the absolute line f not coinciding with the absolute point F.
I.7.1. No connecting straight line of the fundamental points is an isotropic line.
I.7.2. One connecting straight line of the fundamental points is an isotropic line.

I.8. Three fundamental points are finite points, and the point on the absolute line f coincides with the absolute point F.

4. FOCAL CURVE

Without becoming less general, we can furtheron observe the normed equations of the fundamental lines and presume that the coefficients are

$a_u = a_v = a_p = a_q = 1,$ (4.1)

if not defined otherwise.

Furthermore, using the group G_3 of motions of isotropic plane we can always map one of the fundamental lines (e.g. line v) onto the line $y = 0$, and one (e.g. line p) adjust so that it passes through the point of origin of the coordinate system. If it is not defined otherwise, we shall therefore presume furtheron that the coefficients are

$a_v = 0,\ b_v = 1,\ c_v = 0,\ c_p = 0.$ (4.2)

4.1. PENCIL I.1.

The characteristic of the pencil - subtype **I.**1.: The fundamental points (A, B, C, D) are at finiteness and no connecting straight line of the fundamental points is an isotropic line.

The common characteristic for all the pencils of the discussed subtype, according the focal curve, is established by the following proposition.

Proposition 2. *Focal curve k_f^3 of each pencil-subtype **I.**1. has no double points.*

Proof. Let us presume otherwise, i.e. let k_f^3 have a double point T. That means that a common tangent of two curves of the pencils k_1 and k_2 ($k_1 \neq k_2$) is passing through the point T. Every two conics of the pencil have only 4 fundamental points in common. If $T \neq A$, B, C, and D, hence the conics k_1 and k_2 have 5 mutual points, so $k_1 = k_2$. The point T cannot coincide with one of the fundamental points A, B, C, or D, since it is double, and the fundamental points are real and various.

PENCIL I.1.1.

The characteristic of the pencil-case **I.**1.1.:

The main points (K, L, M) are in the finiteness.

Let the coordinates of the fundamental points be

$A(0,0),\ B(b_1,0),\ b_1>0,\ C(c_1,c_2),\ c_1,c_2 \neq 0,$
$D(d_1,d_2),\ d_1,d_2 \neq 0,\ b_1 \neq c_1 \neq d_1,\ c_2 \neq d_2.$ (4.3)

The fundamental straight lines

$v := AB,\ p := AD,\ q := BC,\ u := CD$

are given in the equations:

$v \ldots\ y = 0.$

$p \ldots\ y = \varphi_p x,$ where $\varphi_p = \dfrac{d_2}{d_1}.$

If we put $b_p = -\dfrac{1}{\varphi_p}$,

it follows $x + b_p y = 0.$

$q \ldots\ y = \varphi_q + v_q,$

where $\varphi_q = \dfrac{c_2}{c_1 - b_1}$ $v_q = -\dfrac{b_1 c_2}{c_1 - b_1}.$

If we put $b_q = -\dfrac{1}{\varphi_q}$, and $c_q = \dfrac{v_q}{\varphi_q} = -b_1,$

it follows $x + b_q y + c_q = 0.$

$u \ldots\ y = \varphi_u x + v_u,$

where $\varphi_u = \dfrac{d_2 - c_2}{d_1 - c_1}$ $v_u = \dfrac{c_2 d_1 - c_1 d_2}{d_1 - c_1}.$

If we put $b_u = -\dfrac{1}{\varphi_u}$, and $c_u = \dfrac{v_u}{\varphi_u} = \dfrac{c_2 d_1 - c_1 d_2}{d_2 - c_2},$

it follows $x + b_u y + c_u = 0.$ (4.4)

The coordinates of the fundamental points described through b_p, b_q, c_q, b_u and c_u are

$A\ (0,0),\quad B\ (-c_q,0),$

$C\ \left(\dfrac{b_u c_q - b_q c_u}{b_q - b_u}, \dfrac{c_u - c_q}{b_q - b_u}\right),\quad D\ \left(-\dfrac{b_p c_u}{b_p - b_u}, \dfrac{c_u}{b_p - b_u}\right),$

where, according (4.3), we have

$b_q,\ b_u,\ b_p \neq 0,\ c_u,\ c_q \neq 0$ and $b_q \neq b_u,\ b_p \neq b_u.$ (4.5)

The fundamental conic section determined by the lines u, v is given in the equation

$G\ (x,y) \equiv u\ v = 0,$ that is

$G\ (x,y) \equiv (x + b_u y + c_u)\ y = xy + b_u y^2 + c_u y = 0.$

The quadratic form in the above equation has the matrix

$$\sigma = \begin{bmatrix} 0 & 1/2 \\ 1/2 & b_u \end{bmatrix},$$

and the determinant of the matrix is

$m = det\ \sigma = -1/4.$

It is the matter of the hyperbolic type of a conic.

The fundamental conic section determined by the lines p, q is

$F\ (x,y) \equiv p\ q = 0,$ that is

$F\ (x,y) \equiv (\ x + b_p y\ )(\ x + b_q y + c_q\ ) =$
$= x^2 + (b_p + b_q)xy + b_p b_q y^2 + c_q x + b_p c_q y = 0.$

The quadratic form in the above equation has the matrix

$$\sigma = \begin{bmatrix} 1 & (b_p + b_q)/2 \\ (b_p + b_q)/2 & b_p b_q \end{bmatrix},$$

and the determinant of the matrix is

$p = det\ \sigma = b_p b_q - (\ b_p + b_q\ )^2/4 = -(\ b_p - b_q\ )^2/4.$

According (4.4), $b_p = b_q$ would meant that the lines p and q are mutually parallel. This would implie that one main point is in the infinity, which is the case that does not belong to the pencils-subtype **I.**1.1. We can conclude that p is always less than zero, wherefrom it follows that it is the matter of the hyperbolic type of a conic.

The pencil generated with the curves $F\ (x,y) = 0$ and $G\ (x,y) = 0$ is

$H\ (x,y) \equiv F\ (x,y) + \lambda G\ (x,y) = 0,$ that is

$H\ (x,y) \equiv x^2 + (b_p + b_q + \lambda)xy +$
$+ (b_p b_q + \lambda b_u)y^2 + c_q x +$
$+ (b_p c_q + \lambda c_u)y = 0.$ (4.6)

Proposition 3.
Conic pencils of the case **I.**1.1. *are up to the motions G_3 of the isotropic plane with five ivariants $\{\varphi_p, \varphi_q, v_q, \varphi_u, v_u\}$, i.e. $\{b_p, b_q, c_q, b_u, c_u\}$ fully determined.*

In order to determine how many and which curves of parabolic type are within this pencil, we need the determinant of quadratic form (2.1), i.e.
$det\ \sigma = m\lambda^2 + n\lambda + p$,
where m, n, p are the values given in relations (2.2).

$$det\ \sigma = 0 \Rightarrow m\lambda^2 + n\lambda + p = 0 \Rightarrow$$

$$\Rightarrow \lambda_{1,2} = \frac{-n \pm \sqrt{n^2 - 4mp}}{2m}. \qquad (4.7)$$

Which case it will be out of (2.3), depends on
$D = n^2 - 4mp$.
$D = (b_u - (b_p + b_q)/2)^2 - 4(-1/4)(-(b_p - b_q)^2/4)$
$= (b_u - b_p)(b_u - b_q)$.

According (2.3) it can be concluded that within the case **I.**1.1. there are three different subcases of conic pencils, depending on whether it is $D > 0$, $D < 0$ or $D = 0$.

FOCAL CURVE WITHIN THE PENCILS I.1.1.
We take the equation (4.6) of the pencil:

$$H(x,y) \equiv x^2 + (b_p + b_q + \lambda)xy +$$

$$+(b_p b_q + \lambda b_u)y^2 + c_q x + (b_p c_q + \lambda c_u)y = 0.$$

One computes

$$\frac{\partial H}{\partial y} \equiv (b_p + b_q + \lambda)x +$$

$$+2(b_p b_q + \lambda b_u)y + (b_p c_q + \lambda c_u) = 0,$$

and therefrom

$$\lambda = -\frac{(b_p + b_q)x + 2b_p b_q y + c_q b_p}{x + 2b_u y + c_u}.$$

Inserting thus received λ in $H(x,y) = 0$, the following focal curve is obtained :

$$k_f^3 \equiv x^3 + 2b_u x^2 y + ((b_p + b_q)b_u - b_p b_q)xy^2 +$$
$$+(c_u + c_q)x^2 + 2b_u c_q xy +$$
$$+(b_u b_p c_q - b_p b_q c_u)y^2 + c_u c_q x = 0. \qquad (4.8)$$

In order to define the obtained 3rd order curve more closely, let us go over to the homogeneous coordinates. Introducing $x = x_1/x_0$, $y = y_1/y_0$, we get

$$k_f^3 \equiv \frac{x_1^3}{x_0^3} + 2b_u \frac{x_1^2 x_2}{x_0^3} +$$

$$+((b_p + b_q)b_u - b_p b_q)\frac{x_1 x_2^2}{x_0^3} + (c_u + c_q)\frac{x_1^2}{x_0^2} +$$

$$+2b_u c_q \frac{x_1 x_2}{x_0^2} + (b_u b_p c_q - b_p b_q c_u)\frac{x_2^2}{x_0^2} + c_u c_q \frac{x_1}{x_0} = 0.$$

Looking for the points on the absolute straight line f, $f \equiv x_0 = 0$, one receives:

i) absolute point $F(0:0:1)$, on the line $x_1 = 0$;
ii) 2nd order equation
$x_1^2 + 2b_u x_1 x_2 + ((b_p + b_q)b_u - b_p b_q)x_2^2 = 0$,
and therefrom

$$\left(\frac{x_1}{x_2}\right)_{1,2} = -b_u \pm \sqrt{B}, \text{ where we have marked}$$

$$B = b_u^2 - (b_p + b_q)b_u + b_p b_q.$$

According i) and ii), there are three possibilities:

a) $B > 0$ ($D > 0$) $\Rightarrow$ There are three points at infinity:
1) absolute point $F(0:0:1)$,
2) point $T_1(0 : b_u - \sqrt{B} : -1)$,
3) point $T_2(0 : b_u + \sqrt{B} : -1)$.

b) $B < 0$ ($D < 0$) $\Rightarrow$ There is only one real point at infinity and that is the absolute point F $(0:0:1)$.

c) $B = 0$ ($D = 0$) $\Rightarrow$ There are two real points at infinity :
1) absolute point $F(0:0:1)$,
2) point $T_1(0 : b_u : -1)$.

PENCIL I.1.1. a)
The characteristic of the pencil - subcase **I.**1.1.a):
$D = (b_u - b_p)(b_u - b_q) > 0 \Rightarrow$
$(b_u > b_q$ and $b_u > b_p)$ or $(b_u < b_q$ and $b_u < b_p)$

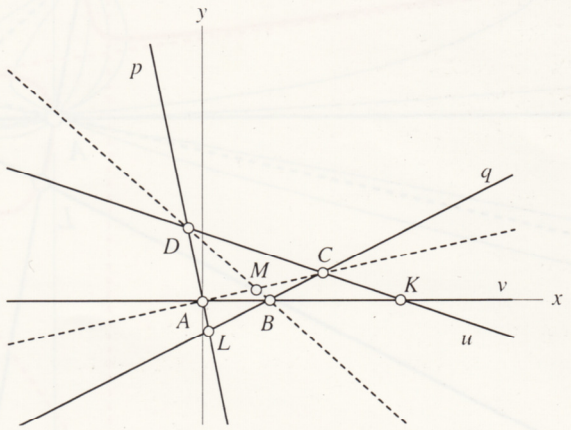

Fig.2: Fundamental points, the accompanying fundamental lines and main points within the pencil **I.**1.1.a), obtained by $b_u > b_q$ and $b_u > b_p$.

Since $D > 0$, it is the case (2.3, v), that is, there are exactly two conics of parabolic type within the pencil which are obtained when the values (4.7) are introduced into the pencil equation. They separate the conics of the hyperbolic from those of elliptic type. Thus, the conic pencil induces on the absolute straight line f one hyperbolic involution ([4], [12]).
Let us write the focal curve k_f^3 in the form
$a y^2 + b y + c = 0$,
where we have marked

$a = ((b_p + b_q)b_u - b_p b_q)\, x + (b_u\, b_p c_q - b_p b_q c_u)$,
$b = 2b_u x^2 + 2b_u c_q x$,
$c = x^3 + (c_u + c_q)x^2 + c_u c_q x$.

The isotropic asymptote, i. e. the asymptote passing through the absolute point F, is obtained from the condition $a = 0$, that is

$$x = \frac{b_p(b_q c_u - b_u c_q)}{b_p(b_u - b_q) + b_q b_u}.$$

Since $D > 0 \Rightarrow B > 0$, the curve k_f^3 of isotropic focuses has three points at infinity. Therefrom, according to the Newton's classification of the 3rd order curves, k_f^3 belongs to the 1. group, i.e. among the curves having three asymptotes and three hyperbolic branches. The curves of this group are called "broken hyperbolas".

The basic forms of the curves from this group are determined with the roots of the auxiliary equation $D_4(x) = 0$, where $D_4(x) = b^2 - 4ac$ is the fourth degree polynomial. The calculation yields

$$D_4(x) = (b_u - b_q)\cdot(b_u - b_p)\cdot$$
$$\cdot x\,(x + c_q)(x + \frac{b_q c_u - b_u c_q}{b_q - b_u})(x - \frac{b_p c_u}{b_u - b_p}),$$

wherefrom it can be seen that the roots of the equation $D_4(x) = 0$ are the abscissas of the fundamental points A, B, C, and D (4.5). As the points are real and various and within the observed pencil there are no isotropic lines, it holds.

Proposition 4.
The focal curve k_f^3 of all pencils of the subcase **I.**1.1.a) *consists of three hyperbolic branches and an oval, or of two hyperbolic branches and one straight line's branch.*

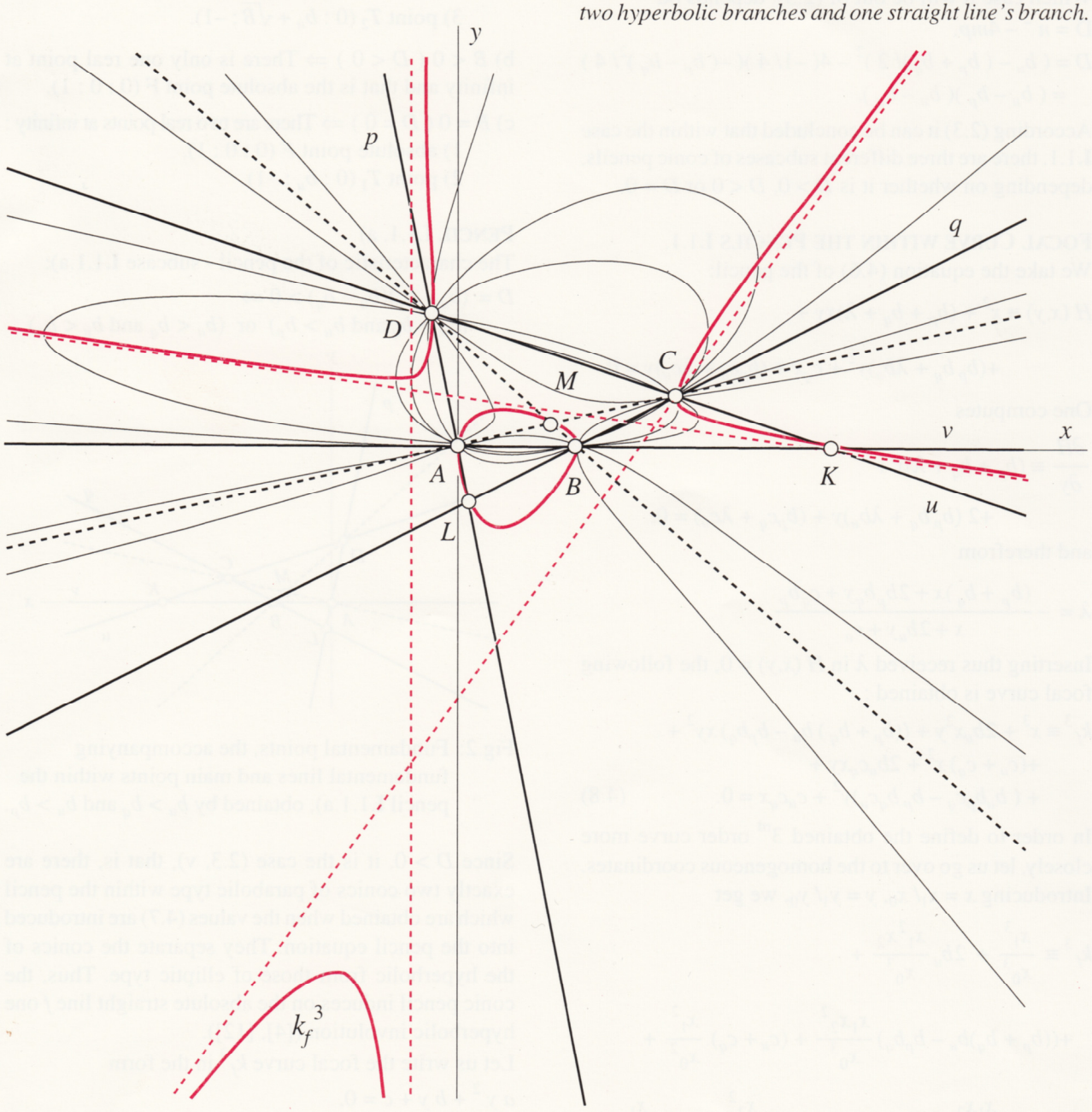

Fig.3: Pencil of conic sections - subcase **I.**1.1.a)

***Pencil* I.**1.1. b)

The characteristic of the pencil - subcase **I.**1.1.b):

$D = (b_u - b_p)(b_u - b_q) \Rightarrow$

$(b_q < b_u < b_p)$ or $(b_p < b_u < b_q)$

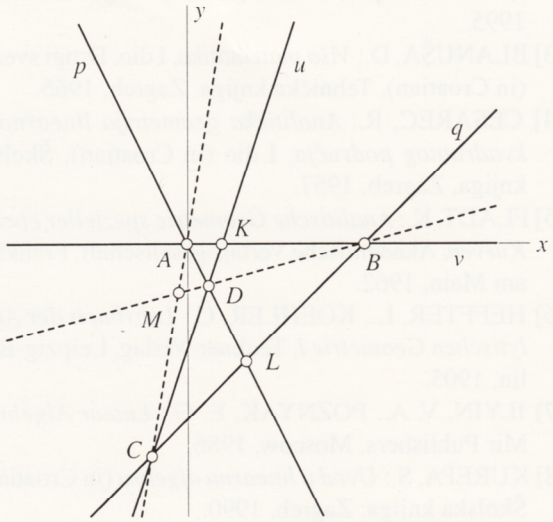

Fig.4: Fundamental points, the accompanying fundamental lines and main points within the pencil **I.**1.1.b), obtained by $b_q < b_u < b_p$.

Since $D < 0$, it is the case (2.3, ii), that is, no conics of parabolic type are within the pencil. As it is always $det\ \sigma < 0$, it can be concluded that the pencil consists only of hyperbolas. Thus, the conic pencil induces on the absolute straight line f one elliptic involution ([4], [12]).

Let us write the focal curve k_f^3 in the form

$a\,y^2 + b\,y + c = 0,$

where we have marked

$a = ((b_p + b_q)b_u - b_p b_q)\,x + (b_u\,b_p c_q - b_p b_q c_u),$

$b = 2b_u x^2 + 2b_u c_q x,$

$c = x^3 + (c_u + c_q)x^2 + c_u c_q x..$

The isotropic asymptote is obtained from the condition $a = 0$, that is

$$x = \frac{b_p(b_q c_u - b_u c_q)}{b_p(b_u - b_q) + b_q b_u}.$$

Since $D < 0 \Rightarrow B < 0$, the curve k_f^3 of isotropic focuses has only one real point at infinity. Therefrom, according to the Newton's classification of the 3. order curves, k_f^3 belongs to the 2. group, i.e. among the curves having one asymptote and one straightline's branch. The curves of this group are called "defective hyperbolas".

The basic forms of the curves from this group are determined with the roots of the auxiliary equation $D_4(x) = 0$, where $D_4(x) = b^2 - 4ac$ is the fourth degree polynomial. The calculation yields

$$D_4(x) = (b_u - b_q)(b_u - b_p)\cdot$$

$$\cdot x\,(x + c_q)(x + \frac{b_q c_u - b_u c_q}{b_q - b_u})(x - \frac{b_p c_u}{b_u - b_p}),$$

wherefrom it can be seen that the roots of the equation $D_4(x) = 0$ are the abscissas of the fundamental points A, B, C, and D (4.5). As the points are real and various and within the observed pencil there are no isotropic lines, it holds.

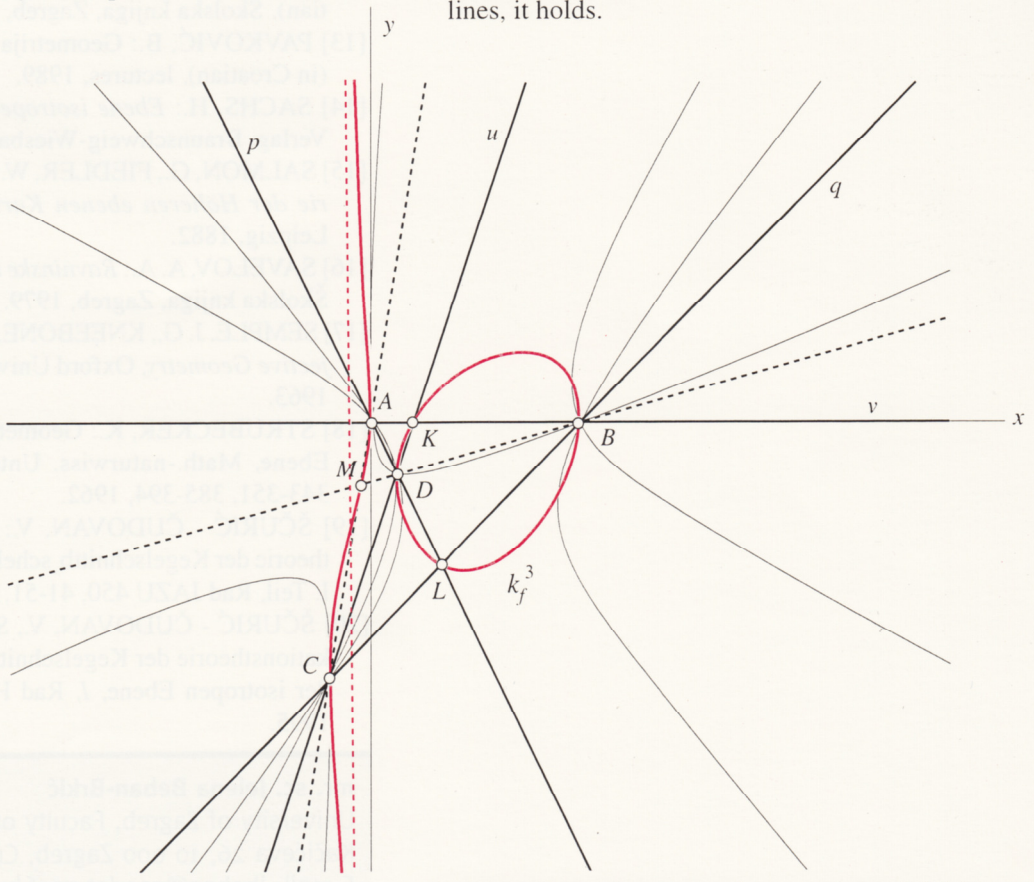

Fig.5: Pencil of conic sections - subcase **I.**1.1.b)

Proposition 5.
The focal curve k_f^3 of all pencils of the subcase **I.**1.1.b) *consists of one straightline's branch and an oval.*

PENCIL I.1.1. c)
The characteristic of the pencil - subcase **I.**1.1.c):
$D = (b_u - b_p)(b_u - b_q) = 0 \Rightarrow b_u = b_p$ or $b_u = b_q$.

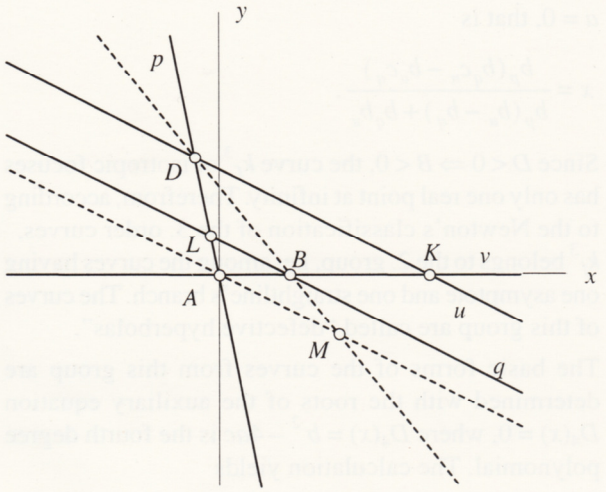

Fig. 6. Fundamental points, the accompanying fundamental lines and main points within the pencil **I.**1.1.c), obtained by $b_u = b_q$.

Since the lines u and p or u and q are mutually parallel, the fundamental point of intersection is in the infinity, so this case does not belong to the pencils - subtype **I.**1.

REFERENCES

[1] ALEKSANDROV, P. S.: *Lekcii po analitičeskoj geometrii* (in Russian), Nauka, Moskva, 1968.
[2] BEBAN-BRKIĆ, J.: Prilog klasifikaciji pramena konika izotropne ravnine (in Croarian), manuscript, 1995.
[3] BLANUŠA, D.: *Viša matematika,* I dio, Drugi svezak (in Croatian), Tehnička knjiga, Zagreb, 1965.
[4] CESAREC, R.: *Analitička geometrija linearnog i kvadratnog područja*, I dio (in Croatian), Školska knjiga, Zagreb, 1957.
[5] FLADT, K.: *Analitische Geometrie spezieller ebener Kurven,* Akademische Verlagsgesellschaft, Frankfurt am Main, 1962.
[6] HEFFTER, L., KOEHLER, C.: *Lehrbuch der Analytischen Geometrie I,* Teubner-Verlag, Leipzig-Berlin, 1905.
[7] ILYIN, V. A., POZNYAK, E. G.: *Linear Algebra* , Mir Publishers, Moscow, 1986.
[8] KUREPA, S.: *Uvod u linearnu algebru* (in Croatian), Školska knjiga, Zagreb, 1990.
[9] LAPAINE, M., JOVIČIĆ, D.: Grafički prikaz konika pomoću računala (in Croatian), KOG, br.1, 19-26, 1996.
[10] LAPAINE, M.: Grafički prikaz pramena konika pomoću raèunala (in Croatian), KOG, br.2, 1997.
[11] MAKAROWA, N. M.: Krivije vtorogo porijatka v ploskoj paraboličeskoj geometrii (in Russian), "Voprosi diferencijaljnoj i neevklidskoj geometrii", Učenije zapiski MG-PI im. Lenina, 222-251, 1963.
[12] NIČE, V.: *Uvod u sintetičku geometriju* (in Croatian), Školska knjiga, Zagreb, 1956.
[13] PAVKOVIĆ, B.: Geometrija Galilejevog prostora (in Croatian), lectures, 1989.
[14] SACHS, H.: *Ebene isotrope Geometrie*, Vieweg-Verlag, Braunschweig-Wiesbaden, 1987.
[15] SALMON, G., FIEDLER, W.: *Analytische geometrie der Höheren ebenen Kurven,* Teubner-Verlag, Leipzig, 1882.
[16] SAVELOV, A. A.: *Ravninske krivulje* (in Croatian), Školska knjiga, Zagreb, 1979.
[17] SEMPLE, J. G., KNEEBONE, G. T.: *Algebraic Projective Geometry,* Oxford University Press, London, 1963.
[18] STRUBECKER, K.: Geometrie in einer isotropen Ebene, Math.-naturwiss. Unterricht 15, 297-306, 343-351, 385-394, 1962.
[19] ŠČURIĆ - ČUDOVAN, V.: Zur Klassifikationstheorie der Kegelschnittb¸schel der isotropen Ebene, I. Teil, Rad JAZU 450, 41-51,1990.
[20] ŠČURIĆ - ČUDOVAN, V., SACHS, H.: Klassifikationstheorie der Kegelschnittbüschel vom Typ IV der isotropen Ebene, *I,* Rad HAZU 470, 119-137, 1995.

mr. sc. Jelena Beban-Brkić
University of Zagreb, Faculty of Geodesy
Kačićeva 26, 10 000 Zagreb, Croatia
E-mail: jbeban@geodet.geof.hr

Stručni rad
Prihvaćeno 27. 01. 1997.

MILJENKO LAPAINE

Grafički prikaz pramena konika pomoću računala

Computer-Aided Graphical Representation of Conic Section Pencils

Abstract

In one of the previous works it has been shown how graphic presentation of an individual conics can be programmed on the basis of the coefficients of its equation in the general form. In this paper the conic section pencil is explained, and it is noted that it cannot contain any number of conics of parabolic type, but that only all of them, or two, or one or none can be of such type. The conic section pencil is illustrated through several examples from cartography.

Keywords: conic, conic section pencils, map projections

Grafički prikaz pramena konika pomoću računala

SAŽETAK

U jednom prethodnom radu pokazano je kako se može programirati grafičko prikazivanje pojedine konike na temelju koeficijenata njezine jednadžbe u općem obliku. U ovome radu objašnjava se pramen konika te uočava da u njemu ne može biti bilo koji broj konika paraboličkog tipa, nego da takve mogu biti samo sve, ili dvije, ili jedna ili niti jedna. Pramen konika ilustrira se na nekoliko primjera iz kartografije.

Ključne riječi: konika, pramen konika, kartografske projekcije

1. UVOD

U radu Lapainea i Jovičića (1996) pokazano je kako se može programirati grafičko prikazivanje pojedine konike na osnovi koeficijenata njene jednadžbe u općem obliku. Takav program može se onda nadopuniti tako da služi za crtanje skupa krivulja koje pripadaju nekom pramenu konika.

Osim u geometriji, pramenovi konika susreću se i u drugim znanstvenim disciplinama. U ovom radu daje se nekoliko primjera pramenova konika koji se pojavljuju u matematičkoj kartografiji pri grafičkom prikazivanju projekcije mreže meridijana i paralela kod perspektivnih i pseudocilindričnih projekcija.

2. KONIKE

Najopćenitija jednadžba drugog stupnja od dvije varijable x i y može se napisati u obliku

$$F(x, y) = ax^2 + 2bxy + cy^2 + 2dx + 2ey + f = 0 \qquad (2.1)$$

gdje su a, b, c, d, e i f realni brojevi, i barem jedan od brojeva a, b i c različit od nule. Geometrijsko mjesto točaka (x, y) u ravnini čije koordinate zadovoljavaju jednadžbu (2.1) zove se krivulja 2. reda, konusni presjek, konika ili čunjosječnica.

Ako je $a = b = c = 0$ tada se radi o specijalnim slučajevima za koje se lako uočava da predstavljaju:

skup svih točaka ravnine, ako je $d = 0, e = 0$ i $f = 0$;

pravac, ako je $d \neq 0$ ili $e \neq 0$; (2.2)

prazan skup, ako je $d = 0, e = 0$ i $f \neq 0$.

Pretpostavimo da je bar jedan od brojeva a, b, c različit od nule. Pomoću rotacije ravnine oko ishodišta i translacije ravnine moguće je svaku koniku prikazati u standardnom ili kanonskom obliku (vidi npr. Lapaine i Jovičić 1996).

Realna simetrična matrica

$$\delta = \begin{bmatrix} a & b \\ c & d \end{bmatrix} \qquad (2.3)$$

od osnovne je važnosti pri analizi jednadžbe (2.1). Njezine svojstvene vrijednosti λ_1 i λ_2 rješenja su kvadratne jednadžbe

$$\lambda^2 - (a+c)\lambda + ac - b^2 = 0 \qquad (2.6)$$

dakle

$$\lambda_1 = \frac{1}{2}\left[a + c + \sqrt{(a+c)^2 - 4(ac - b^2)}\right] \qquad (2.7)$$

$$\lambda_2 = \frac{1}{2}\left[a + c - \sqrt{(a+c)^2 - 4(ac - b^2)}\right] \qquad (2.8)$$

Budući da se izraz ispod korijena može napisati u obliku zbroja kvadrata:

$$(a+c)^2 - 4(ac - b^2) = (a - c)^2 + 4b^2 \qquad (2.9)$$

to najprije zaključujemo da su λ_1 i λ_2 realni brojevi. Zatim, $\lambda_1 = \lambda_2$ ako i samo ako je $a = c$ i $b = 0$. Konačno, ne može biti $\lambda_1 = \lambda_2 = 0$, jer bi tada moralo biti $a = b = c = 0$, što je u suprotnosti s početnom pretpostavkom.

Ako je $\lambda_1 = \lambda_2$ tj. $a = c$ i $b = 0$, tada se lako uočava da je svaki vektor u ravnini svojstveni vektor matrice δ. Ako svojstvene vrijednosti λ_1 i λ_2 nisu međusobno jednake, onda vrijedi relacija

$$\tan\theta = \frac{\lambda_1 - a}{b} \qquad (2.10)$$

gdje smo s θ označili kut što ga svojstveni vektor v_1 koji pripada svojstvenoj vrijednosti λ_1 zatvara s pozitivnim smjerom osi x. Činjenica da osim kuta θ, relaciju (2.10) zadovoljavaju i kutovi oblika $\theta + k\pi$, $k \in Z$, ne otežava daljnju primjenu jer je očito sasvim svejedno koji ćemo od njih uzeti za smjer svojstvenog vektora v_1 (možemo uzeti npr. $\theta \in (-\pi/2, \pi/2)$).

Pri programiranju formule (2.10) moramo voditi računa

o tome da će ona zatajiti u slučaju kad je $b = 0$. Zato taj slučaj treba promatrati odvojeno. Lako se pokaže da tada mora biti $\theta = 0$.

Označimo još

$$\begin{bmatrix}\alpha\\ \beta\end{bmatrix}=\begin{bmatrix}d\cos\theta+e\sin\theta\\ -d\sin\theta+e\cos\theta\end{bmatrix} \tag{2.11}$$

Postoji devet klasa konika, tj. za zadane a, b, c, d, e i f, jednadžba (2.1) jedan je od devet tipova ravninskih krivulja koje se nazivaju konikama. Od njih su dva tipa imaginarna jer u tim slučajevima ne postoje realne točke koje bi zadovoljile jednadžbu (2.1).

Ako je matrica δ regularna, $\lambda_1\lambda_2 \neq 0$, označimo

$$f' = f - \alpha^2 / \lambda_1 - \beta^2 / \lambda_2, \tag{2.12}$$

i imamo sljedeće slučajeve:

(*i*) $\operatorname{sgn}\lambda_1 = \operatorname{sgn}\lambda_2 = \operatorname{sgn} f'$ i $f' \neq 0$,
imaginarna elipsa

(*ii*) $\operatorname{sgn}\lambda_1 = \operatorname{sgn}\lambda_2 \neq \operatorname{sgn} f'$ i $f' \neq 0$
realna elipsa

(*iii*) $\operatorname{sgn}\lambda_1 = \operatorname{sgn}\lambda_2$ i $f' = 0$
točka

(iv) $\operatorname{sgn}\lambda_1 \neq \operatorname{sgn}\lambda_2$ i $f' \neq 0$
hiperbola

(*v*) $\operatorname{sgn}\lambda_1 \neq \operatorname{sgn}\lambda_2$ i $f' = 0$
dva pravca koji se sijeku.

Ako je matrica δ singularna, a $\lambda_1 \neq 0$ i $\lambda_2 = 0$, označimo

$$f' = f - \frac{\alpha^2}{\lambda_1}, \tag{2.13}$$

i imamo sljedeće slučajeve:

(*vi1*) $\beta \neq 0$
parabola

(*vii1*) $\beta = 0$ i $\operatorname{sgn}\lambda_1 \neq \operatorname{sgn} f'$ i $f' \neq 0$,
dva paralelna pravca

(*viii1*) $\beta = 0$ i $\operatorname{sgn}\lambda_1 = \operatorname{sgn} f'$
dva imaginarna pravca

(*ix1*) $\beta = 0$ i $f' = 0$
dvostruki pravac.

Ako je $\lambda_1 = 0$ i $\lambda_2 \neq 0$, tada označimo

$$f' = f - \frac{\beta^2}{\lambda_2} \tag{2.14}$$

i imamo sljedeće slučajeve:

(*vi2*) $\alpha \neq 0$
parabola

(*vii2*) $\alpha = 0$ i $\operatorname{sgn}\lambda_2 \neq \operatorname{sgn} f'$ i $f' \neq 0$,
dva paralelna pravca

(*viii2*) $\alpha = 0$ i $\operatorname{sgn}\lambda_2 = \operatorname{sgn} f'$
dva imaginarna pravca

(*ix2*) $\alpha = 0$ i $f' = 0$
dvostruki pravac.

Za krivulje tipa (*i*) - (*iii*) kaže se da su eliptičkog, dok su krivulje tipa (*iv*) - (*v*) hiperboličkog, a (*vi*) - (*ix*) paraboličkog tipa. U prethodnom je radu (Lapaine i Jovičić 1996) potanko prikazano kako se dolazi do opisane klasifikacije te kako se svaka od navedenih realnih krivulja može nacrtati uz pomoć računala i odgovarajuće jednadžbe krivulje u parametarskom obliku.

3. PRAMEN KONIKA

Neka su

$$F(x, y) = a_1x^2 + 2b_1xy + c_1y^2 + 2d_1x + 2e_1y + f_1 = 0 \tag{3.1}$$

$$G(x, y) = a_2x^2 + 2b_2xy + c_2y^2 + 2d_2x + 2e_2y + f_2 = 0 \tag{3.2}$$

jednadžbe dviju konika. Za proizvoljni $\mu \in R$ sastavimo izraz

$$H(x, y) = F(x, y) + \mu G(x, y) \tag{3.3}$$

Polinom H je oblika

$$H(x, y) = ax^2 + 2bxy + cy^2 + 2dx + 2ey + f \tag{3.4}$$

gdje smo označili

$$a = a_1 + \mu a_2, \ldots\ldots, f = f_1 + \mu f_2 \tag{3.5}$$

Za svaki pojedini $\mu \in R$, izraz

$$H(x, y) = F(x, y) + \mu G(x, y) = 0 \tag{3.6}$$

jednadžba je konike u smislu definicije iz prethodnog poglavlja, ako je barem jedan od brojeva a, b i c različit od nule. Za zadane realne brojeve $a_1, b_1, \ldots, f_1, a_2, b_2, \ldots, f_2$ i $\mu \in R$ skup svih konika obuhvaćenih jednadžbom (3.6) zove se pramen konika. Konike pomoću kojih je pramen definiran i kojima odgovaraju jednadžbe $F(x, y)$ i $G(x, y)$ zovu se osnovne konike pramena. Bez većih teškoća moguće je proširiti razmatranja na pramenove čije su osnovne krivulje reda ≤ 2.

Za svaki čvrsti $\mu \in R$ jednadžba (3.4) predstavlja jednu krivulju iz pramena ili u specijalnom slučaju prazan skup. Tip krivulje ovisit će prvenstveno o svojstvenim vrijednostima λ_1, λ_2 matrice δ. Njena determinanta je

$$\det(\delta) = \lambda_1\lambda_2 = ac - b^2 = m\mu^2 + n\mu + p \tag{3.7}$$

gdje smo označili

$$\begin{aligned} m &= a_2c_2 - b_2^2,\\ n &= a_1c_2 + c_1a_2 - 2b_1b_2,\\ p &= a_1c_1 - b_1^2. \end{aligned} \tag{3.8}$$

Determinanta matrice δ jednaka je nuli u sljedećim slučajevima:

1. za svaki $\mu \in R$, ako je
   $m = n = p = 0$,
2. ni za koji $\mu \in R$, ako je
   $m = n = 0$, $p \neq 0$ ili $m \neq 0$, $D < 0$
3. za $\mu = -p/n$, ako je
   $m = 0$, $n \neq 0$
4. za $\mu = -p/2m$, ako je
   $m \neq 0$, $D = 0$
5. za $\mu_{1,2} = (-n \pm \sqrt{D}) / 2m$, ako je
   $m \neq 0$, $D > 0$,

gdje je $D = n^2 - 4mp$.

Odatle možemo zaključiti da u pramenu konika ne može biti bilo koji broj konika paraboličkog tipa, nego takve mogu biti samo sve, ili jedna, ili dvije ili niti jedna. Pramenovi krivulja 2. reda mogu se zadavati i istraživati na različite načine. Tako je npr. Cesarec (1957) vrlo detaljno opisao dvije njihove klasifikacije: projektivnu i afinu.

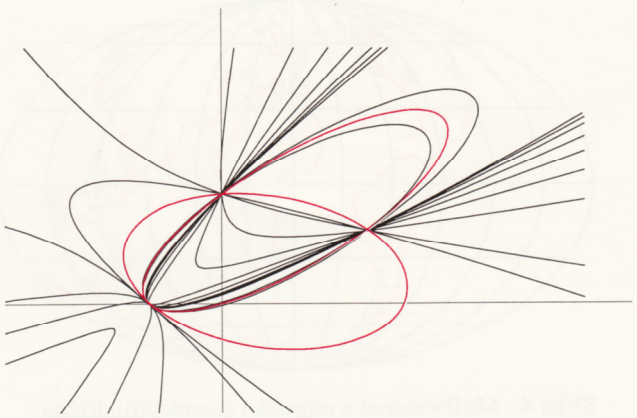

Slika 1: Pramen konika
$(24x^2+18xy+80y^2-72x-160y-240)+$
$+\mu(84x^2-202xy+200y^2+168x-600y)=0$
Crvenom linijom prikazane su osnovne konike pramena

Pri ispitivanjima pramenova konika znatno mogu pomoći odgovarajući grafički prikazi. S obzirom na relativnu složenost takvih crteža, treba klasični mukotrpni i dugotrajni način crtanja zamijeniti crtanjem uz primjenu računala. U radu Lapainea i Jovičića (1996) pokazano je kako se može programirati grafičko prikazivanje pojedine konike na osnovi koeficijenata njezine jednadžbe u općem obliku. Takav program može se sada nadopuniti, tako da služi za crtanje skupa krivulja koje pripadaju nekom pramenu. U skladu s time, autor ovog rada sastavio je odgovarajući program za crtanje proizvoljnog pramena konika. Pomoću spomenutoga programa izrađen je crtež pramena na slici 1 (primjer preuzet od Cesarca (1957)).
U sljedećih pet poglavlja opisuju se neki primjeri pramenova konika u kartografiji.

4. GNOMONSKA ILI CENTRALNA PROJEKCIJA

Jedan od lijepih primjera pramena konika u kartografiji skup je paralela u gnomonskoj ili centralnoj projekciji Zemljine sfere. Uzmimo za model Zemlje sferu polumjera $R > 0$,

$$\mathcal{S} = \{(X, Y, Z) \in \mathbf{R}^3 : X^2+Y^2+Z^2 = R^2\} \qquad (4.1)$$

i parametrizirajmo je pomoću preslikavanja

$[-\pi/2, \pi/2]\times[-\pi, \pi] \to \mathbf{R}^3$ zadanog formulama

$$\begin{aligned} X &= R\cos\phi\cos\lambda, \\ Y &= R\cos\phi\sin\lambda, \\ Z &= R\sin\phi. \end{aligned} \qquad (4.2)$$

Tako definirana parametrizacija regularna je do na zanemariv skup. Parametri ϕ i λ geografska su širina, odnosno duljina, a parametarske su krivulje paralele (ϕ = const.) i meridijani (λ = const.). Gnomonska ili centralna projekcija može se geometrijski opisati kao perspektivno projiciranje sfere na ravninu s centrom projiciranja smještenim u središtu sfere. Ako ravnina projekcije tangira sferu u točki određenoj koordinatama $(\phi_0, 0)$ tada se jednadžbe gnomonske projekcije mogu napisati (lijevi koordinatni sustav!) u obliku (Borčić 1955):

$$x = \frac{R(\sin\phi_0\cos\lambda - \cos\phi_0\tan\phi)}{\sin\phi_0\tan\phi + \cos\phi_0\cos\lambda},$$

$$y = \frac{R\sin\lambda}{\sin\phi_0\tan\phi + \cos\phi_0\cos\lambda} \qquad (4.3)$$

Lako se može izvesti da su projekcije meridijana u toj projekciji pravci koji pripadaju pramenu

$$y = \tan\lambda\,(x\sin\phi_0 + R\cos\phi_0) \qquad (4.4)$$

dok su projekcije paralela određene pramenom

$$(x\cos\phi_0 - R\sin\phi_0)^2 - \\ -\tan^2\phi[(\cos\phi_0 - R\sin\phi_0)^2 + y^2] = 0 \qquad (4.5)$$

Ako je $\phi_0 \in (0, \pi/2)$, tada su projekcije paralela:

hiperbole	ako je	$\phi \in (-\pi/2, \phi_0)$
parabola		$\phi = \phi_0$
elipse		$\phi \in (\phi_0, \pi/2)$
dvostruki pravac		$\phi = 0$
točka		$\phi = -\pi/2$ ili $\phi = \pi/2$.

Mreža meridijana i paralela u gnomonskoj projekciji uz $\phi_0 = \pi/4$ prikazana je na slici 2.

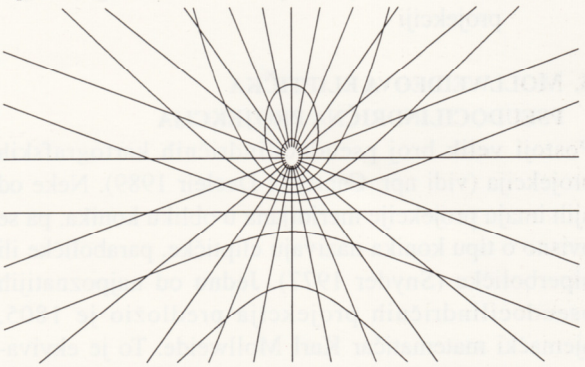

Slika 2: Mreža meridijana i paralela u gnomonskoj projekciji

5. STEREOGRAFSKA PROJEKCIJA

Neka je sfera polumjera R parametrizirana geografskom parametrizacijom (vidi prethodno poglavlje). Stereografska projekcija može se geometrijski opisati kao perspektivno projiciranje sfere na njezinu proizvoljnu tangencijalnu ravninu. Središte je projiciranja u točki što leži na sferi, dijametralno suprotno diralištu tangencijalne ravnine. Ako ravnina projekcije tangira sferu u točki određenoj koordinatama $(\phi_0, 0)$, tada se jednadžbe stereografske projekcije mogu napisati u obliku (Borčić 1955):

$$x = \frac{R(\sin\phi_0\cos\phi\cos\lambda - \cos\phi_0\sin\phi)}{1+\sin\phi_0\sin\phi + \cos\phi_0\cos\phi\cos\lambda},$$

$$y = \frac{R\sin\lambda\cos\phi}{1+\sin\phi_0\sin\phi + \cos\phi_0\cos\phi\cos\lambda} \qquad (5.1)$$

Lako se može izvesti da projekcije meridijana u toj kartografskoj projekciji pripadaju pramenu

$$Ry + \tan\lambda\cos\phi_0\,(x^2 - 2Rx\tan\phi_0 + y^2 - R^2) = 0 \qquad (5.2)$$

dok su projekcije paralela iz pramena

$$x^2 + y^2 + \frac{2R\cos\phi}{\sin\phi_0 + \sin\phi}x = 0 \qquad (5.3)$$

Iz relacije (5.2) i (5.3) može se izvesti da su za $\phi_0 \in (0, \pi/2)$, projekcije meridijana kružnice ili pravac, dok su projekcije paralela kružnice ili točka. Mreža meridijana i paralela u stereografskoj projekciji uz $\phi_0 = \pi/4$ prikazana je na slici 3.

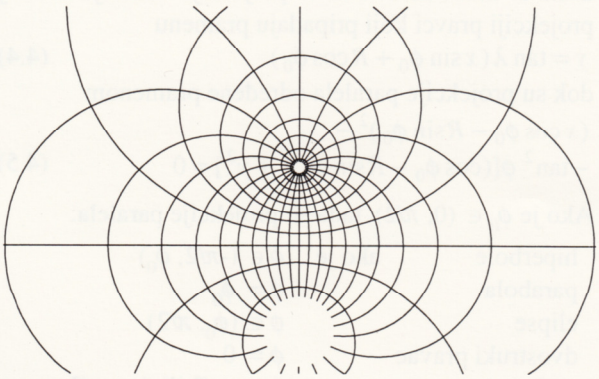

Slika 3: Mreža meridijana i paralela u stereografskoj projekciji

6. MOLLWEIDEOVA ELIPTIČKA PSEUDOCILINDRIČNA PROJEKCIJA

Postoji velik broj pseudocilindričnih kartografskih projekcija (vidi npr. Canters i Decleir 1989). Neke od njih imaju projekcije meridijana u obliku konika, pa se ovisno o tipu konika nazivaju eliptičke, paraboličke ili hiperboličke (Snyder 1977). Jednu od najpoznatijih pseudocilindričnih projekcija predložio je 1805. njemački matematičar Karl Mollweide. To je ekvivalentna pseudocilindrična projekcija s eliptičnim meridijanima, koja se prema svome autoru zove Mollweideova projekcija.

Neka je sfera polumjera R parametrizirana geografskom parametrizacijom (vidi 4. poglavlje). Mollweideova je projekcija definirana jednadžbama

$$x = R\sqrt{2}\sin\beta, \quad y = \frac{2R\sqrt{2}\,\lambda}{\pi}\cos\beta \qquad (6.1)$$

gdje je β pomoćni kut koji zadovoljava transcendentu jednadžbu

$$\sin\beta + 2\beta = \pi\sin\phi \qquad (6.2)$$

Projekcije meridijana u toj kartografskoj projekciji pripadaju pramenu elipsa:

$$\pi^2 y^2 + 4\lambda^2(x^2 - 2R^2) = 0 \qquad (6.3)$$

dok su paralele dijelovi međusobno paralelnih pravaca

$$x = R\sqrt{2}\sin\beta \qquad (6.4)$$

Na slici 4. prikazane su mreža meridijana i paralela i konture kontinenata u Mollweideovoj projekciji.

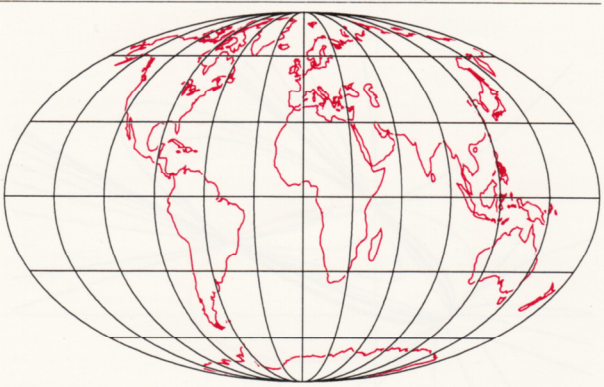

Slika 4: Mollweideova eliptička pseudocilindrična projekcija

7. CRASTEROVA PARABOLIČKA PSEUDOCILINDRIČNA PROJEKCIJA

Neka je sfera polumjera R parametrizirana geografskom parametrizacijom (vidi 4. poglavlje). Potpukovnik Craster predložio je 1929. paraboličku pseudocilindričnu projekciju koja je definirana jednadžbama (Steers 1965, Canters i Decleir 1989):

$$x = \sqrt{3\pi}\,R\sin\frac{\phi}{3}, \quad y = \sqrt{3\pi}\,R\lambda\left(2\cos\frac{2\phi}{3} - 1\right) \qquad (7.1)$$

Projekcije meridijana u toj kartografskoj projekciji dijelovi su parabola koje pripadaju pramenu:

$$\pi\sqrt{3\pi}\,Ry + \lambda(4x^2 - 3\pi R^2) = 0 \qquad (7.2)$$

dok su paralele dijelovi međusobno paralelnih pravaca

$$x = \sqrt{3\pi}\,R\sin\frac{\phi}{3} \qquad (7.3)$$

Na slici 5. prikazani su mreža meridijana i paralela i konture kontinenata u Crasterovoj projekciji.

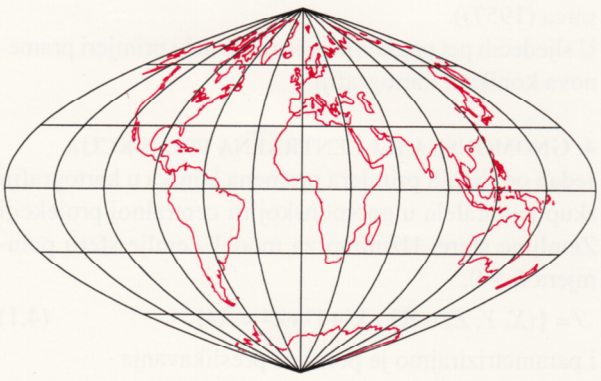

Slika 5: Crasterova parabolička pseudocilindrična projekcija

8. PUTNINŠOVA P_5 HIPERBOLIČKA PSEUDOCILINDRIČNA PROJEKCIJA

R. V. Putniņš predložio je 1934. dvanaest pseudocilindričnih projekcija, a svaka od njih ima meridijane u obliku elipsa, parabola ili hiperbola (Putniņš 1934).

Neka je sfera polumjera R parametrizirana geografskom parametrizacijom (vidi 4. poglavlje). Putninšova P_5 hiperbolička pseudocilindrična projekcija definirana je jednadžbama

$$x = k R \phi, \quad y = k R \lambda (2 - \sqrt{1 + 12\phi^2 / \pi^2}) \qquad (8.1)$$

gdje je k = 1.01346. Projekcije meridijana u toj kartografskoj projekciji dijelovi su hiperbola koje pripadaju pramenu:

$$(x - k R \lambda)^2 - \lambda^2 (12 y^2 / \pi^2 + k^2 R^2) = 0 \qquad (8.2)$$

dok su paralele dijelovi međusobno paralelnih pravaca

$$x = k R \phi \qquad (8.3)$$

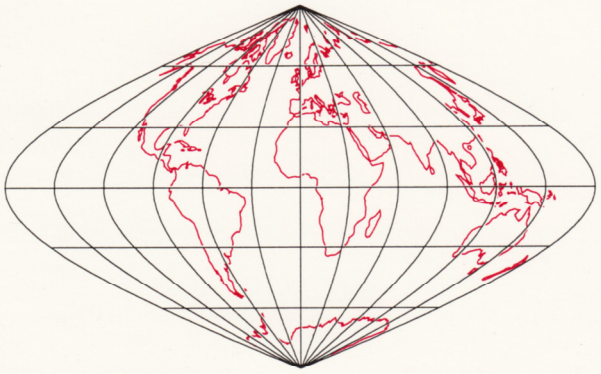

Slika 6: Putninšova P_5 hiperbolička pseudocilindrična projekcija

Na slici 6. prikazani su mreža meridijana i paralela i konture kontinenata u Putninšovoj P_5 projekciji. Uočava se da je pramen (8.2) oblika

$$F(x,y) + \lambda G(x,y) + \lambda^2 H(x,y) = 0$$

Autoru ovoga rada nije poznato jesu li se matematičari bavili proučavanjem takvih pramenova konika.

LITERATURA

BORČIĆ , B. (1955): *Matematička kartografija*, Tehnička knjiga, Zagreb.

CANTERS, F. i DECLEIR, H. (1989): *The World in Perspective*, John Wiley & Sons, Chichester, New York, Brisbane, Toronto, Singapore.

CESAREC, R. (1957): *Analitička geometrija linearnog i kvadratnog područja*, I. dio. Školska knjiga, Zagreb.

LAPAINE, M. i JOVIČIĆ, D. (1996): Grafički prikaz konika pomoću računala, KoG, 1, 19-26.

PUTNINŠ, R. V. (1934): Jaunas projekcijas pasaules kartem, Geografiski raksti, Folia Geographica 3 and 4, 180-209.

SNYDER, J. P. (1977): A Comparison of Pseudocylindrical Map Projections, The American Cartographer, Vol 4, No. 1, 59-81.

STEERS, J. A. (1965): *An Introduction to the Study of Map Projections,* University of London Press Ltd, London.

Doc. dr. sc. Miljenko Lapaine
Geodetski fakultet Sveučilišta u Zagrebu
10 000 Zagreb, Kačićeva 26
tel.: 456 1222,
faks: 482 8081
e-mail: Miljenko.Lapaine@public.srce.hr

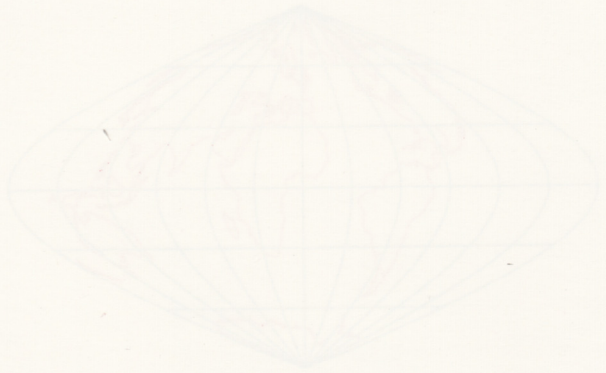

Professional paper
Accepted 27.04. 1997

DAGMAR SZARKOVÁ

Computer Aided Calculation of Characteristics Points of Some Envelope Helical Surfaces

Computer Aided Calculation of Characteristics Points of Some Envelope Helical Surfaces
ABSTRACT
Presented calculations and the choice of variables $u,v \in [0,1]$ of the given basic surface φ enable the creation of a versatile programme for the graphical processing of the characteristics not only of the helical but also of the rotational envelope surface Φ defined by the conical or cylindrical surface. Basic (conical or cylindrical) surface j can be generated from the basic curve defined by the vector function $\mathbf{r}(u)$, for $u \in [0,1]$ (1) applying a class of transformations defined by the matrix $\mathbf{T}(v)$, for $v \in [0,1]$ (2). The combined analytical and synthetical method resultes in the parametric equations of the characteristics (3) and in the coordinates of the meridian section points.
Keywords:
envelope surface, characteristics, meridian section, creative space, creative representation

Izračunavanje karakterističnih točaka ovojnice helikoidne plohe pomoću računala
SAŽETAK
Prikazana izračunavanja i izbor varijabli $u,v \in [0,1]$ zadane osnove plohe φ omogućavaju kreiranje programa za grafičku obradu osobitosti ne samo helikoidne, već i rotacijske ovojne plohe Φ definirane stožastom ili valjkastom plohom. Osnovna (stožasta ili valjkasta) ploha j može biti generirana iz osnovne krivulje definirane vektorskom funkcijom $\mathbf{r}(u)$, za $u \in [0,1]$ (1) primjenjujući klasu transformacija definiranu matricom $\mathbf{T}(v)$, za $v \in [0,1]$ (2). Kombinirana analitička i sintetička metoda rezultira parametarskim jednadžbama karakteristika (3) i koordinatama točaka meridijanskih presjeka.
Ključne riječi:
ovojna ploha, karakteristike, meridijanski presjek, kreativni prostor, kreativni prikaz

An envelope surface Φ is created by a continuous movement of a basic surface φ. Characteristics is a curve segment along which the envelope surface Φ touches the basic surface φ. At any point of the characteristics there exists a common tangent plane τ and a normal $\mathbf{c}$ to the basic surface φ and the envelope surface Φ.

The same envelope surface Φ can be created by the continuous movement of either characteristics, or the basic surface φ.

Let us deal with an envelope helical surface Φ created by a helical movement (this movement is a geometric transformation concatenated from a revolution about the axis o and a translation in the direction of the vector collinear to the axis o of revolution) of a conical or cylindrical surface φ. An envelope rotational surface is a special type of the envelope helical surface with the helical movement pitch $|\mathbf{z}_v|$ ($\mathbf{z}_v$ is the translation vector corresponding to the angle of revolution equal to 2π) equal to zero.

Study and realization of the construction of the envelope helical and rotational surface characteristics points are very important in the mechanical engineering practise. The classical construction of the characteristics points (mentioned in Kopincová [1]) can be substituted by computer processing and following graphical output.

In the Creative space (defined in Velichová [6] and described in Velichová [5]), in which we work with homogeneous coordinates (in correspondence with Qiulin [2]), let us create the basic surface φ. Let us define the basic curve segment of the conical or the cylindrical surface by a vector function

$$\mathbf{r}(u) = (x(u), y(u), z(u), 1) \qquad (1)$$

such, that it is defined and at least $C^{(1)}$ for $u \in [0,1]$ and its first derivative $(x'(u), y'(u), z'(u), 0)$ is a non-zero vector for $u \in [0,1]$.

Let the generating principle be the class of transformations represented by a regular square matrix of rank 4 in a form

$$\mathrm{T}(v) = \begin{pmatrix} q(v) & 0 & 0 & 0 \\ 0 & q(v) & 0 & 0 \\ 0 & 0 & q(v) & 0 \\ x_1 v & y_1 v & z_1 v & 1 \end{pmatrix} \quad v \in [0,1] \qquad (2)$$

where function $q(v) = 1 - v$ is pertinent to the conical

surface and function $q(v) = 1$ to the cylindrical surface. Constants x_1, y_1, z_1 are coordinates of the conical surface vertex or they are coordinates of the cylindrical surface direction vector.

The analytic representation of the basic conical or the cylindrical surface φ can be then expressed as follows

$\mathbf{r}(u,v) = \mathbf{r}(u) \,.\, \mathbf{T}(v) =$

$= (x(u)\, q(v) + x_1\, v,\ y(u)\, q(v) + y_1\, v,\ z(u)\, q(v) + z_1\, v,\ 1)$

where $(u,v) \in [0,1] \times [0,1]$.

Let the clockwise helical movement with the axis o in the coordinate axis z be defined by the reduced pitch $v_0 = |\mathbf{z}_v|/2\pi$ (with respect to Velichová [6]) (see Fig.1).

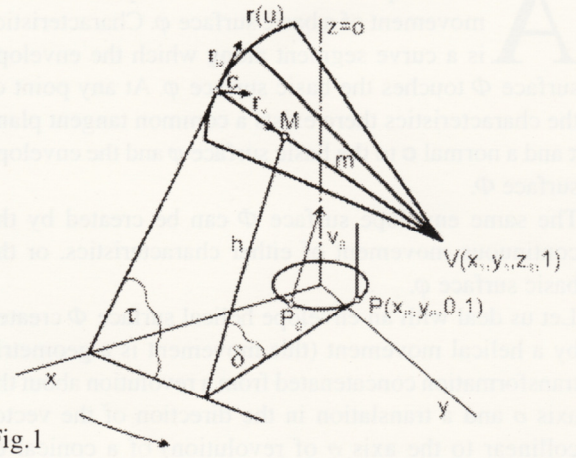

Fig.1

The point M of the characteristics can be determined as the intersection point of the line m on the surface φ and the auxiliary characteristics h of the tangent plane τ to the surface φ incident with the line m.. Characteristics h is a line on the surface of tangents to the helics (i.e. the envelope surface created from the tangent plane τ by the given helical movement). Characteristics $h = \tau \cap \delta$, where δ is a plane determined by the point P, the direction vector $\mathbf{c}$ and the direction vector (0,0,1,0) of the axis o.

Parametric equations of the envelope helical surface characteristics (if it exists) will be

$$\begin{aligned} x &= x(u)\, q(\,\xi(u)\,) + x_1\, \xi(u) \\ y &= y(u)\, q(\,\xi(u)\,) + y_1\, \xi(u) \\ z &= z(u)\, q(\,\xi(u)\,) + z_1\, \xi(u) \end{aligned} \qquad (3)$$

for those values $u \in [0,1]$, for which $\xi(u) \in [0,1]$, while

$$\xi(u) = \frac{c_2(x(u) - x_P) + c_1(-y(u) + y_P)}{-c_2(x(u)\,a + x_1) + c_1(y(u)\,a + y_1)} \qquad (4)$$

and

$$\begin{aligned} c_1 &= a(y'(u)\,z(u) - z'(u)\,y(u)) + y'(u)\,z_1 - z'(u)\,y_1 \\ c_2 &= a(-x'(u)\,z(u) + z'(u)\,x(u)) - x'(u)\,z_1 + z'(u)\,x_1 \\ c_3 &= a(x'(u)\,y(u) - y'(u)\,x(u)) + x'(u)\,y_1 - y'(u)\,x_1 \end{aligned}$$

$$x_P = \frac{v_0\, c_2\, c_3}{c_1^2 + c_2^2}(-1)^i$$

$$x_P = \frac{-v_0\, c_1\, c_3}{c_1^2 + c_2^2}(-1)^i$$

$a = q'(v) = \text{const}$

where vector $\mathbf{c} = (\,c_1\,,\, c_2\,,\, c_3\,,\, 0\,)$ is the direction vector of the basic surface φ normal and therefore it is also the direction vector of the envelope Φ normal in the point M of the characteristics.

$x_P\,,\ y_P$ - are coordinates of the auxiliary point $P(x_P\,,\ y_P,\ 0,1)$.

Constant value $i = 1$ is valid for clockwise and $i = 2$ for anticlockwise helical movement.

A special attention must be payed to the situations, in which the value c_1 and the value of the denominator of the relation (4) are equal to zero.

The shape of the envelope surface can be better comprehended by its meridian section than by the characteristics, which is usually a space curve segment. Coordinates of the point $M^* = (x^*, y^*, z^*, 1)$ located on the meridian section in the xz-plane can be obtained from the coordinates of the point $M = (x_M\,,\ y_M\,,\ z_M\,,\ 1)$ on the characteristics as the solutions of the following equations

$$x^* = \pm\sqrt{x_M^2 + y_M^2}$$

$$y^* = 0$$

$$z^* = z_M + \omega\, v_0$$

where ω is the directed angle of the revolution about the axis o to the xz-plane oriented in the helical movement direction.

Presented calculations and the choice of variables $(u,v) \in [0,1] \times [0,1]$ of the given basic surface enable the creation of a versatile programme for the graphical processing of the characteristics not only of the helical but also of the rotational (if $v_0 = 0$) envelope surface defined by the conical or cylindrical surface - see figures. In the Fig.2 there is presented the characteristics and the principal meridian of the envelope rotational surface created by the revolution of a conical surface with the basic curve in a spatial Viviani curve.

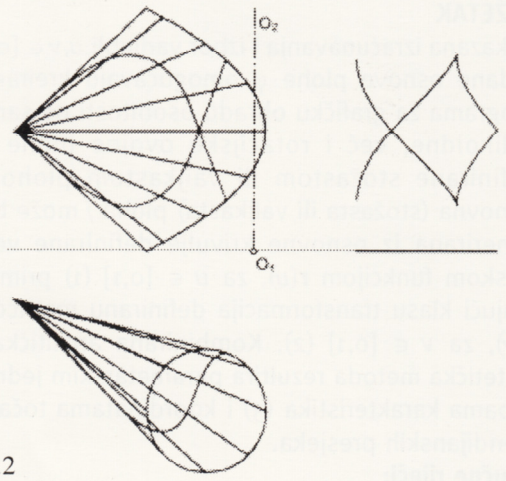

Fig.2

The illustration of the envelope surface generated by the helical movement of the basic conical surface characteristics, the basic curve of which is the circle, is in the Fig.3. The same movement of the envelope helical surface meridian produces the same envelope surface (see Fig.4).

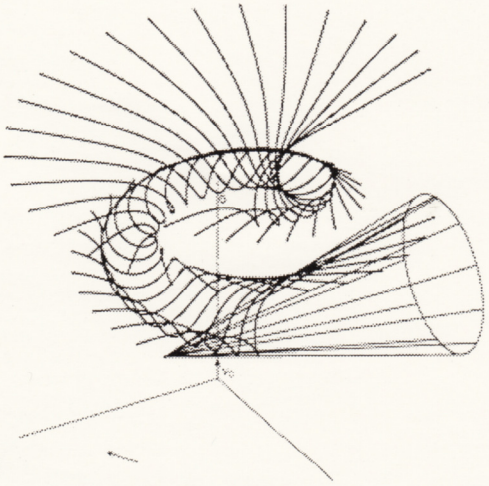

Fig.3

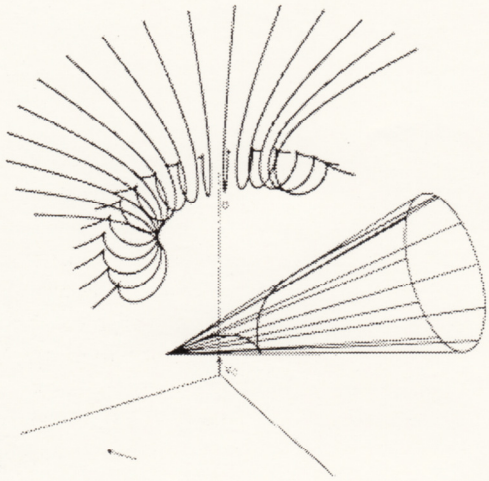

Fig.4

Fig.5 ilustrates a helical surface created by the characteristics of a basic cylindrical surface which basic curve segment is a circle. Other examples of the envelope surfaces can be found in the papers Szarková [3] and Szarková [4].

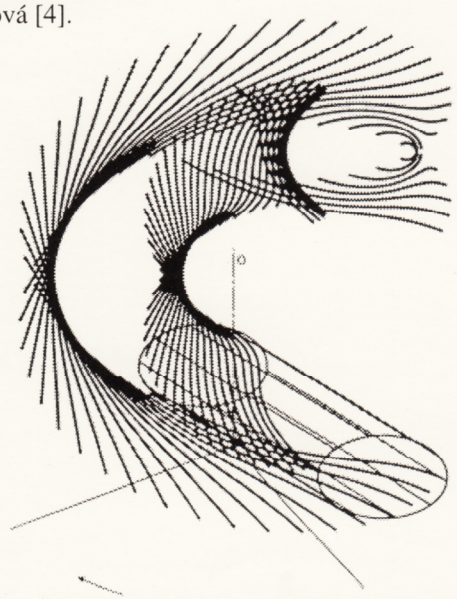

Fig.5

Graphical access to the processing of the given problematic enables a more effective function in the sphere of the machining tool design, because the basic surface of the desirable envelope surface can be fixed interactively and also all irregular cases, when the envelope surface cannot be defined or it is of an unsuitable shape, can be omitted.

Presented figures are examples of the characteristics, the meridian section and the basic surface φ of the envelope surface Φ in Monge projection method and Axonometry projections are outputs of the programme (written by the autor) on the screen and digital plotter.

REFERENCES

[1] KOPINCOVÁ, E.: Počítačem podporovaná konstrukce obalové plochy, Sborník 13. semináre odborné skupiny pro deskriptivní geometrii, počítačovou grafiku a technické kreslení, Pernink 14.-17.9.1993, JČMF Západočeská univerzita v Plzni, 1993, Czech republic, pp. 84-88

[2] QIULIN, D., DAVIES, B. J.: *Surface Engineering Geometry for Computer - Aided Design and Manufacture*, Ellis Horwood Limited, Chichester, 1987

[3] SZARKOVÁ, D.: Graphical Processing of a Characteristic and Meridian Section of a Rotational Envelope Surface Created by a Conical or Cylindrical Surface, Abstract, Konstruktive Geometrie, Balatonföldvár 27.9.-1.10.1993, Budapest, August 1993, Hungary

SZARKOVÁ, D.: Grafické spracovanie charakteristiky a meridiánového rezu rotačnej obalovej plochy vytvorenej kužel'ovou a valcovou plochou, Sborník 13. semináre odborné skupiny pro deskriptivní geometrii, počítačovou grafiku a technické kreslení, Pernink 14.-17.9.1993, JČMF Západočeská univerzita v Plzni, 1993, Czech republic, pp. 94-97

[4] SZARKOVÁ, D.: Graphical Processing of a Characteristic and Meridian Section of a Helical Envelope Surface, Proceedings of Seminars on Computational Geometry, SjF STU Bratislava and MtF STU Trnava, 1993/94, Slovak republic, pp. 24-29

SZARKOVÁ, D.: Grafické spracovanie skrutkovej obalovej plochy vyvorenej kužel'ovou a valcovou plochou, Sborník 14. semináre odborné skupiny pro deskriptivní geometrii, počítačovou grafiku a technické kreslení, Bílá 19.-22.9.1994, Západočeská univerzita v Plzni, 1994, Czech republic, pp. 55-60

[5] VELICHOVÁ, D.: Creative Geometry, Procedings of the 6th International Conference on Engineering Computer Graphics and Descriptive Geometry, Tokyo 1994, Japan, pp. 302-304

[6] VELICHOVÁ, D.: *Konštrukčná geometria*, Vydavatel'stvo STU, Bratislava,1996, Slovak Republic

RNDr. Dagmar Szarková
Department of Mathematics,
Mechanical Engineering Faculty
Slovak Technical University
Námestie Slobody 17, 812 31 Bratislava, Slovakia
tel: +4217 3596 394, fax: +4217 325 749
email: szarkova@dekan.sjf.stuba.sk

Professional paper
Accepted 29.04.1997

DANIELA RICHTÁRIKOVÁ

3D Polyhedra Scenes and the Triangulation

3D Polyhedra Scenes and the Triangulation
ABSTRACT.
One of the possible utilizations of the planar region triangulation is presented in this paper - a part of the visibility solution in the visualization of the general 3D scene consisting of disjoint polyhedra by the means of computer.
Keywords:
triangulation, potential visibility, polyhedra scene visibility, triangle intersection

3D poliedarne scene i triangulacija
SAŽETAK
Jedna od mogućih primjena triangulacije područja u ravnini prikazana je u ovom radu - dio rješenja vidljivosti pri vizualizaciji opće 3D scene koji se sastoji u rastavljanju poliedra uz pomoć računala.
Ključne riječi:
triangulacija, potencijalna vidljivost, vidljivost scene poliedra, presjek trokuta

INTRODUCTION

The term *triangulation* is used here for the decomposition of the connected planar region bounded by closed polygons (not intersecting each other) into elemental regions - triangles. The triangulation gives an opportunity to solve some of the problems in computer geometry of polyhedra in simply and easy understandable way, e.g. visualisation of polyhedra, determination and drawings of their intersections, calculation of their boundary surface, etc, and more, in order to simplify and make this field more understandable and attractive for students it can be used in teaching process at universities as well.

ASSUMPTIONS

The visualization of the scene can be obtained in a user specified view and polyhedra arrangement. The scene is defined by all the faces of disjoint polyhedra. They are filed in attaching the same exterior orientation.
The face orientation determines potential visibility. *Potentially visible* faces (abr. PV faces) are concidered to be the faces of the same orientation as their images in the projection plane [8].

SCENE ANALYSIS

Three different groups of PV faces arrangements can be distinguished, according to their mutual location to the centre of projection:

1. group. PV faces do not overlay; i.e. no PV face is hidden behind another one of the same or other polyhedron.
Solution: All PV faces are displayed.

2. group. PV faces are hidden behind other ones. Their images intersect in a "planar" intersection (bounded planar region containing at least three noncollinear points). PV faces can be ordered in the sequence $\{F_i\}_{i=1}^{n}$ according to their mutual position towards the centre of projection (Fig.1).

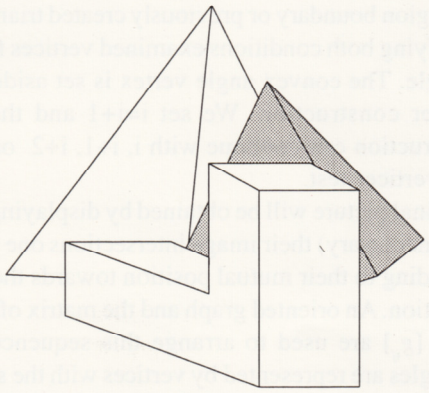

Fig. 1

The mutual position of two plain regions can be determined by any of those region points that lay on one projecting ray (projector) and so produce their image intersection (Fig. 2).

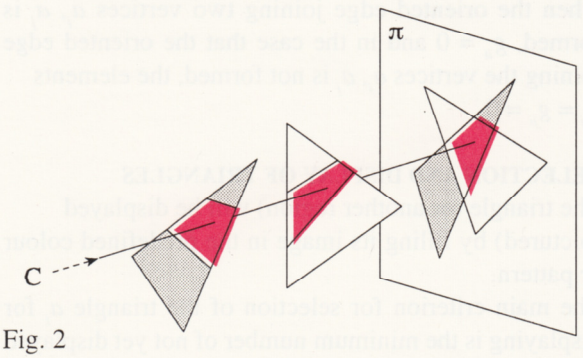

Fig. 2

Solution: PV faces are displayed gradually in the order corresponding to the sequence $\{F_i\}_{i=1}^{n}$.

3. group. Images of PV faces intersect in a "planar" region but faces cannot be ordered in the sequence $\{F_i\}_{i=1}^{n}$ (Fig. 3).

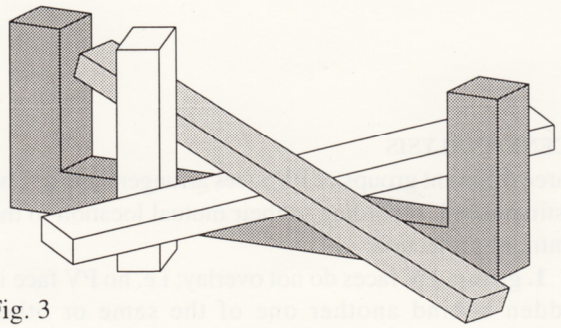

Fig. 3

Solution:: PV faces are triangulated - decomposed into elemental figures - triangles a_i, i=1,..n. For this purpose several algorithms can be used [e.g.3]. Our method is based on the triangle generation test of three suceeding polygon vertices: i, i+1, i+2 [8]. Two conditions are examined:

a) the vertices create the convex angle

b) none of the currently created edges intersect the region boundary or previously created triangle edges.

Satisfying both conditions examined vertices formed the triangle. The convex angle vertex is set aside from the further construction. We set i=i+1 and the triangle construction can continue with i, i+1, i+2 or i+2, i+3, i+4 vertices test.

The final picture will be obtained by displaying triangles or (if necessary) their image intersections one after other according to their mutual position towards the centre of pojection. An oriented graph and the matrix of incidence $\mathbf{G}_n = [g_{ij}]$ are used to arrange this sequence [1], [5]. Triangles are represented by vertices with the same notes a_i, i =1,..n. The directed edge joining two vertices a_i, a_j is formed only if the triangles a_i, a_j are located in two different faces and their images intersect in the "planar" region; the triangle a_i is located closier to the centre of projection than the triangle a_j and so the former overlays the latter (Fig. 2). Corresponding elements in the matrix of incidence $\mathbf{G}_n$ are defined in this way: $g_{ij} = 1$, $g_{ji} = 0$ when the oriented edge joining two vertices a_i, a_j is formed, $g_{ii} = 0$ and in the case that the oriented edge joining the vertices a_i, a_j is not formed, the elements $g_{ij} = g_{ji} = 0$.

SELECTION AND DISPLAY OF TRIANGLES

The triangle (or another region) will be displayed (pictured) by filling its image in the predefined colour or pattern.

The main criterion for selection of the triangle a_i for displaying is the minimum number of not yet displayed triangles laying "under" (or behind) the triangle a_i, i.e. the triangles that are located in the longer distance to the centre of projection than the triangle a_i and have a "planar" intersection with the triangle a_i in images. So these triangles are overlayed by the triangle a_i in the predefined view. This fact is examined in the matrix $\mathbf{G}_n$ via the parameter $S_i = \sum_{j=1}^{n} g_{ij}$ for the current i.

If $S_i = 0$ then non of not yet displayed triangles is located "under" the triangle a_i. The triangle a_i can be displayed and as follows, eliminated from the further process. Corresponding row and column are omitted in the matrix $\mathbf{G}_n$. The next triangle can be examined.

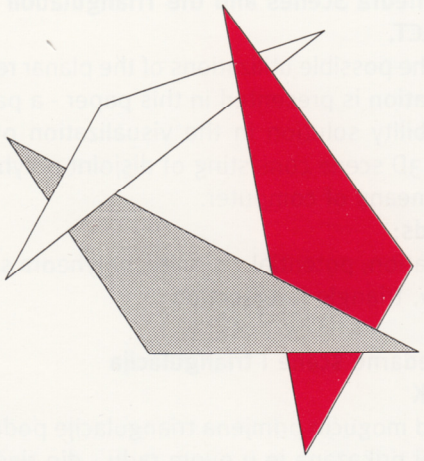

Fig. 4

If $S_i > 0$ for all i = 1,...n no triangle lays "under" the other ones (Fig. 4). Let $S_{min} = minS_i$. Two cases are possible:

1. $S_i = S_{min}$ for unique one i. The triangle a_i is selected.

2. $S_i = S_{min}$ for i of number $f, f > 1$. Let $\{r_k\}_{k=1}^{n}$ is the sequence of indexes i. Now the triangle a_i will be selected only from the triangles a_{r_k} according to the main criterion (minimum number of not yet displayed triangles a_{r_k} laying "under" the triangle a_i) with respect to the mutual position of triangles a_{r_k} only. If $S_{min} = S_{r_k}$ for all r_k, the triangle will be selected in the comparisn test of the mutual position of triangles in pairs. That triangle in the tested pair will be chosen which is "under" the other one. The selected triangle will be repeatedly compared to the next triangle from the sequence $\{a_{r_k}\}_{k=1}^{f}$.

Selected triangle a_i can be displayed immediately, and the information about not yet displayed trianges a_j laying "under" the triangle a_i have to be stored, for instance in a row b_i of another matrix $\mathbf{P}_n = [b_{lh}]$ - the matrix of intersections, by setting the elements b_{ij} =1. After each triange a_j displaying the intersection of the triangle a_i, a_j images will be filled in the colour of the triangle a_i (The triangle a_i was displayed before the triangle a_j although the triangle a_i is located over the triangle a_j).If several triangles a_i, $i = r_v$, v = 1,...t, have been already displayed in the time of triangle a_j displaying, (filling in the intersections of triangles a_{r_v}, a_j images will be ordered and realised with respect to the main criterion.

The problem of selecting a triangle is solved in all levels by using the same algorithm that can be recursively called and applied on the current sequence of triangles and so the scene with arbitrary overlaying faces can be visualized.

DETERMINATION OF THE TRIANGLE IMAGES INTERSECTION

Construction of the intersection of the triangle images is based on the region orientation of the boundary polygon vertices [7].

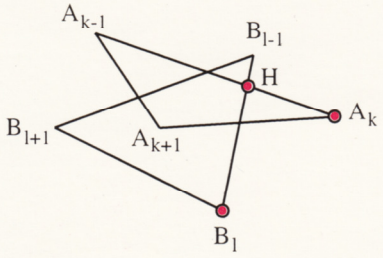

Fig. 5

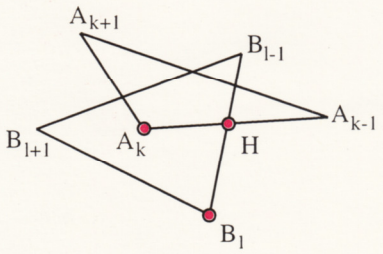

Fig. 6

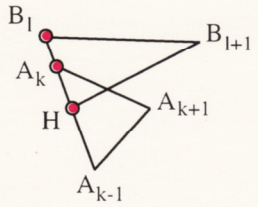

Fig. 7

Let *A*, *B* be the concordantly oriented images of the triangles. The first vertex of the intersection can be an intersection point of two arbitrary sides. The succesor can be found as the intersection point of sides or as the vertex on the boundary of that triangle *A*, for which the three points H, A_k, B_l (H-topical vertex of the intersection, A_k - the successive vertex of the triangle *A* and B_l - the successive vertex of the triangle B (Fig. 5, 6, 7) are in the same orientation as the both triangles *A*, *B*. Having found the succeding vertex equal to the first one the determination of the intersection is finished (Fig. 8).

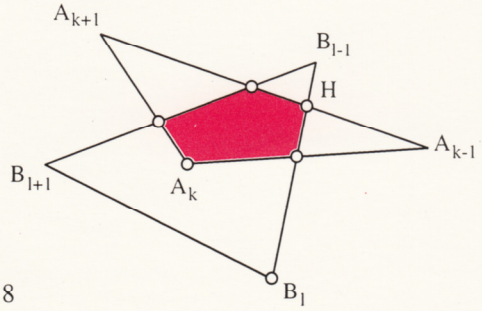

Fig. 8

CONCLUSION

Visibility represents quite an important and big part in the field of computer graphics. There have been a lot of visibility algorithms worked out [6]. They differ in various ways with respect to complexity, universality, the choice of examined phenomena, methods, etc. Our algorithm can be tabled next to the Newell's and Sancha's one [2] in which the polyhedra faces are ordered into the display sequence according to the "z- depth", z denotes the direction of the view. The problem of cyclic overlaying (Fig. 4) is suggested to be solved by the division of the problematic polygon into two parts, that are to be ordered then as new polygons into the sequence. The aim of the paper is to describe the visibility problem solving in displaying the general polyhedra scenes *via the triangulation* of polyhedra faces. This method was elaborated for the purposes of the educational process. It solves the problem in understandable way and enables to visualize polyhedra scenes in any view and arrangement. Even very complex scenes with overlaying of polyhedra faces (rare in the space) are allowed.

REFERENCES

[1] BEKA, J., HIC, P.: Charakteristické polynómy turnajov, Zbornik Matem 2. Nitra, PdF 1982

[2] NEWELL, M.E., NEWELL, R.G., SANCHA, T.L.: A New Approach to the shaded Picture Problem, Proc.ACM Nat. Conf.,1972

[3] PREPARATA, F., SHAMOS, M.I.: *Computational Geometry*, Springer - Verlag, New York, 1985

[4] RICHTÁRIKOVÁ, D., ZÁMOŽIK, J.: Námety s využitim triangulácie, Zbornik 23. Konference o matematice na VŠTEP, Praha 1994

[5] RICHTÁRIKOVÁ, D., ZÁMOŽIK, J.: Guided Split on Directed Graph, Proceedings of Seminars on Computational Geometry, SjF STU Bratislava, MtF STU Trnava 1993/1994

[6] RUŽICKÝ, E., FERKO, A.: Počitačová grafika a spracovanie obrazu, Vydavatel'stvo Sapetia, Bratislava 1995

[7] SUROVÁ, A., ZÁMOŽIK, J.: The Analysis of the Operations upon Regions Via Method of Determinants, Proceedings of Seminar on Computational Geometry, STU 1992/1993

[8] ZÁMOŽIK, J., VRANKOVÁ, E., MIŠÚTOVÁ, M., STÚPALOVÁ, H.: Základy počítačovej grafiky, Vydavatel'stvo STU, Bratislava1996

RNDr.Daniela Richtáriková
Department of Mathematics,
Mechanical Engineering Faculty
Slovak Technical University
Námestie Slobody 17, 812 31 Bratislava, Slovakia
tel: +4217 3596 394, fax: +4217 325 749
email: richtarikova@dekan.sjf.stuba.sk

Stručni rad
Prihvaćeno 28.11.1997.

SONJA GORJANC

Izvođenje pet tipova pravčastih ploha 4. stupnja

Generation of Five Types of Ruled Quartics
ABSTRACT
According to Sturm ([4], [7]), the ruled quartics are classified into twelve types. In this paper only five types, where directing curves can be conics and straight lines are selected and there is one or more examples given for each of them. In these examples we described the constructive generation of the surfaces, and by means of their parametric equations we made the graphics in *Mathematica* 3.0.
Keywords: ruled quartics, ruled surfaces

Izvođenje pet tipova pravčastih ploha 4. stupnja
SAŽETAK
Između dvanaest vrsta pravčastih ploha 4. reda, po Sturmovu ([4], [7]) razvrstavanju, izdvojeno je pet kod kojih se za ravnalice mogu odabrati konike i pravci. Za svaku od tih pet vrsta ploha dan je jedan ili više primjera. U primjerima su opisani načini njihova konstruktivnog izvođenja, a pomoću parametarskih jednadžbi napravljeni su crteži u programu *Mathematica* 3.0.
Ključne riječi: pravčate kvartike, pravčaste plohe

UVOD

Svakom točkom pravčaste plohe prolazi barem jedan pravac te plohe, što daje velik broj mogućnosti primjene pravčastih ploha u graditeljstvu. Stoga je konstruktivna obrada tih ploha sadržaj gotovo svake knjige koja se upotrebljava u nastavi geometrije na tehničkim fakultetima u nas (npr. [1], [2], [5], [8]). Cilj je ovoga rada prikazati jednostavnost njihova izvođenja i raznolikost njihovih oblika. Za grafičke prikaze ploha upotrijebiti ćemo programski sustav *Mathematica 3.0.*

1. OPĆENITO O ALGEBARSKIM PRAVČASTIM PLOHAMA

U ovom poglavlju navodimo neke opće definicije i teoreme vezane uz pravčaste plohe. Navodimo ih bez dokaza, za koje se čitatelja upućuje na bilo koju od knjiga [10], [7], [8] ili [9].

Prostor za naša razmatranja proširen je euklidski prostor (model projektivnog prostora), tj. euklidski prostor nadopunjen neizmjerno dalekim elementima. Prostor sadrži ∞^3 točaka i ∞^4 pravaca. Stoga se u njemu mogu promatrati:

plohe - skupovi od ∞^2 neprekinuto povezanih točaka,
krivulje - skupovi od ∞^1 neprekinuto povezanih točaka,
kompleksi - skupovi od ∞^3 neprekinuto povezanih pravaca,
kongruencije - skupovi od ∞^2 neprekinuto povezanih pravaca,
pravčaste plohe - skupovi od ∞^1 neprekinuto povezanih pravaca.

Pravčasta ploha nastaje neprekinutim gibanjem nekog pravca pri kojem se on sam u sebi ne pomiče. Osnovna je podjela tih ploha je na *razmotljive*, koje se mogu razviti u jednu ravninu bez kidanja, i *vitopere* kod kojih je takvo razvijanje nemoguće. Skup točaka kojih Kartezijeve koordinate zadovoljavaju neku algebarsku jednadžbu n-toga stupnja nazivamo *algebarskom* plohom n-toga reda. U ovom radu bavit ćemo se isključivo vitoperim algebarskim pravčastim plohama.

Algebarske plohe i krivulje, kompleksi i kongruencije razvrstavaju se prema njihovu redu i razredu. Konstruktivnoj obradi prostora primjerene su geometrijske interpretacije tih pojmova kojima se služi sintetička geometrija.

— Red (razred) algebarske plohe jednak je broju njezinih točaka (dirnih ravnina) incidentnih s nekim pravcem. Ako su red i razred plohe jednaki onda taj broj nazivamo njezinim stupnjem.

— Red prostorne krivulje jednak je broju njezinih točaka incidentnih s nekom ravninom, dok joj je razred jednak broju dirnih ravnina incidentnih s nekim pravcem.

— Red ravninske krivulje jednak je broju njezinih sjecišta s nekim pravcem incidentnim s ravninom krivulje, dok joj je razred jednak broju tangenata incidentnih s nekom točkom ravnine krivulje.

— Red kompleksa jednak je redu stošca što ga čine sve zrake (pravci koji pripadaju kompleksu) incidentne s nekom točkom, dok mu je razred jednak razredu krivulje koju omataju sve njegove zrake u nekoj ravnini. Red i razred nekog kompleksa uvijek su jednaki.

— Red (razred) kongruencije jednak je broju njezinih zraka incidentnih s nekom točkom (ravninom).

Pri tim prebrojavanjima računaju se realni i imaginarni elementi.

Izvođenje

Pravčaste plohe kao sustave od ∞^1 neprekinuto povezanih pravaca u prostoru možemo najopćenitije promatrati kao presjeke triju kompleksa ili kao presjek jedne kongruencije i jednoga kompleksa. Dosljedno sprovođenje tog drugog načina izvođenja zahtijevalo bi, međutim,

značajnije udubljivanje u pravčasti prostor. Zbog toga će predmet našeg proučavanja biti uglavnom one pravčaste plohe koje nastaju kao presjek triju kompleksa zadanih algebarskim krivuljama. U tom smislu pravčaste se plohe mogu promatrati kao skupovi od ∞^1 neprekinuto povezanih pravaca koji sijeku tri algebarske krivulje k_1, k_2 i k_3. Krivulje k_1, k_2 i k_3 nazivamo *ravnalicama*, a pravce koji ih sijeku *izvodnicama* plohe. (Slika 1)

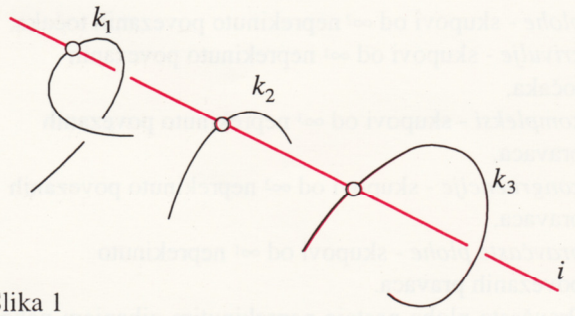

Slika 1

Red i razred

Ako su redovi krivulja k_1, k_2, k_3 redom n_1, n_2 i n_3 te ako se one ne sijeku, red pravčaste plohe jednak je $2\,n_1 n_2 n_3$. Ako se, međutim, krivulje k_2 i k_3 sijeku u jednoj točki raspast će se pravčasta ploha reda $2\,n_1 n_2 n_3$ na stožac s vrhom u tom sjecištu i osnovicom k_1 (slika 2) te plohu reda $2\,n_1 n_2 n_3 - n_1$.

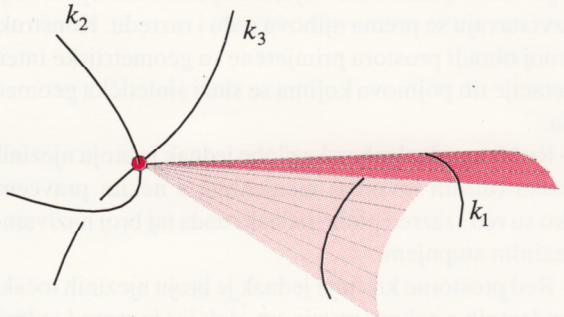

Slika 2

Stoga općenito vrijedi: ako se krivulje k_1 i k_2 sijeku u s_3 točke, krivulje k_1 i k_3 u s_2 točke, a krivulje k_2 i k_3 u s_1 točki tada je red pravčaste plohe koju ćemo promatrati jednak

$$2\,n_1 n_2 n_3 - (s_1 n_1 + s_2 n_2 + s_3 n_3). \qquad (1)$$

Ako ploha nastaje kao presjek kongruencije n-tog reda, m-tog razreda i kompleksa r-tog stupnja red plohe jednak je $r\,(n + m)$. Koliko će se i kakvi stošci pojaviti pri raspadu te plohe može se diskutirati u konkretnim slučajevima.

Red i razred pravčaste plohe uvijek su jednaki. Stoga pravcaste plohe imaju određeni stupanj.

Višestruke linije

Višestruke linije vitopere pravčaste plohe njezine su ravnalice k_1, k_2 i k_3, a strukost im je redom

$$n_2 n_3 - s_1,\ n_1 n_3 - s_2 \text{ i } n_1 n_2 - s_3. \qquad (2)$$

To se lako zaključuje na temelju činjenice da svakom točkom npr. krivulje k1 prolazi $n_2 n_3$ izvodnica plohe koje su presjek stožaca s vrhom u toj točki i osnovicama k_2 i k_3 (slika 3).

Napomena: u slučajevima kada se radi o pravčastoj ravnalici koja je ujedno i izvodnica tih stožaca koji su dijelovi raspada pravčaste plohe gornja se formula mora modificirati ovisno o tome koliko je puta pravčasta ravnalica brojena pri raspadu.

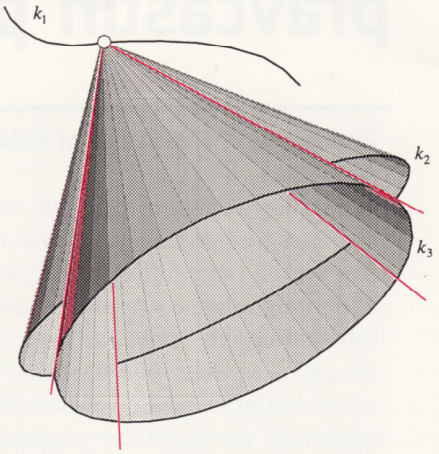

Slika 3

Sustavi izvodnica

Vitopere pravčaste plohe 2. reda (jednoplohi i parabolični hiperboloidi) jedine su plohe s dva sustava izvodnica, tj. u svakoj točki takve plohe sijeku se dvije njezine izvodnice. Sve pravčaste plohe reda većeg od 2 imaju samo jedan sustav izvodnica, tj. svakom njihovom točkom, koja ne leži na višestrukoj liniji, prolazi jedinstvena izvodnica plohe.

Dirne ravnine

Dirna ravnina u nekoj točki vitopere pravčaste plohe reda n sadrži izvodnicu koja prolazi diralištem te siječe plohu po krivulji reda $n-1$.

Pramen dirnih ravnina uzduž jedne izvodnice vitopere pravčaste plohe projektivno je pridružen nizu njihovih dirališta na toj izvodnici.

Konoidalne plohe i konoidi

Konoidalna pravčasta ploha nastaje onda kada je jedna od njezinih ravnalica neizmjerno daleki pravac. Ako ploha uz taj neizmjerno daleki pravac sadrži kao ravnalicu još i jedan pravac u konačnosti, nazivamo je konoidom.

Torzalni i oskularni pravci

Izvodnicu uzduž koje postoji jedinstvena dirna ravnina što plohu siječe još i u krivulji reda n –2 nazivamo *torzalnim* pravcem 1. *reda*, a onu uzduž koje jedinstvena dirna ravnina siječe plohu još i po krivulji reda $n-s$, *torzalnim* pravcem *reda* $s-1$, $s = 2,\ldots,n-1$. Torzalni pravac 2. reda nazivamo i *oskularnim* pravcem plohe.

Kuspidalne točke

Kuspidalne ili šiljaste točke one su točke dvostruke linije plohe u kojima dvije tangencijalne ravnine koincidiraju. Na pravčastim plohama to su točke presjeka torzalnih pravaca i dvostrukih linija plohe. Svaki ravninski presjek kroz takvu točku imat će u njoj šiljak. One su ujedno i točke koje na dvostrukim linijama razdvajaju dijelove što sadrže čvorove od onih što sadrže izolirane dvostruke točke* ravninskih presjeka plohe.

*Dvostruku točku ravninske krivulje nazivamo čvorom, šiljkom ili izoliranom dvostrukom točkom ako su u njoj dvije tangente krivulje realne i različite, realne i jednake ili konjugirano imaginarne.

2. PRAVČASTE PLOHE 4. STUPNJA

Neraspadnuta ravninska krivulja 4. reda može imati najviše tri dvostruke i najviše jednu trostruku točku. Stoga se na plohama 4. reda kao dvostruke krivulje mogu pojaviti samo prostorne krivulje 3. reda, konike ili pravci, a kao trostruka linija jedino pravac.

Pravčaste kvartike (plohe 4. reda) mogu se razvrstavati prema građi njihovih algebarskih jednadžbi [10, str. 203-213]. U geometrijskoj interpretaciji to je razvrstavanje prema redu i položaju njihovih ravnalica, te vrsti i broju torzalnih pravaca. Prema [4] prvu je takvu klasifikaciju načinio Cremona, a doradio Sturm. U knjizi [7, str. 246-294] pravčaste su kvartike detaljno obrađene prema Sturmovoj klasifikaciji po kojoj postoji dvanaest tipova. U daljnjem ćemo se izlaganju pozivati na to razvrstavanje prema kojemu su plohe obrađene i u radnji [6], a u knjigama [8] i [9] navedene su osnovne karakteristike pojedinih tipova. U knjizi [10] Salmon navodi Cayleyjevu klasifikaciju (također dvanaest tipova) te dodaje i svoju (trinaest) tipova. U knjizi [4, str. 76-80] dana je usporedba Cremonine, Sturmove i Cayleyjeve klasifikacije.

3. PRIMJERI PRAVČASTIH PLOHA 4. STUPNJA ZADANIH PRAVCIMA I KONIKAMA

Prema Sturmovu razvrstavanju postoji pet vrsta pravčastih kvartika kod kojih se kao ravnalice mogu odabrati konike i pravci. To su tipovi V, VII, VIII, IX i XI. U ovom ćemo poglavlju svaki od navedenih tipova ilustrirati s jednim ili više primjera.

Parametarske jednadžbe ploha, povoljne za crtanje u *Mathematici*, izvest ćemo u prvom primjeru dok ćemo ih u ostalima samo navesti. One se, naime, za svaki od idućih slučajeva izvode na sličan način.

Torzalne pravce plohe također ćemo istaknuti jedino u prvom primjeru. Dosljedno određivanje njihove vrste, realnosti, imaginarnosti ili podudaranja zahtijevalo bi zntnije zalaženje u područje diferencijalne geometrije ili pak, pri sintetičkom pristupu, vrlo dugačke opise.

3.1. VII. VRSTA U STURMOVOJ KLASIFIKACIJI

Taj tip pravčastih kvartika nastaje kada su ravnalice dva mimosmjerna pravca i konika koja ih ne siječe. Možemo ih promatrati kao presjek triju kompleksa određenih tim ravnalicama, ali i kao presjek kompleksa 2. stupnja određenog konikom i hiperboličke linearne kongruencije određene mimosmjernim pravcima. (Skup od ∞^2 transverzala dvaju mimosmjernih pravaca nazivamo linearnom *hiperboličkom* kongruencijom). Ploha iste vrste nastaje i ako se bilo koji drugi kompleks 2. stupnja odabere kao temeljni.

Mimosmjerni su pravci dvostruke linije tih ploha.

Plohe upravo toga tipa najčešći su primjeri pravčastih kvartika u literaturi ([1, str.177], [3, str.313], [5, str. 180]).

***Primjer* 3.1.1.**

Ravnalice plohe su kružnica u ravnini xy i dva mimosmjerna pravca paralelna s koordinatnim osima (slika 4).

c.....$x^2 + y^2 = 1,\ z = 0$

l_1.....$y = 0,\ z = 2$

l_2.....$x = 0,\ z = 1$

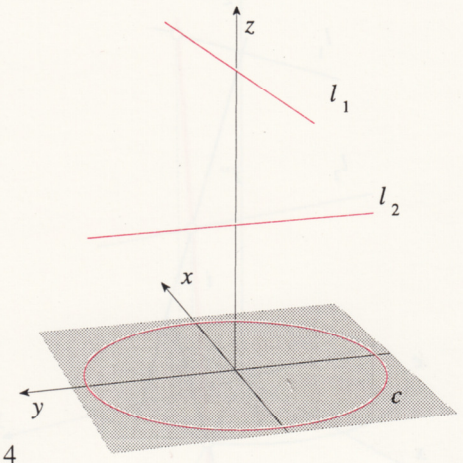

Slika 4

Izvodnice te plohe mogu se konstruirati kao spojnice probodišta pravca l_2 i kružnice c s ravninama pramena $[l_1]$ (slika5), ili kao spojnice probodišta pravca l_1 i kružnice c s ravninama pramena $[l_2]$ (slika6).

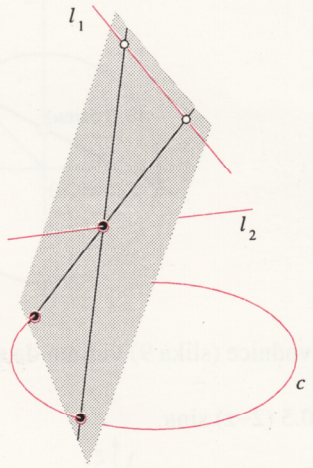

Slika 5

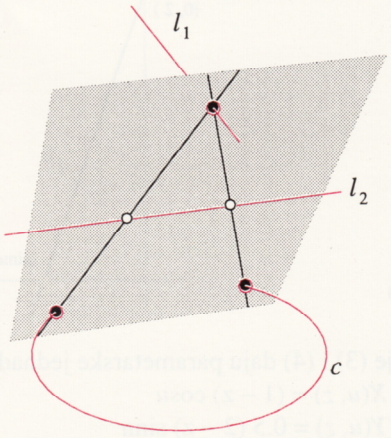

Slika 6

Za dobivanje grafičkog prikaza plohe u programu *Mathematica* najprikladnije je upotrijebiti njezine parametarske jednadžbe. Poznavajući samo osnove analitičke i

nacrtne geometrije one se u ovom slučaju vrlo jednostavno izvode. Zbog ravnomjerne raspoređenosti izvodnica parametrizirat ćemo plohu pomoću veličina u i z (slika 7).

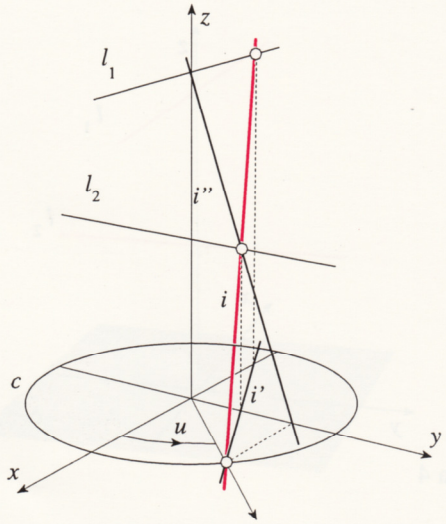

Slika 7

Iz tlocrta izvodnice (slika 8) zaključujemo da ona leži u ravnini

$$y = 0.5\ (x \tan u + \sin u). \qquad (3)$$

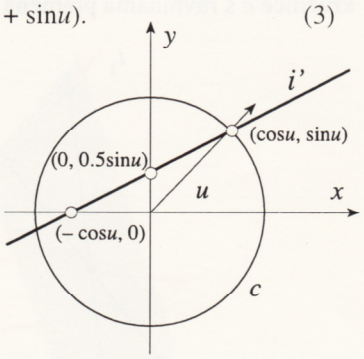

Slika 8

Iz nacrta izvodnice (slika 9) vidimo da se ona nalazi i u ravnini

$$y = 0.5\ (2-z)\ \sin u. \qquad (4)$$

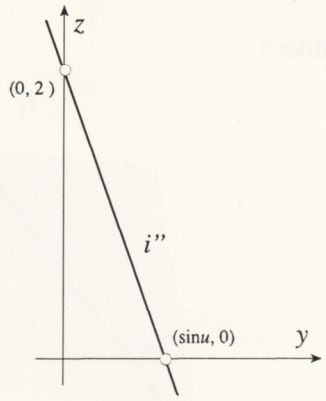

Slika 9

Relacije (3) i (4) daju parametarske jednadžbe plohe

$$X(u, z) = (1 - z)\ \cos u$$
$$Y(u, z) = 0.5\ (2 - z)\ \sin u$$
$$Z(u, z) = z, \quad u \in [0, 2\pi],\ z \in R. \qquad (5)$$

Na slici 10 prikazan je dio plohe omeđen ravninama $z = 0$ i $z = 2$ te naredba za crtanje.

```
<<Graphics'ParametricPlot3D';
ParametricPlot3D[
   {(1-z) Cos[u],0.5(2-z) Sin[u],z},
   {u,0,2Pi,Pi/20}, {z,0,2,1},
ViewPoint->{-3.5,2,1.75},
Boxed->False,Axes->None,
ColorOutput->GrayLevel]
```

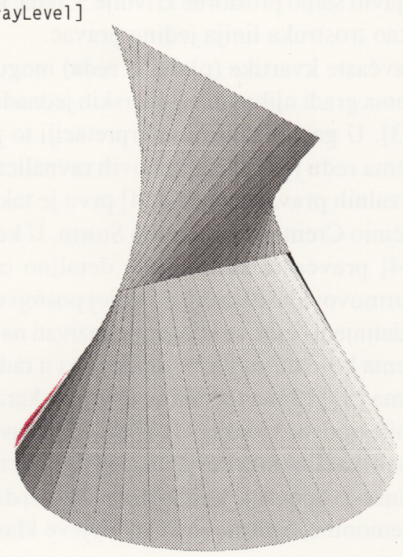

Slika 10

Torzalni pravci leže u onim ravninama pramenova $[l_1]$ i $[l_2]$ koje su dirne za kružnicu c. U svakoj od tih ravnina dvije izvodnice koje se sijeku na dvostrukom pravcu padaju zajedno u torzalni pravac. Ravnina pramena zajednička je dirna ravnina za sve točke torzalnog pravca, osim za kuspidalne. Kuspidalna točka, sjecište dviju neizmjerno blizih izvodnica, nalazi se na dvostrukom pravcu koji nije nosilac pramena kojem pripada ravnina (slika 11).

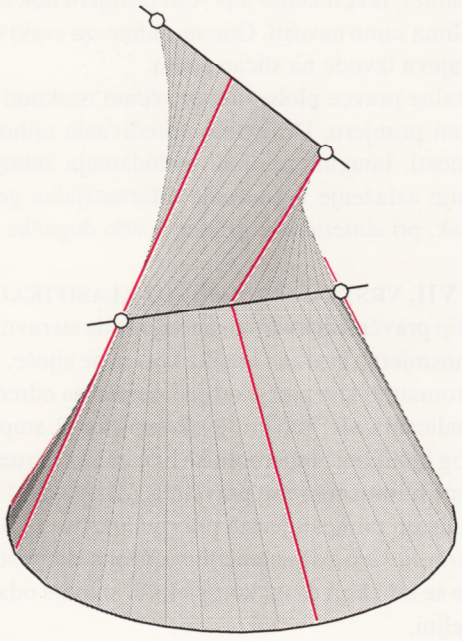

Slika 11

Pomoću programa *Mathematica* moguće je dobiti i prikaze koji, barem djelomice, otkrivaju i unutarnju stranu plohe. Na slici 12 dan je takav prikaz dijela plohe omeđenog ravninama $z = -0.5$ i $z = 2.5$ te naredba za crtanje.

```
Show[
  Table[
ParametricPlot3D[{(1-z) Cos[u],0.5(2-z) Sin[u],z},
{u,0,2Pi,Pi/24},{z,i,i+3/31,3/31}],{i,-.5,2.5-3/31,6/31},
DisplayFunction->Identity],
  Table[
ParametricPlot3D[{(1-z) Cos[u],0.5(2-z) Sin[u],z},
{u,j,j+Pi/24,Pi/24},{z,-.5,2.5,3/31}],{j,0,2Pi-Pi/12,Pi/12},
DisplayFunction->Identity]],
   ViewPoint->{-3.5,2,1.75},
   Boxed->False,Axes->None,
   ColorOutput->GrayLevel,
   DisplayFunction->$DisplayFunction]]
```

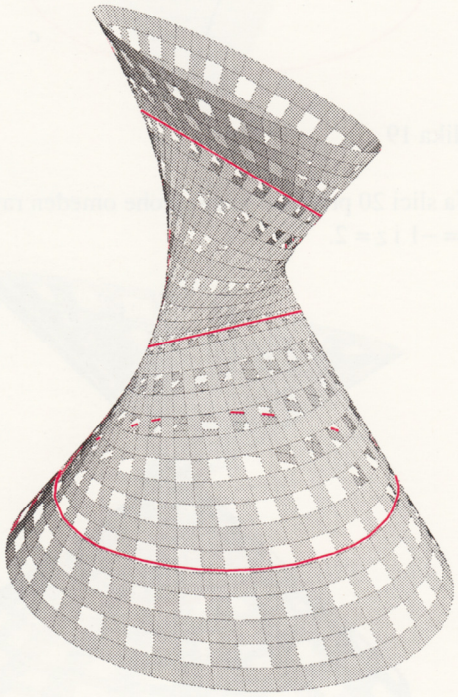

Slika 12

Primjer 3.1.2.

Ravnalice konoida su kružnica u xy ravnini, pravac paralelan s osi x te neizmjerno daleki pravac ravnine yz. (Neizmjerno daleki pravac prostora analitički ćemo zadavati pramenom paralelnih ravnina, dok ćemo pri grafičkom prikazu upotrebljavati bilo koju ravninu tog pramena, tzv. *direkcijsku.*) (Slika 13)

c.....$x^2 + y^2 = 1, \quad z = 0$

l_1.....$y = 0, \quad z = 1.5$

l_2^∞....$x = t, \quad t \in \mathrm{R}$

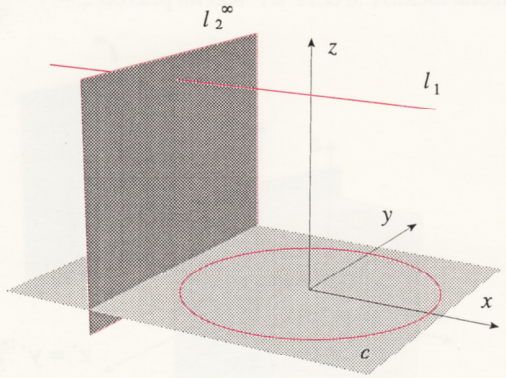

Slika 13

Izvodnice konoida određuju se kao spojnice probodišta pravca l_1 i kružnice c s ravninama pramena paralelnih ravnina $[l_2^\infty]$ (slika14), ili u ravninama pramena $[l_1]$ kao paralele s direkcijskom ravninom kroz probodišta kružnice s ravninama pramena (slika15).

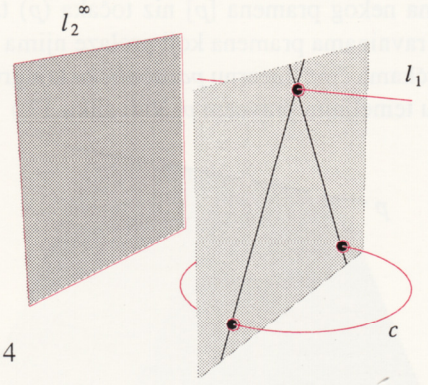

Slika 14

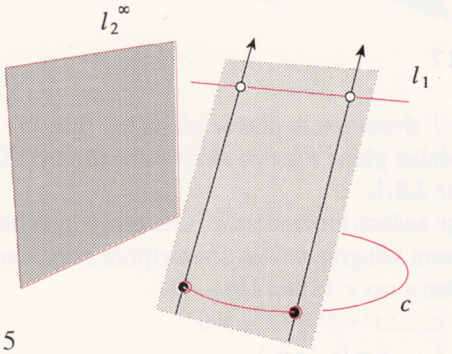

Slika 15

Za iste parametre kao u prethodnom primjeru parametarske su jednadžbe tog konoida:

$$X(u, z) = \cos u$$

$$Y(u, z) = \frac{3 - 2z}{3} \sin u$$

$$Z(u, z) = z, \quad u \in [0, 2\pi], \quad z \in \mathrm{R}. \qquad (6)$$

Na slici 16 prikazan je dio konoida omeđen ravninama $z = -0.8$ i $z = 2.3$.

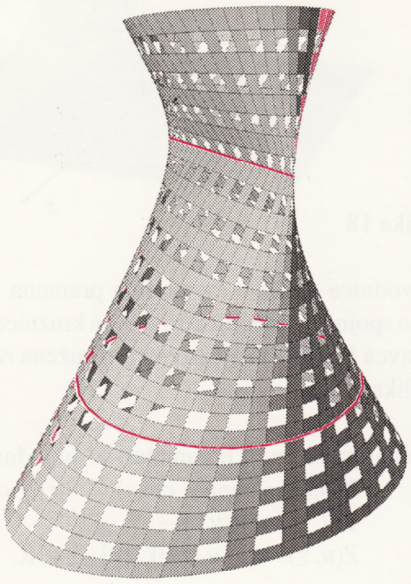

Slika 16

3.2. VIII. VRSTA U STURMOVOJ KLASIFIKACIJI

Taj tip ploha nastaje iz prethodnog ako se pravci l_1 i l_2 podudaraju, tj. izvodnice plohe su zajedničke zrake kompleksa 2. stupnja i linearne paraboličke kongruencije s temeljnim pravcem $l = l_1 = l_2$. (Pridruži li se projektivno ravninama nekog pramena $[p]$ niz točaka (p) tada svi pravci u ravninama pramena koji prolaze njima pridruženim točkama čine linearnu *paraboličku* kongruenciju određenu temeljnim pravcem p. Vidi sliku 17.)

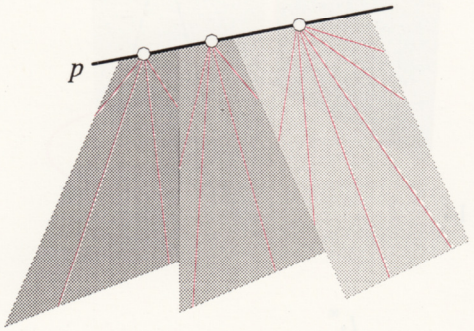

Slika 17

Pravac l dvostruki je pravac ploha tog tipa.
Konoidalne plohe tog tipa nazivamo *cilindroidima*.

***Primjer* 3.2.1.**

Ploha je zadana kružnicom u xy ravnini te paraboličkom linearnom kongruencijom s temeljnim pravcem koji je paralelan s osi x. (Slika 18)

c.....$x^2 + y^2 = 1, \quad z = 0$

l.....$y = 0, \quad z = 1$

Projektivitet između niza točaka (l) i pramena ravnina $[l]$, koji određuje paraboličku linearnu kongruenciju, zadan je na sljedeći način:

$A \leftrightarrow \alpha \quad \Leftrightarrow \quad x_A = \tan v,\ v = \angle(\alpha, z),\ A \in (l),\ \alpha \in [l].$

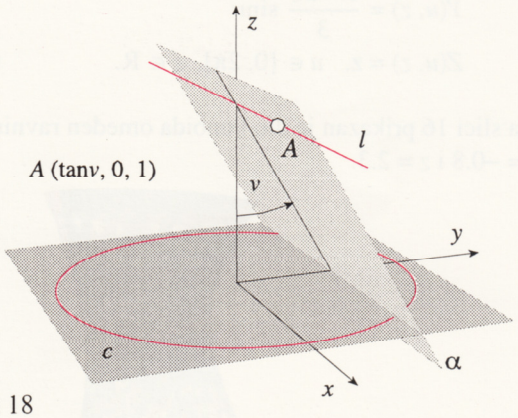

Slika 18

Izvodnice plohe u ravninama pramena $[l]$ određuju se kao spojnice probodišta ravnine s kružnicom c i one točke pravca l koja je projektivno pridružena ravnini pramena (Slika 19).

Za parametre u i z parametarske su jednadžbe plohe:

$$X(u, z) = (\sin u - \cos u)(1 - z) + \cos u$$
$$Y(u, z) = \cos u\,(1 - z)$$
$$Z(u, z) = z, \quad u \in [0, 2\pi],\ z \in \mathrm{R}. \qquad (7)$$

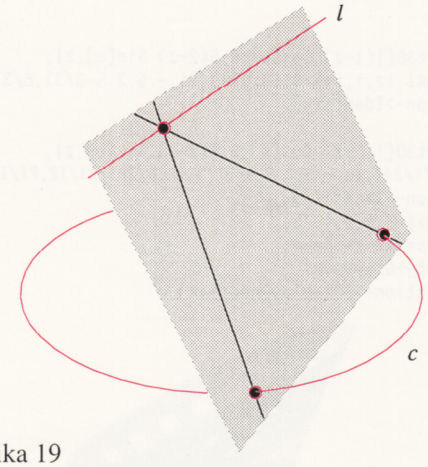

Slika 19

Na slici 20 prikazan je dio plohe omeđen ravninama $z = -1$ i $z = 2$.

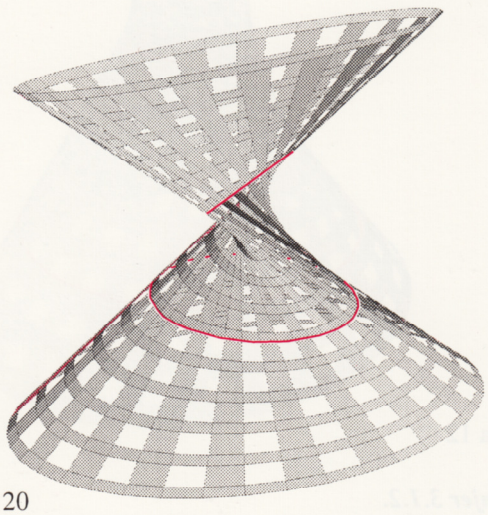

Slika 20

***Primjer* 3.2.2.**

Cilindroid je zadan kružnicom u ravnini xz, neizmjerno dalekim pravcem ravnine yz te paraboličkom linearnom kongruencijom kojoj je taj pravac temeljni (slika 21).

c.....$x^2 + z^2 = 1, \quad y = 0$

l^∞.....$x = t, \quad t \in \mathrm{R}$

Projektivitet $[l^\infty] \overline{\wedge} (l^\infty)$ određen je na sljedeći način: Ako je ravnina $\alpha \in [l^\infty]$ dana jednadžbom $x = t$, tada njoj pridružena točka $A^\infty \in \alpha, A^\infty \in l^\infty$ leži na pravcu $z = y \dfrac{\tan t}{5}$.

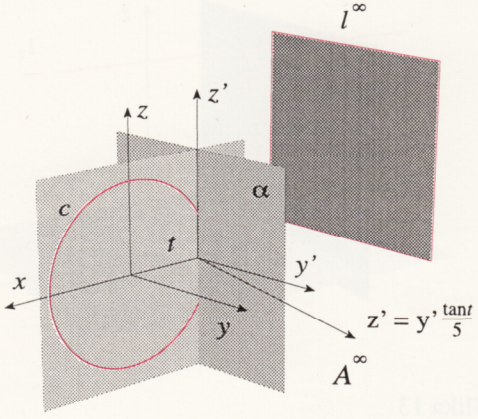

Slika 21

Izvodnice plohe u ravninama pramena $[l^{\infty}]$ određuju se kao spojnice probodišta ravnine s kružnicom c i one točke pravca l^{∞} koja je projektivno pridružena ravnini pramena (slika 22).

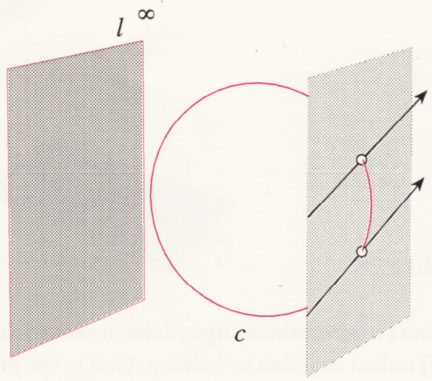

Slika 22

Za ravnine pramena $[l^{\infty}]$ u kojima leže realne izvodnice cilindroida možemo uvesti supstituciju $t = \cos u$, $u \in [0, \pi]$. Sada su parametarske jednadžbe plohe, za parametre u i y, dane sa:

$$X(u, y) = \cos u$$
$$Y(u, y) = y$$
$$Z_{1,2}(u, y) = y\,\frac{\tan(\cos u)}{5} \pm \sin u,$$
$$u \in [0, \pi],\ y \in \mathrm{R} \qquad (8)$$

Na slici 23 prikazan je dio plohe omeđen ravninama $y = -3$ i $y = 3$.

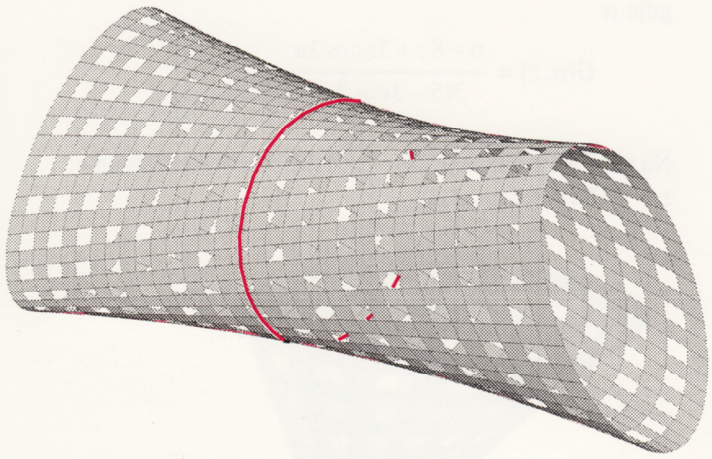

Slika 23

3.3. IX. vrsta u Sturmovoj klasifikaciji

Plohe tog tipa nastaju onda ako se kao ravnalice odaberu dvije konike koje se ne sijeku i jedan pravac što svaku od njih siječe u jednoj točki, dok su tangente konika u tim sjecištima s pravcem mimosmjerne. Pravac je trostruka linija ploha. Prema formuli (3) izašlo bi da je to četverostruka linija. Međutim, taj se pravac, iako se konike ne sijeku, pojavljuje kao zajednička izvodnica stožaca koji nastaju pri raspadu plohe osmoga reda te pri računanju njegove višestrukosti treba od vrijednosti izraza (3) oduzeti broj 1.

***Primjer* 3.3.1.**

Ploha je zadana elipsom u ravnini xy, kružnicom u ravnini paralelnoj s ravninom xy te s osi z (slika 24).

$$e\ldots\ldots(2x - 1)^2 + (5y - \sqrt{3})^2 = 4,\ z = 0$$
$$c\ldots\ldots(2x - 1)^2 + (2y - 1)^2 = 2,\ z = 1$$
$$l\ \ldots\ldots x = 0,\ y = 0$$

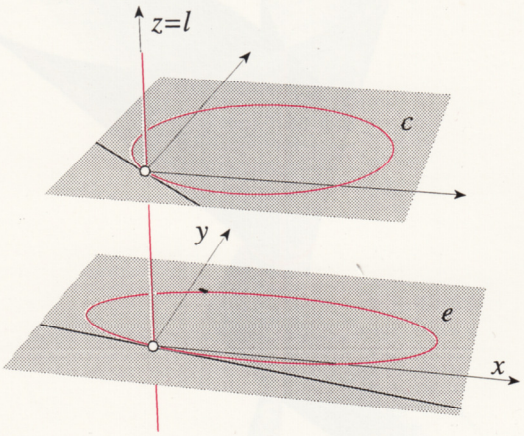

Slika 24

U svakoj ravnini pramena $[l]$ nalazi se jedna izvodnica te plohe. Ona je spojnica probodišta ravnine s konikama c i e (slika 25). Izvodnice plohe mogu se također dobivati i kao prodorne izvodnice dvaju stožaca kojima je vrh u točki pravca l, a osnovice konike c i e. To je ujedno i način na koji se pokazuje da je pravac l trostruki pravac plohe.

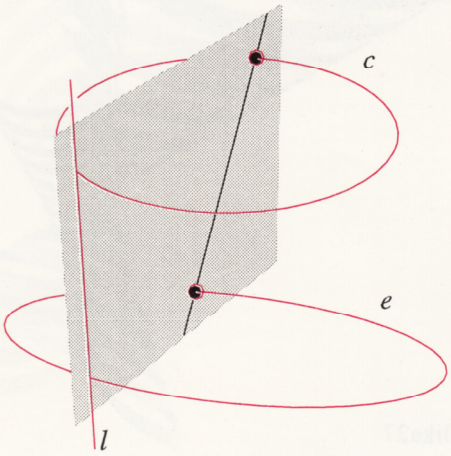

Slika 25

Za parametre u i z parametarske su jednadžbe plohe:

$$X(u, z) = \frac{\cos u}{58 - 42\cos 2u}\,F(u, z)$$
$$Y(u, z) = \frac{\sin u}{58 - 42\cos 2u}\,F(u, z)$$
$$Z(u, z) = z,\quad u \in [0, \pi],\ z \in \mathrm{R}, \qquad (9)$$

gdje je

$$F(u, z) = \cos u\,(16 + 21z) - 21z\cos 3u$$
$$- 40\sqrt{3}\sin u\,(z - 1) + 2z\sin u\,(29 - 21\cos 2u).$$

Na slikama 26 i 27 prikazan je dio te plohe omeđen ravninama $z = -5$ i $z = 8$.

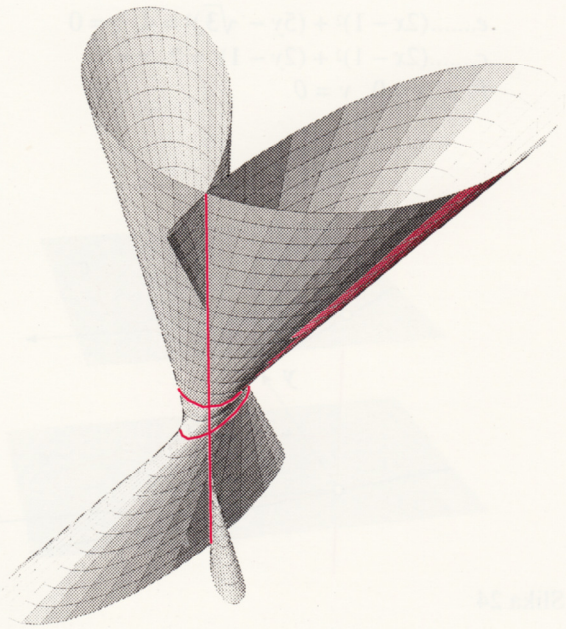

Slika 26

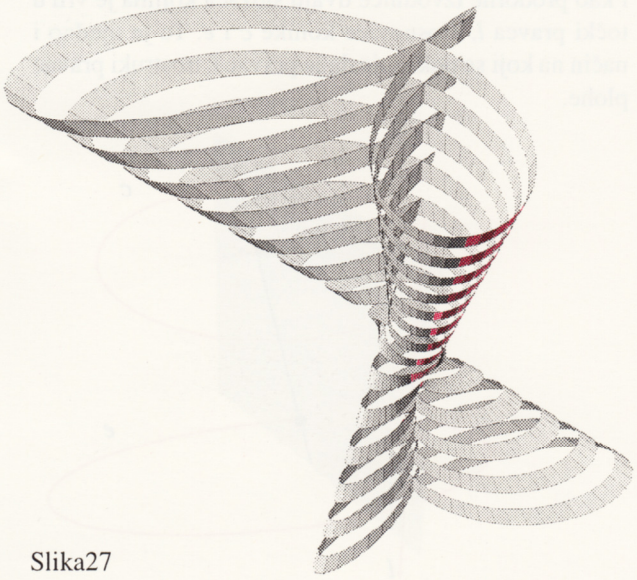

Slika27

3.4. XI. VRSTA U STURMOVOJ KLASIFIKACIJI

Kod ploha tog tipa ravnalice su jednake onima u prethodnom tipu, samo što tangente konika u njihovim sjecištima s pravcem leže u istoj ravnini.

***Primjer* 3.4.1.**

Ploha je zadana elipsom u ravnini xy, kružnicom u ravnini paralelnoj s ravninom xy, te s osi z. Tangente konika u njihovim sjecištima s osi z paralelne su (slika 28).

e.....$(x-1)^2 + 4y^2 = 1,\ z = 0$

c.....$(3x+1)^2 + 9y^2 = 4,\ z = 2$

l .....$x = 0,\ y = 0$

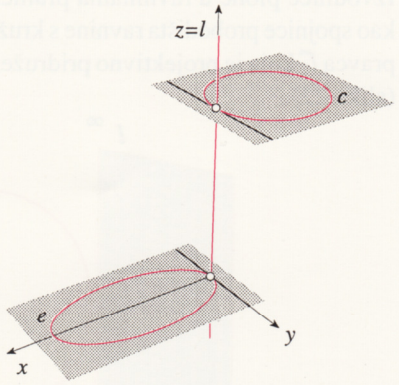

Slika 28

Kao i u prethodnom tipu plohe, u svakoj ravnini pramena $[l]$ nalazi se jedna izvodnica. Ona je spojnica probodišta ravnine s konikama c i e (slika 29).

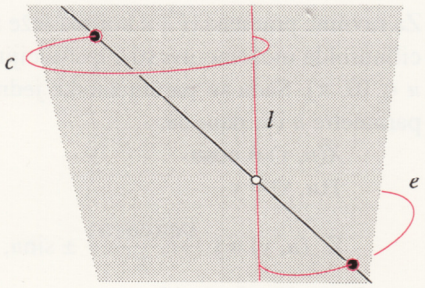

Slika 29

Za parametre u i z parametarske su jednadžbe plohe:

$$X(u, z) = 2\cos^2 u\, G(u, z)$$
$$Y(u, z) = \sin 2u\, G(u, z)$$
$$Z(u, z) = z, \quad u \in [0, \pi],\ z \in \mathrm{R}, \qquad (10)$$

gdje je

$$G(u, z) = \frac{6 - 8z + 3z\cos 2u}{3(5 - 3\cos 2u)}.$$

Na slici 30 prikazan je dio ove plohe omeđen ravninama $z = -0.5$ i $z = 2.5$.

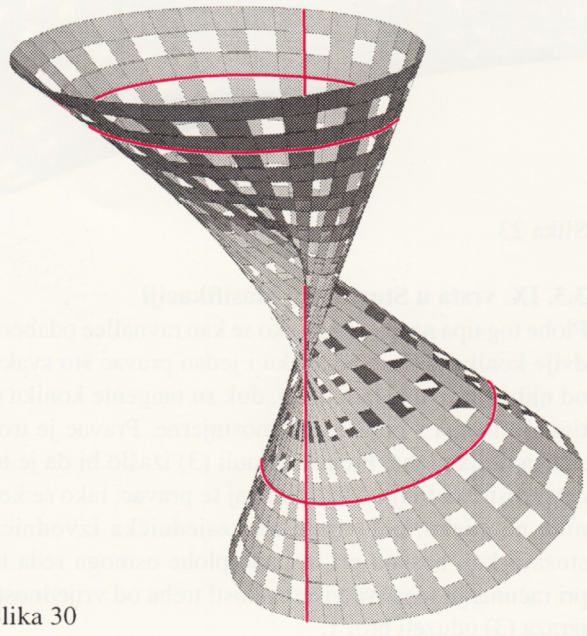

Slika 30

***Primjer* 3.4.2.**

Konoidalna ploha zadana je dvjema parabolama koje leže u ravninama xz i xy te neizmjerno dalekim pravcem ravnine paralelne s njihovim osima (slika 31). Tangente parabola u njihovim neizmjerno dalekim točkama leže u neizmjerno dalekoj ravnini prostora.

p_1.....$z = -0.5x^2 + 2$, $y = 0$

p_2.....$y = 0.5x^2 + 2$, $z = 0$

l^∞.....$x = t$, $t \in R$

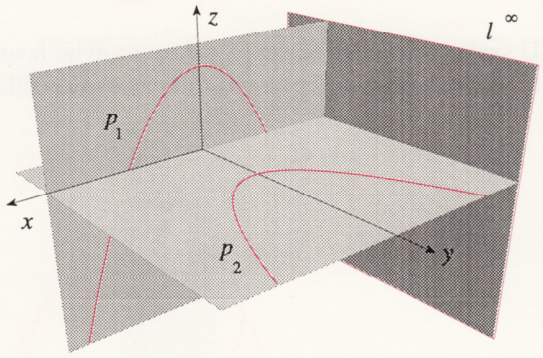

Slika 31

Izvodnice plohe u paralelnim ravninama pramena $[l^\infty]$ određuju se kao spojnice probodišta ravnine s parabolama (slika 32). One se također mogu dobivati i kao prodorne krivulje paraboličkih valjaka kojima su izvodnice paralelne s direkcijskom ravninom.

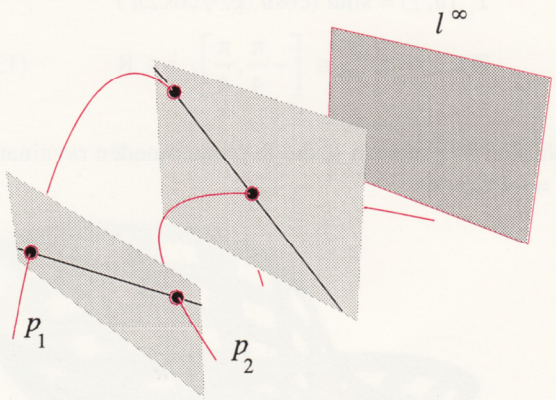

Slika 32

Za crtanje u Mathematici eksplicitni oblik jednadžbe plohe prikazat ćemo parametarski.

$$X(x, y) = x$$
$$Y(x, y) = y$$
$$Z(x, y) = \frac{-x^4 - 8y + 2x^2y + 16}{2(4 + x^2)}, \quad x \in R, \; y \in R. \quad (11)$$

Na slici 33 prikazan je dio plohe omeđen ravninama $x = -3.9$, $x = 3.9$, $y = -0.5$ i $y = 6.5$.

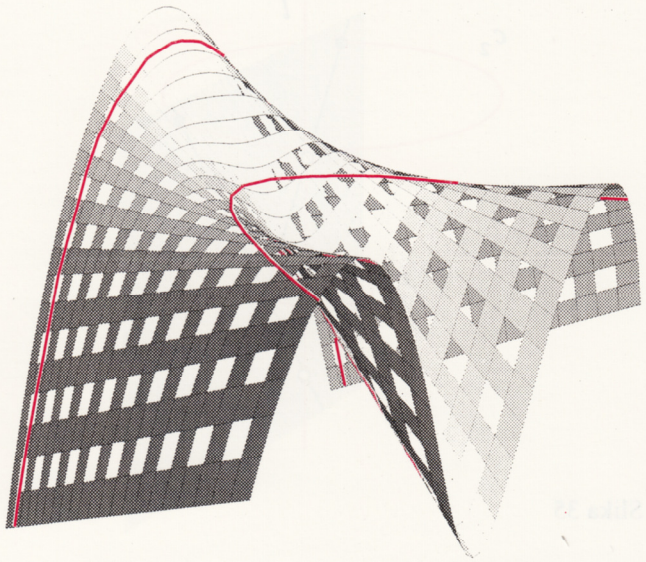

Slika 33

3.5. V. VRSTA U STURMOVOJ KLASIFIKACIJI

Plohe tog tipa mogu se zadati dvjema konikama koje se sijeku u dvjema točkama, te pravcem koji u jednoj točki siječe jednu od njih. Pravac i konika koja se s njim siječe dvostruke su linije tih ploha.

***Primjer* 3.5.1.**

Ploha je zadana dvjema kružnicama koje leže u ravninama paralelnim s ravninom xy. (Budući da svaka kružnica prolazi parom apsolutnih točaka neizmjerno dalekog pravca njezine ravnine, te su točke sjecišta svih kružnica u ravninama paralelnog pramena). Jedna od kružnica siječe os z koja je također ravnalica plohe (slika 34). Takav je primjer obrađen u knjizi [3, str.318]

c_1.....$(x - 1)^2 + y^2 = 1$, $z = 0$

c_2.....$(x - 2)^2 + y^2 = 9$, $z = 4$

l .....$x = 0$, $y = 0$

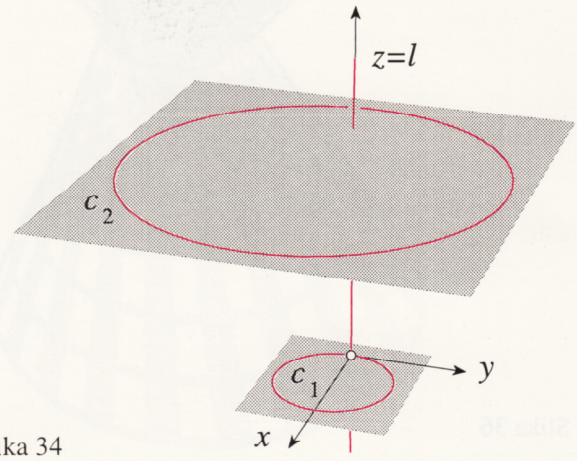

Slika 34

U svakoj ravnini pramena $[l]$ nalaze se dvije izvodnice te plohe koje se sijeku na dvostrukoj kružnici c_1 (slika 35). Izvodnice se također mogu dobiti i kao prodorne izvodnice dvaju stožaca kojima se vrhovi nalaze na pravcu l, a osnovice su im kružnice c_1 i c_2. Svaka dva takva stošca sijeku se u paru izotropnih izvodnica te u dvjema izvodnicama plohe.

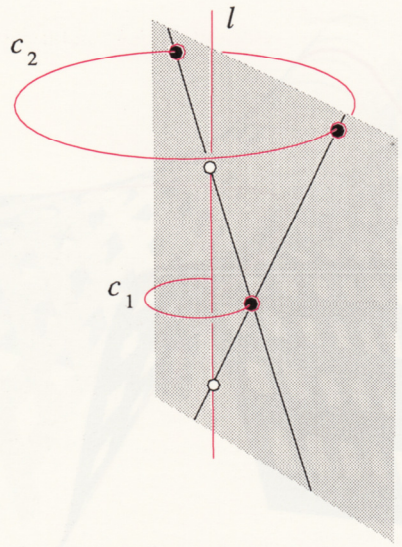

Slika 35

Za parametre u i z parametarske su jednadžbe plohe:

$$X(u, z) = 1 + \cos 2u + 0.25\, z \cos u \sqrt{7 + 2\cos 2u}$$
$$Y(u, z) = \sin 2u + 0.25\, z \cos u \sqrt{7 + 2\cos 2u}$$
$$Z(u, z) = z, \quad u \in [0, 2\pi],\ z \in \mathrm{R}. \qquad (12)$$

Na slici 36 prikazan je dio ove plohe omeđen ravninama $z = -4$ i $z = 4$.

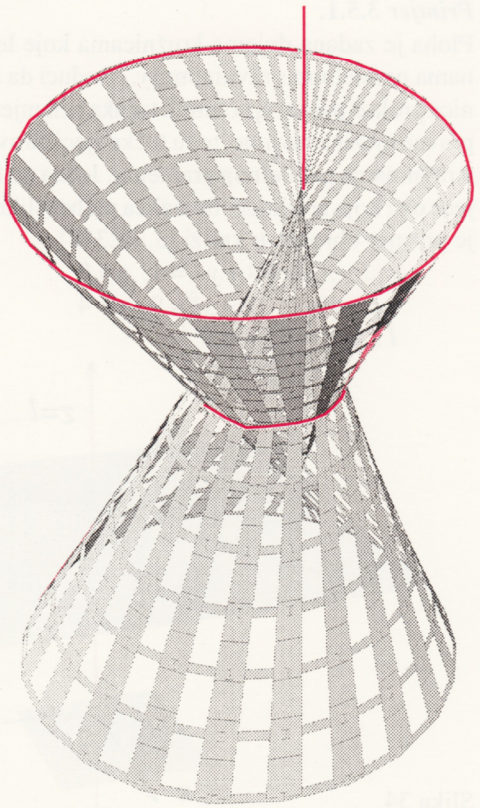

Slika 36

***Primjer* 3.5.2.**
Ploha je zadana s dvije kružnice koje se sijeku u dvije realne točke. Jedna od kružnica siječe os z koja je također ravnalica plohe. (Slika 37)

c_1.....$(x - 1)^2 + y^2 = 1,\ z = 0$
c_2.....$y^2 + z^2 = 1,\ x = 1$
l .....$x = 0,\ y = 0$

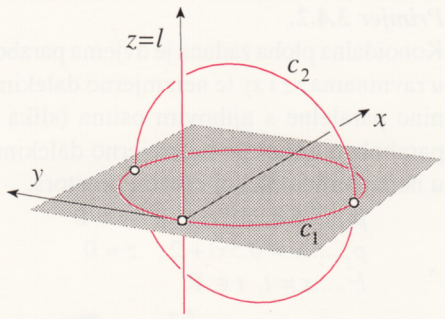

Slika 37

U svakoj ravnini pramena $[l]$ nalaze se dvije izvodnice ove plohe koje se sijeku na dvostrukoj kružnici (slika 38).

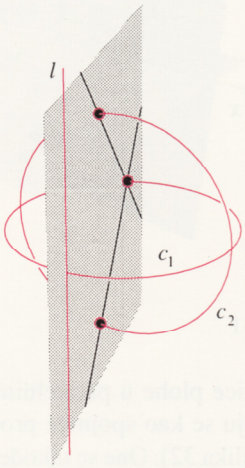

Slika 38

Za parametre u i z parametarske jednadžbe plohe su:

$$X_{1,2}(u, z) = \cos u\, (\cos u \pm z\sqrt{\cos 2u}\,)$$
$$Y_{1,2}(u, z) = \sin u\, (\cos u \pm z\sqrt{\cos 2u}\,)$$
$$Z(u, z) = z, \quad u \in \left[-\frac{\pi}{4}, \frac{\pi}{4}\right],\ z \in \mathrm{R}. \qquad (13)$$

Na slici 39 prikazan je dio te plohe omeđen ravninama $z = -4$ i $z = 4$.

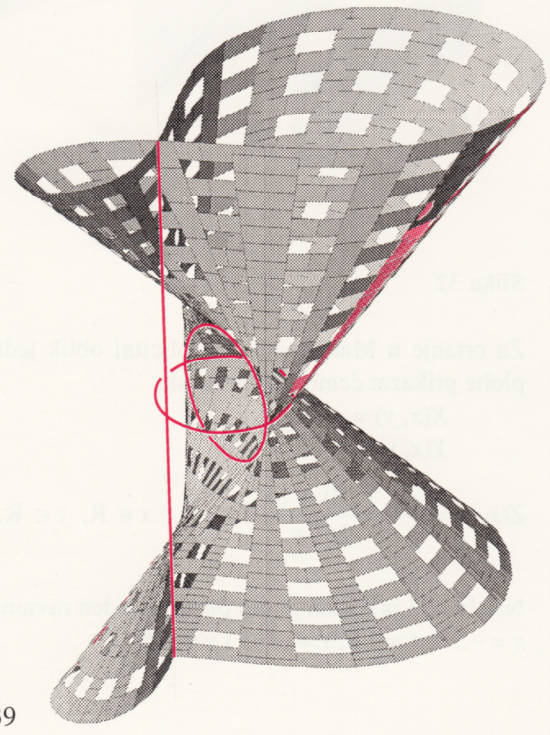

Slika 39

***Primjer* 3.5.3.**

Konoidalna ploha tog tipa zadana je kružnicom i parabolom koje se sijeku te neizmjerno dalekim pravcem u ravnini paralelnoj s osi parabole, tj. pravcem koji siječe parabolu u njezinoj neizmjerno dalekoj točki. Parabola i neizmjerno daleka ravnalica dvostruke su linije te plohe (slika 40).

c.....$x^2 + z^2 = 1,\ y = 0$

p.....$y = x^2 - 1,\ z = 0$

l^∞.....$x = t,\ t \in \mathrm{R}$

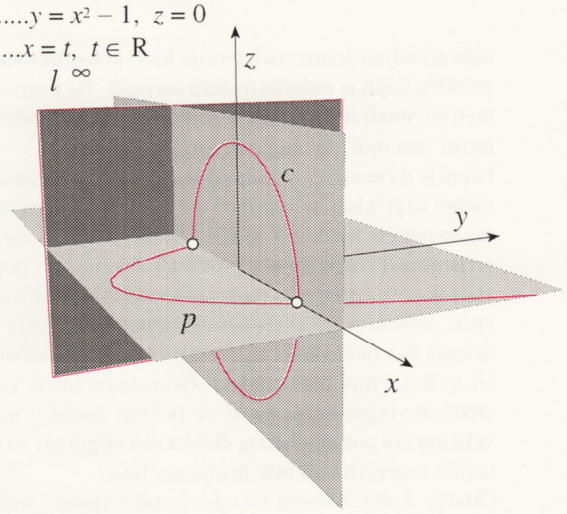

Slika 40

U svakoj ravnini paralelnoj s ravninom yz nalaze se dvije izvodnice te plohe koje se sijeku u točki parabole (slika 41).

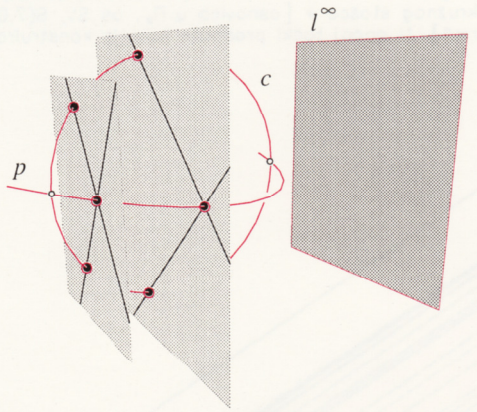

Slika 41

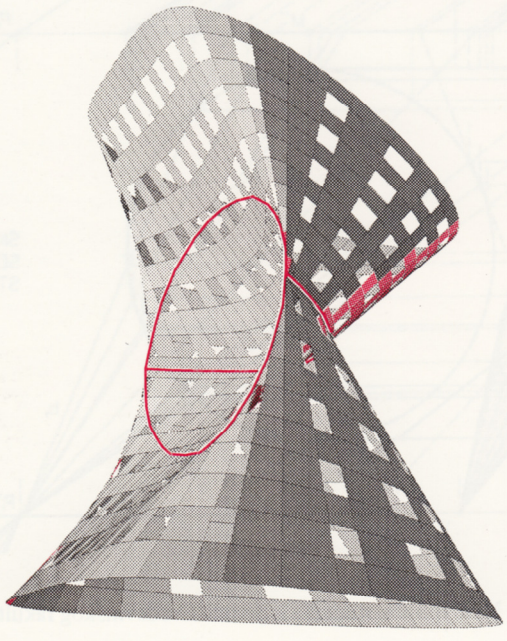

Slika 42

U ravninama $x = t$ izvodnice plohe dane su jednadžbama $y = t^2 \pm z\sqrt{1-t^2} - 1$. Stoga se parametarske jednadžbe plohe mogu napisati:

$$X(x, z) = x$$
$$Y_{1,2}(x, z) = x^2 \pm z\sqrt{1-x^2} - 1$$
$$Z(x, z) = z, \quad x \in [-1, 1]\ z \in \mathrm{R}. \qquad (14)$$

Na slici 42 prikazan je dio konoida omeđen ravninama $z = -2$ i $z = 2$.

ZAKLJUČAK

Na principima izvođenja sprovedenim u ovom radu mogu se lako dobiti brojni oblici različitih pravčastih ploha 4. stupnja, kako odabirom položaja ravnalica tako i odabirom vrsta konika.

Kako su one nastavne teme koje snažnije potiču kreativnost studenata nedvojbeno plodonosnije u smislu ostvarenja obrazovnih ciljeva, sklona sam zaključiti da bi znatnije uključivanje takvih sadržaja u nastavu geometrije, u prvom redu na fakultetima graditeljskih usmjerenja, pridoinijelo njezinoj kvaliteti.

Skice generirane u programu *Mathematica* 3.0, dorađene su za tisak u programu *FreeHand* 7.0.

LITERATURA

[1] BABIĆ, I., GORJANC, S., SLIEPČEVIĆ, A., SZIROVICZA, V.: Konstruktivna geometrija - vježbe, IGH, Zagreb, 1994.

[2] BRAUNER, H., KICKINGER, W.: *Geometrija u graditeljstvu I*, (prijevod: P. Kurilj, B. Hajsig) Školska knjiga, Zagreb, 1980.

[3] FLADT, K., BAUR, A.: *Analytische Geometrie spezieller Flächen und Raumkurven*, Friedr. Viewg &Sohn, Braunschweig 1975.

[4] JESSOP, C. M.: *A Treatise on the Line Complex* Chelsa Publishing Company, New York, 1969. (reprint)

[5] KUČINIĆ, B., KRISTOFOROVIĆ, O., SALER, I.: *Oble forme u graditeljstvu*, Zagreb, 1992.

[6] KURILJ, P.: Konstruktivna obrada pravčastih ploha 3. i 4. stupnja, magistarski rad, Zagreb, 1968.

[7] MÜLLER, E., KRAMES, J. L.: *Konstruktive Behandlung der Regelfächen*, Franc Deuticke, Leipzig und Wien, 1931.

[8] NIČE, V.: *Deskriptivna geometrija II*, Školska knjiga, Zagreb, 1980.

[9] NIČE ,V.: *Uvod u sintetičku geometriju*, Školska knjiga, Zagreb, 1956.

[10] SALMON, G.: *A Treatise on the Analytic Geometry of Three Dimensions*, Chelsa Publishing Company, New York, 1965. (reprint)

Mr. sc. Sonja Gorjanc
Građevinski fakultet Sveučilišta u Zagrebu
Kačićeva 26, 10000 Zagreb
e-mail: sgorjanc@grad.hr

VLASTA SZIROVICZA

AutoCAD u konstruktivnoj geometriji

Iako je programski paket AutoCAD kao profesionalni crtački program u praksi postao nezamjenjiv, geometričari još uvijek postavljaju pitanje njegove svrhovitosti pri kompliciranim konstrukcijama iz područja konstruktivne geometrije. Radi se o relativno crtački kompliciranim konstrukcijama kod kojih nema ponavljanja istog zadatka ili nekog njegova dijela, odnosno svaki je crtež samo taj, nema umnožavanja. Neupućeni smatraju da posjedovanje određenog crtačkog programa rješava sve probleme, a zaboravljaju da je računalo samo alat. Za neke vrste crtanja u tehnici razrađeni su programi koji ubrzavaju posao služeći se umnožavanjem, analogijom s prijašnjim zadatkom, pa su tako nastali specijalizirani programi kao što je ArchiCAD. No tu je riječ o konstruktivno-geometrijskim zadacima za edukaciju studenata iz predmeta Konstruktivna geometrija, odnosno Nacrtna geometrija. Pokušaji da crtež (program) dobijemo od studenata koji se znaju služiti AutoCAD-om završili su neuspjehom zbog toga što oni nisu dovoljno dobro znali teoriju kao i konstruktivne postupke pomoću kojih je zadatke trebalo ostvariti. Ne poznavajući geometriju, imali su utisak da se svaki zadatak jednostavnije i brže može "nacrtati" računalom. Što je prava istina ?

Istina je da se crtački kompliciraniji zadaci sporije crtaju računalom nego klasičnim priborom: olovkom, šestarom i trokutima na papiru. Međutim, nakon crtanja olovkom crtež je potrebno istuširati i tu nastupaju problemi. Ne smije se pogriješiti jer se svaka mala pogreška mukotrpno ispravlja, a ako su pogreške veće, pametnije je crtež tuširati iznova. Svakako je paus-papir nekada bio rješenje da se crtež u olovci nije trebao ponoviti, ali to baš i nije bilo utješno. Osim toga, taj se crtež morao crtati dovoljno velik da bi se poslije smanjio na potrebnu veličinu (za potrebe nekog članka ili knjige), pa su time eventualne nepreciznosti bile manje uočljive.

Crtanje AutoCAD-om također je tako sporo i mukotrpno, u nekim elementima čak i sporije nego crtanje rukom. Pretpostav-

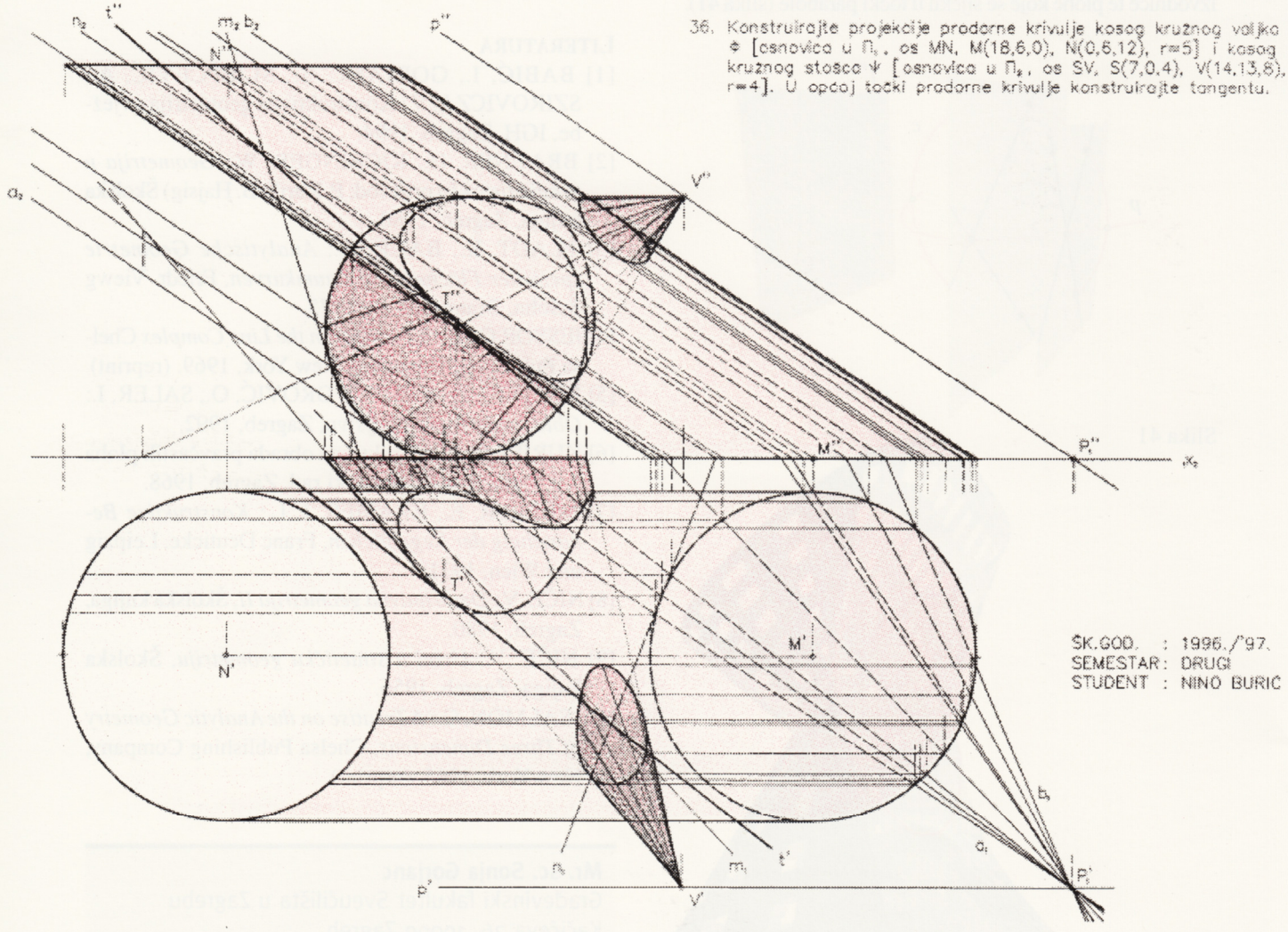

Studentski rad u AutoCAD-u Nine Burića, studenta I. godine Građevinskog fakulteta u Zagrebu.

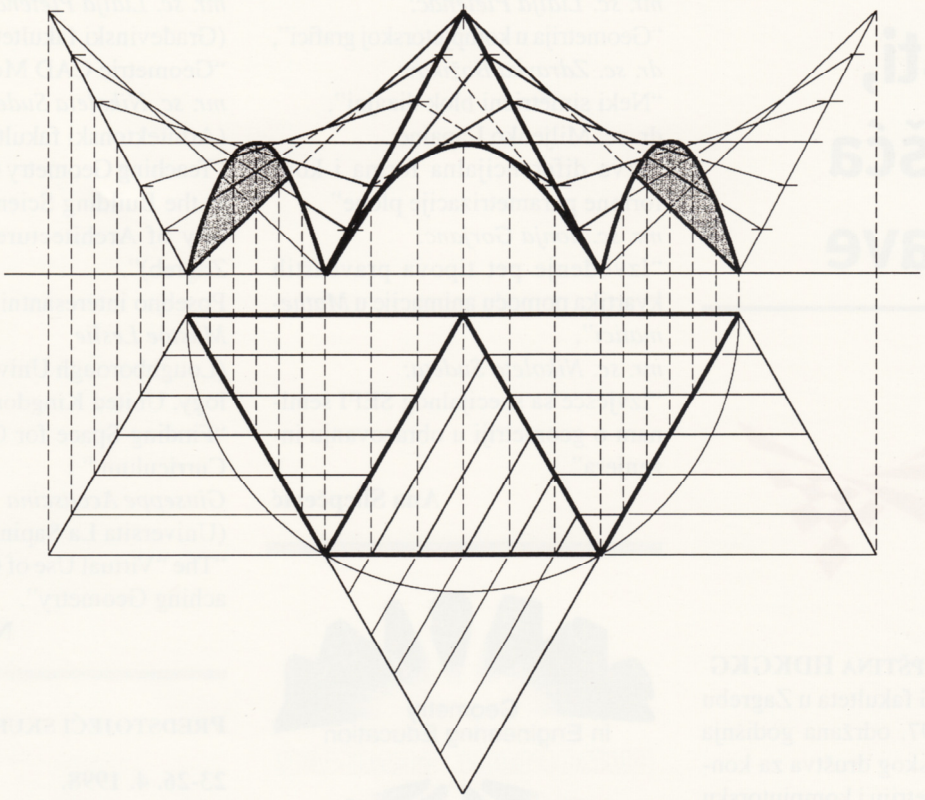

ka je takvog crtanja uz dovoljno dobro osobno računalo, veličina zaslona, svakako ne manja od dijagonale 17". Bez obzira na to što se svaki nejasni dio crteža može povećati naredbom Zoom, potrebno je ipak crtež sagledati u cjelini, odnosno za neke konstrukcije povući pravce duž cijelog formata crteža. Velika je prednost crtanja računalom savršena preciznost koja se naprosto ne može postići klasičnim crtanjem, bez obzira na oštrinu vida crtača i veličinu crteža. Ta se preciznost odnosi na debljine linija, izbor kojih nije ograničen debljinom crtaćeg pera (rapidografa) ili položajem ruke crtača, ali još više, pri crtanju pravca koji prolazi sjecištem dvaju pravaca ili središtem kružnice i sl.

Pri crtanju paralela i okomica nema bojazni da će se trokuti pomaknuti, odnosno da zbog lošeg crtaćeg pribora konstrukcija neće biti točna. Jednako tako nema bojazni da nultočka neće biti točno u sjecištu dvaju pravaca ili da tangenta točno ne dira krivulju, te još mnogo sličnih crtačkih dilema pri crtanju računalom nestaje.

Problem ipak nastaje pri "izvlačenju" krivulje. Ona se, kao i pri klasičnom crtanju, izvlači spajanjem dovoljnog broja njezinih točaka. Dok se ručno izvlačila pomoću krivuljara (što je zahtijevalo strpljenje pri traženju "prave" zakrivljenosti), računalo je crta kao poligonalnu liniju koju naredbom Pedit-Spline pretvara u krivulju. Taj je dio posla najteži odnosno najpreciznji i najmukotrpniji i zahtijeva najveću rutinu crtača. Nemoguće je konstruirati dovoljan broj točaka tražene krivulje (crtež bi bio nepregledan!), pa je tu potrebna određena improvizacija.

Koja je ipak prednost AutoCAD programa u navedenoj primjeni? Iako nešto sporije crtanje od klasičnog, zapravo je ipak brže, ako se sjetimo da crtež treba ponoviti tušem. Sama mogućnost ispravljanja pogrešaka daje dovoljnu prednost da odmah zaboravimo klasično crtanje. Pomoćne konstrukcije pri kojima upotrebljavamo samo rezultat, a pridonose nepreglednosti crteža, naprosto izbrišemo. Nenadoknadiva je prednost pri rješavanju zadataka kod kojih se koristi temeljni zadatak naredbom COPY umnožavamo i zatim nadopunjava novim konstrukcijama. Uz to AutoCAD pruža mogućnost translacije (naredba MOVE) i rotacije (naredba ROTATE) cijelog zadatka ili nekog njegova dijela. Naredbu MOVE upotrebljavamo često pri smještaju oznaka točaka, pravaca, kuteva i dr., dakle pri dotjerivanju crteža. Tu su svakako na pomoći i naredbe BREAK i TRIM. Prvu upotrebljavamo pri brisanju suvišnih dijelova linija, brisanju crte prekrivene slovom i sl., a druga je najkorisnija pri uništavanju linija unutar nultočke. Promjena vrste linije rješava se naredbom CHANGE, a njezina debljina naredbom PEDIT. To su samo neke od prednosti crtanja računalom.

Navedene su naredbe upotrijebljene pri konstrukciji projekcija prodorne krivulje dviju ploha Mongeovom metodom. Sliku je izradio Nino Burić, student I. godine Građevinskog fakulteta u Zagrebu. Redoslijed crtanja identičan je onome koji se upotrebljava pri crtanju na papiru. Crtanje usporava izvlačenje vidljivosti pojedine izvodnice na plohi jer su njezini dijelovi linije različite vrste i različitih debljina, a to se mijenja nakon što je ona nacrtana. Uz to stvarnu debljinu, pa čak i vrstu pojedine linije možemo sa sigurnošću provjeriti tek pomoću ASSIST-INQUIRY-LIST ili na kraju ispisom, budući da ono što vidimo na ekranu nije stvarni rezultat našeg crtanja.

Iako su za crtanje računalom potrebni velika koncentracija i napor, može se reći da štedi vid. Priloženi crtež, relativno crtački kompliciran i jasan na papiru, nije tako jasan i pregledan na ekranu, osim ako se njegovi detalji pomnije ne promotre s pomoću naredbu Zoom. To se ne odnosi na njegov ispis.

Učenje upotrebe AutoCAD-a ili kojeg drugog profesionalnog crtačkog programa ne treba nikako miješati s učenjem geometrije. Nepoznavatelji geometrijskih odnosa i dometa te, najstarije znanosti vjeruju da će uporaba računala ukinuti tu granu matematike. Zaboravljaju da je računalo samo alat koji pomaže i ubrzava ostbarenje onog što se stvara u glavama ljudi, u prvom redu onih stručnjaka koji su stekli teorijske spoznaje kao pretpostavku za usavršavanje i unapređivanje znanosti. A za one ostale računalo će ostati samo dobra "pisaća mašina" ili zanimljiva igračka.

Vijesti, izvješća i najave

GODIŠNJA SKUPŠTINA HDKGKG

U vijećnici AGG fakulteta u Zagrebu je 29. rujna 1997. održana godišnja skupština Hrvatskog društva za konstruktivnu geometriju i kompjutorsku grafiku. Predsjednica Društva dala je pregled rada i događaja od prethodne godišnje skupštine do danas. Istaknuta je uspješna prezentacija prvog broja časopisa KoG, te izraženo zadovoljstvo na reagiranja iz cijelog svijeta povodom njegova izlaska. Osim po sveučilišnim centrima u Hrvatskoj, časopis je razaslan na pedesetak adresa diljem svijeta (Austrija, Mađarska, Poljska, Slovačka, Japan, USA, Australija...) i odasvud su stizale samo pohvale.

Izašao je novi sveučilišni udžbenik Nacrtna geometrija za studente strojarstva i brodogradnje autorica I. Babić i K. Horvatić.

Tajnica Društva izvijestila je o financijskom poslovanju, a zatim su slijedila kratka izvješća Izdavačkog savjeta i Nadzornog odbora. Istaknuta je potreba za češćim sastancima Društva. Skupu je prisustvovalo dvadesetak članova, a pristupilo je i dvoje novih članova, od kojih je jedan iz Bosne i Hercegovine.

Sljedeći sastanak planiran je u veljači 1998.

Istoga dana održan je i Znanstveno-stručni kolokvij sa sljedećim izlaganjima:

mr. sc. Jelena Beban-Brkić:
"Krivulje fokusa pramenova konika u I_2",
mr. sc. Lidija Pletenac:
"Geometrija u kompjutorskoj grafici",
dr. sc. Zdravka Božikov:
"Neki simetrični blok dizajni",
dr. sc. Miljenko Lapaine:
"Prva diferencijalna forma i konformne parametrizacije plohe"
mr. sc. Sonja Gorjanc:
"Izvođenje pet tipova pravcastih kvartika pomoću animacije u *Mathematici*",
mr. sc. Nikoleta Sudeta:
"Izvješće sa specijalnog SEFI seminara o geometriji u obrazovanju inženjera"

Ana Sliepčević

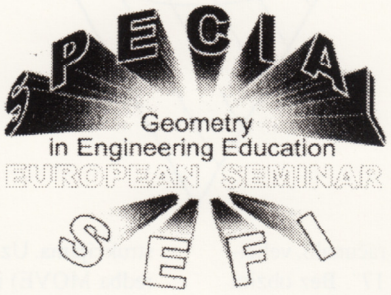

U Smolenicama (Slovačka) je od 25. do 29. kolovoza 1997. održan "Specijalan Europski seminar za geometriju u inženjerskoj edukaciji" *(Special European Seminar on Geometry in Engineering Education)*. Organizirali su ga Tehničko sveučilište u Bratislavi i Evropsko društvo za inženjersku edukaciju SEFI (European Society for Engineering Education).

Seminaru je prisustvovalo četrdesetak sudionika iz dvanaest zemalja Evrope i Japana.

Teme Seminara bile su nastavni planovi geometrije, uloga kompjutora u nastavi geomatrije, komjutorska geometrija.

Članice našeg Društva imale su zapažene referate i aktivno su sudjelovale na Okruglom stolu o nastavi geometrije na fakultetima. Referirale su:

mr. sc. Jelena Beban-Brkić
(Geodetski fakultet, Zagreb):
"Vector Equations of Second Degree Curves",
mr. sc. Sonja Gorjanc
(Građevinski fakultet, Zagreb):
"Generation of Ruled Quartics in Mathematica",
mr. sc. Lidija Pletenac
(Građevinski fakultet, Rijeka):
"Geometric CAD Modeling",
mr. sc. Nikoleta Sudeta
(Arhitektonski fakultet, Zagreb):
"Teaching Geometry (Descriptive and in the Building Sciences) at the Faculty of Architecture University of Zagreb)".

Posebno interesantni referati bili su:
Mustoe Leslie
(Loughborough University of Tehnology, United Kingdom):
"Finding Space for Geometry in the Curriculum " i
Giuseppe Accascina
(Universita La Sapinza, Roma):
"The "Virtual Use of Computer in Teaching Geometry".

Nikoleta Sudeta

PREDSTOJEĆI SKUPOVI

23-26. 4. 1998.
Dani hrvatskih geodeta
X. susret, Hrvatsko geodetsko društvo, Dubrovnik, Hrvatska.

27-30. 4. 1998.
Modern Preparation and Response Systems for Earthquake, Tsunami and Volcanic Hazards, IUGG International Conference, Santiago, Chile.

20-22. 5. 1998.
100 godina fotogrametrije u Hrvatskoj, Geodetski fakultet, Zagreb, Hrvatska.

15-17, 6. 1998.
9th SEFI European Seminar on Mathematics in Engineering Education, Espoo, Finland

16-19. 6. 1998.
ITI '98, 20th International Conference Information Technology Interfaces, Pula, Croatia.

2-4. 7. 1998.
4. susret nastavnika matematike Republike Hrvatske, Hrvatsko matematičko društvo i Ministarstvo prosvjete i športa RH, Zagreb, Hrvatska.

9-11. 7. 1998.
Duane C. Brown, International Summer School in Geomatics, New Tech-

nologies for Geospatial Data Acquisition, Ohio, USA.

19-26. 7. 1998.
FIG 98 XXI International Congress of Surveyors, Brighton, UK.

30. 7. - 3. 8. 1998.
8th International Conference on Engineering Computer Graphics and Descriptive Geometry, Austin, Texas, USA.

18-27. 8. 1998.
Internationale Mathematik-Kongreß· 1998, TU Berlin, Deutschland.
http://elib.zib-berlin.de/icm98

14-18. 9. 1998.
Konstruktive Geometrie, Balatonföldvár, Hungaria

23-25. 9. 1998.
9th International Symposium on Information Systems IS '98, Faculty of Organization and Informatics Varaždin, Croatia.
http://www.foi.hr/simpozij

28. 9. 1998.
4. znanstveno - stručni kolokvij HDKGKG-a, (Hrvatskog društva za konstruktivnu geometriju i kompjutorsku grafiku)

3-6. 10. 1998.
Mapping Japan, 17th International Symposium of the International Map Collectors' Society - IMCoS, Tokyo, Japan.

6-16. 10. 1998.
1. međunarodna nagradna izložba GIS grafike, GIS udruga, Osijek, Hrvatska.

5-17. 10. 1998.
Prvi hrvatski kongres INSEA, znanstveni simpozij "Počeci i razvoj nastave likovne izobrazbe u europskom školstvu", izložba "Crtež u znanosti", Odbor za obilježavanje 210 godina prvih crtarskih škola i kontinuiteta nastave likovne izobrazbe u hrvatskom školstvu, Zagreb, Hrvatska.

4-6. 11. 1998.
"Geometrie für Leben", Tangung des ADG in Strobl, Österreich

4-8. 11. 1998.
Vasco da Gama, Men, Voyages and Cultures, International Conference. CNCDP, Torre do Tombo, Lisbon, Portugal.

studeni, 1998.
18. skup o prometnim sustavima "Automatizacija u prometu '97", KoREMA, Hrvatska.

11-16. 7. 1999.
18th International Conference on the History of Cartography, Athens, Greece.

14-21. 8. 1999.
19th International Cartographic Conference and 11th General Assembly of the International Cartographic Association, Ottawa, Canada.

Prikazi

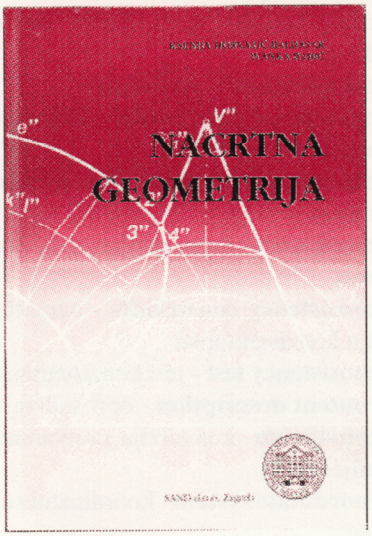

KSENIJA HORVATIĆ I IVANKA BABIĆ:
NACRTNA GEOMETRIJA

U izdanju nakladnika SAND d.o.o. iz Zagreba izašla je 1997. godine Nacrtna geometrija prof.dr.sc. Ksenije Horvatić i doc.dr.sc. Ivanke Babić. Knjiga ima 152 stranice i sadrži šest poglavlja: Osnovni pojmovi, Ortogonalno projiciranje na dvije i više ravnina, Kosa aksonometrija, Kosa projekcija, Presjeci rotacijskih ploha, Prodori rotacijskih ploha, Zavojnica i zavojne plohe. Takav Izbor poglavlja uvjetovan je stručnim razlozima i potrebama. Naime, u predgovoru o namjeni knjige autorice kažu: "Ovaj je udžbenik napisan na temelju dugogodišnjeg iskustva autorica u nastavi nacrtne geometrije na Fakultetu strojarstva i brodogradnje (FSB). Prema tome je i prvenstveno namijenjen studentima tog fakulteta. Može, međutim, dobro poslužiti i slušačima Tekstilnotehnološkog fakulteta, djelomično i studentima Rudarskogeološko-naftnog i njima srodnih fakulteta i visokih škola. Kao osnovni vodič kroz kolegij Nacrtna geometrija, dobro će doći i studentima mnogih drugih fakulteta." Možemo još samo dodati da se isvaki drugi čitatelj može u ovoj knjizi upoznati s osnovnim idejama nacrtne geometrije.

U prvom poglavlju ukratko je opisan osnovni pojam nacrtne geometrije - projiciranje. Drugo je poglavlje najopsežnije i osnova mu je Mongeova metoda projiciranja na dvije okomite ravnine. U njemu su riješene sve najvažnije zadaće u svezi s točkama, pravcima i ravninama te ravninskim likovima i geometrijskim tijelima. Kako ta metoda ne daje uvijek zornu predodžbu predmeta i objekata, važnu za praktične realizacije, u trećem je poglavlju dan opis dviju aksonometrijskih metoda: kose aksonometrije i kose projekcije, kojima se taj cilj lakše postiže. Slijede dva standardna poglavlja u svakom udžbeniku nacrtne geometrije: presjeci i prodori. Obrada tih tema ograničena je iz ranije navedenih razloga samo na rotacijske plohe. Posebna je vrijednost tih poglavlja u opisanoj primjeni presjeka i prodora u strojarstvu (tehnički predmeti, strojni dijelovi, alati, postrojenja i dr.). Zahtjevniji čitatelji, koji žele proširiti produbiti znanje iz pojedinih područja nacrtne geometrije, upućuju se na literaturu na kraju knjige. Podrobniji uvid u tu literaturu mogu naći već na početku knjige u tabelarnom prikazu. Metodički postupak obrade karakteriziraju jasnoća, postupnost i jednostavan matematički jezik. Tekst obiluje brojnim riješenim primjerima. Tome treba dodati precizno izvedene crteže korisne ilustracije. Pred nama je vrijedan sveučilišni udžbenik.

Zdravko Kurnik

OSNOVI KVALITETE PROSTORNIH PODATAKA
ENGLESKO-HRVATSKI RJEČNIK

Knjiga Elementi kvalitete prostornih podataka (Elements of spatial data quality) koju su uredili S. C. Guptill i J. L. Morrison objavljena je 1995. u izdanju Međunarodnog kartografskog društva i izdavačke kuće Elsevier Science, Oxford, NewYork, Tokio. U predgovoru što ga je napisao prethodni predsjednik Međunarodnoga kartografskog društva D. R. F. Taylor stoji da je kvaliteta prostornih podataka od ključne važnosti u doba kada postojeće elektronske tehnologije i mrežne komunikacije, kao što je primjerice Internet, omogućuju lagan pristup prostornim podacima u digitalnom obliku. Kartografi su oduvijek bili posebno zainteresirani za kvalitetu prostornih podataka i treba pozdraviti ovaj vrijedan doprinos Povjerenstva za kvalitetu prostornih podataka Međunarodnoga kartografskog društva na pojašnjenju složenog skupa pitanja. Ova knjiga, napisana od vodećih autoriteta u tom području, daje smjernice za upotrebu digitalnih prostornih podataka. U njoj su dane definicije osnovnih elemenata uključenih u kvalitetu prostornih podataka, koja je višedimenzionalna i objedinjuje mnogo više od same položajne točnosti.
Knjigu je preveo Dražen Tutić, student Geodetskog fakulteta Sveučilišta u Zagrebu uz pomoć Miljenka Lapainea. Za taj rad D. Tutić je 1997. godine primio Rektorovu nagradu. U okviru toga rada nastao je i sljedeći englesko-hrvatski rječnik osnovnih pojmova iz područja kvalitete prostornih podataka. Literatura upotrijebljena pri izradi ovog rječnika navedena je na kraju rada.

A
abstract universe - apstraktni univerzum
abstraction - apstrakcija
accuracy - točnost
acquisition - skupljanje, prikupljanje
aggregation - spajanje, agregacija
association - asocijacija, sažimanje
attribute - atribut
attribute accuracy - točnost atributa
attribute completeness - potpunost atributa
audit trail - kontrolno praćenje

B
bias - pristranost

C
cell - ćelija
cell complex - ćelijski kompleks
classification - klasifikacija
commit - potvrđivati, izvršavati
compilation - sastavljanje, prevođenje
completeness - potpunost
conceptual data model - konceptualni model podataka
conceptual schema - konceptualna shema
consistency - konzistentnost, dosljednost
consistency constraints - ograničenja konzistentnosti
consistency test - test konzistentnosti
content description - opis sadržaja
conversion - konverzija, pretvaranje, mijenjanje
coordinate system - koordinatni sustav
correction - korekcija
currency - aktualnost

D
data collection - prikupljanje podataka, zbirka podataka
data completeness - potpunost podataka
data description - opis podataka
data modeling - modeliranje podataka
database time - vrijeme baze podataka
datum - datum
derivation - izvođenje
description fields - opisna polja
Digital Geographic Information Exchange Standard (DIGEST) - jedna od normi za prijenos digitalnih geografskih informacija
digitizing - digitalizacija
domain - domena
domain consistency - konzistentnost domene
duration - trajanje

E
elevation - visina
entity object - entitet, objekt
entity instance - pojava entiteta
error - pogreška
error propagation - prirast pogrešaka
evaluation matrix - matrica procjene
event time - vrijeme događaja
extrapolation - ekstrapolacija

F
fair draught - reprodukcijski original
feature - objekt
feature completeness - potpunost objekata
feature instance - pojava objekta
fitness for use - pogodnost za uporabu
formal completeness - formalna potpunost

G
Gaussian distribution - Gaussova razdioba, normalna razdioba
generalization - generalizacija, uopćavanje
graph - graf

H
history - povijest
homeomorphism - homeomorfizam

I
incompleteness - nepotpunost
integrity - integritet, cjelovitost
interpolation - interpolacija
interpretation - interpretacija
interval - interval
ISO 9000 - ISO 9000

K
Kappa - *k*, kapa

L
lattice - rešetka
liability - obveza, odgovornost

life cycle - životni ciklus
lineage - porijeklo, podrijetlo
logical consistency - logička konzistentnost

M
map projection - kartografska projekcija
maximum error - maksimalna pogreška
metadata - metapodaci, podaci o podacima
misclassification matrix - matrica pogrešne klasifikacije
model completeness - potpunost modela
modeling - modeliranje
Monte Carlo simulation - Monte Carlo simulacija, Monte Carlo metoda

N
national map accuracy standard - nacionalne norme za točnost karata
nominal - nominalni
null values - nul vrijednosti

O
object - objekt
observation time - vrijeme opažanja
order - poredak
ordinal - ordinalni
origin - ishodište, polazište

P
parameter - parametar
pedigree - pedigre
perceived reality - opažana stvarnost
planimetry - planimetrija
poset - skraćeno od partially ordered set = parcijalno uređen skup
positional accuracy - položajna točnost, horizontalna točnost
precision - preciznost

Q
quality norm - norma kvalitete
quality assessment - procjena kvalitete
quality report - izvješće o kvaliteti

R
ratio - odnos, proporcija
reference field - referentno polje
reference source - referentni izvor
reference system - referentni sustav
referential consistency - referentna konzistentnost
relational database - relacijska baza podataka
relationship - odnos
reliability diagram - dijagram pouzdanosti, skica o pouzdanosti karte
resolution - rezolucija, razlučljivost
revision - održavanje
root mean square error (RMSE) - srednja pogreška

S
scalar - skalar, broj
scale - mjerilo, skala
scene consistency - konzistentnost scene, konzistentnost prikaza
semantic accuracy - semantička točnost
semantics - semantika
simplex - simpleks
simplicial complex - simplicijalni kompleks
simplification - pojednostavljenje
source - izvor
space - prostor
spatial component - prostorna komponenta
Spatial Data Transfer Standard (SDTS) - jedna od normi za prijenos prostornih podataka
specification - specifikacija
standard deviation - standardno odstupanje
standard - norma
surface - ploha

T
temporal - vremenski
temporal attribute - vremenski atribut
thematic attributes - tematski atribut
theme - tema
time - vrijeme
time stamp - vremenska oznaka
time zone - vremenska zona
time slice - vremenski isječak
topological relations - topološke relacije
topological consistency - topološka konzistentnost
topological space - topološki prostor
topology - topologija
total quality management - upravljanje ukupnom kvalitetom
transaction - izmjena, transakcija
transformation - transformacija
truth in labeling - istinitost u označavanju

U
uncertainty - nesigurnost

V
variance - varijanca
version - verzija, inačica
visualization - vizualizacija, prikaz

LITERATURA

Anić, V. (1991): Rječnik hrvatskoga jezika, Novi Liber, Zagreb.

ASCE/ACSM/ASPRS, (1994): Glossary of the mapping sciences, ASCE/ ACSM/ ASPRS, Bethesda, New York.

ACSM/ASCE (1989): Definitions of surveying and associated terms, ACSM/ASCE, Bethesda, New York.

Borčić, B., Kreiziger, I., Lovrić, P. i Frančula, N. (1977): Višejezični kartografski rječnik, Geodetski fakultet sveučilišta u Zagrebu, Zbornik radova - Publikacija br. 15, Zagreb.

Frančula, N. (1996): Digitalna kartografija, Interna skripta, Sveučilište u Zagrebu, Geodetski fakultet, Zagreb.

Gibson, C. (urednica, 1990): The Pan dictionary of mathematics, Pan Books, London, Sydney, Auckland.

Guptill, S. C. i Morrison, J. L. (urednici, 1995): Elements of spatial data quality, International Cartographic Association, Elseiver Science, Kidlington, New York, Tokyo.

Gusić, I. (1995): Matematički rječnik, Element, Zagreb.

IfAG (1971): Fachwörterbuch, Benennungen und Definitionen im deutschen Vermessungswesen, Institut für Angewandte Geodäsie, Frankfurt.

Kiš, M., Buljan, J., Vuković, S. i Anić, O. (1993): Englesko-hrvatski informatički rječnik s računalnim nazivljem, Školska knjiga, Zagreb.

Klaić, B. (1978): Rječnik stranih riječi, Nakladni zavod Matice hrvatske, Zagreb.

Manturov, O. V., Solncev, J. K., Sorkin, J. I. i Fedin, N. G. (1969): Rečnik matematičkih termina sa tumačenjima, Naučna knjiga, Beograd.

Varga, M. (1994): Baze podataka, DRIP - Društvo za razvoj informacijske znanosti, Zagreb.

Woodcock, J. (1995): Microsoft Press Informatički rječnik, Znak, Zagreb.

Dražen Tutić
Miljenko Lapaine

AUTODESK 3D STUDIO 4.0

Autodesk 3D Studio (ver. 4.0) kompjutorski je 3D-program namijenjen stvaranju grafike i animacija.

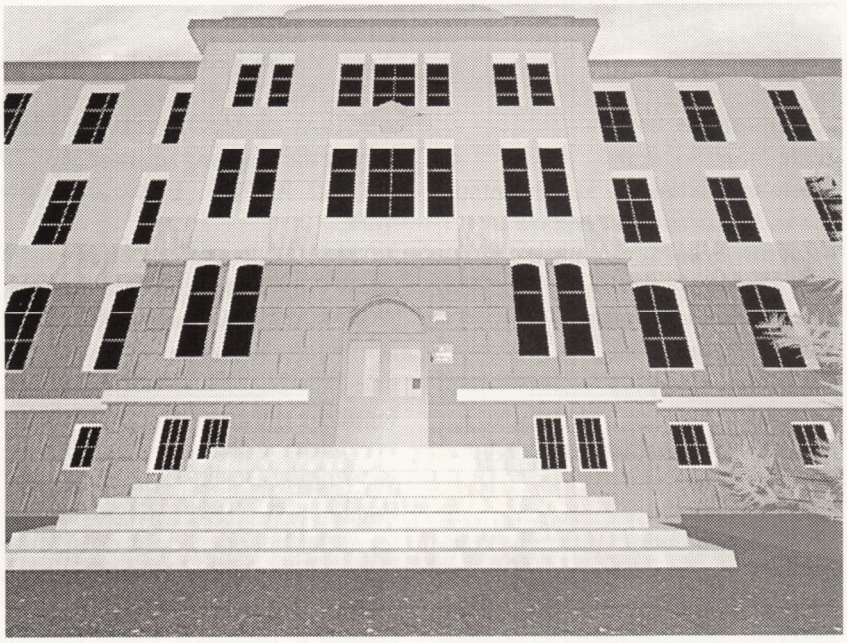

Sučelje programa sastoji se od nekoliko dijelova. Stvaranje dvodimenzionalnih objekata izvodi se u **2D-shaperu.** Taj dio programa omogućuje stvaranje dvodimenzionalnih primitiva (osnovni, jednostavni objekti koji su određeni parametarskim vrijednostima), te obradom primitiva vrlo složene dvodimenzionalne oblike. Objekte iz 2D-shapera prebacujemo u 3D-lofter, dio programa koji objektima "izvlači" treću dimenziju. On ima mogućnost izvođenja niza složenih efekata koji stvaraju najsloženije objekte i površine. Nakon obrade u 3D-lofteru objekte prebacujemo u treći, najvažniji dio programa: 3D-editor. To je dio obrade kojom se objektima određuje boja, površina i smještaj u prostoru (scena). Daljnja obrada uključuje stvaranje izvora svjetlosti (uz određivanje boje, dometa, oblika izvora...) i postavljanje kamera. Treba napomenuti da se u tijeku obrade vide samo mreže objekata, a ne i boje, površine i svjetlost. Uzrok je tome nedovoljna brzina računala. U sastavni dio programa ulazi i tzv. **material editor**, koji, kako mu i ime govori, služi za uređivanje materijala. Uz već gotovi izbor materijala moguće je stvaranje novih. 3D Studio, kao i većina 3D-programa, ima mogućnost namještanja različitih perspektiva gledanja, što uključuje i pogled iz postavljenih kamera i izvora svjetlosti. Keyframer je četvrti, posljedni dio programa. Njegova je glavna uloga stvaranje animacija (kretanje objekata u prostoru) slično izradi filmova. Naime, pokret nastaje određivanjem određenog broja sličica (frame) kroz koje objekti mijenjaju položaj u prostoru. Brzina izmjena sličica omogućuje filmsku kvalitetu pokreta, ali i više od toga. Završni je postupak obrade Render, tj. kompjutorska obrada koja prikazuje scenu (u slučaju animacije skupinu sličica) u konačnom obliku. To podrazumijeva boje, površine, svjetlost, sjene i drugo. Sliku je moguće sačuvati u različitim formatima (*.3ds, *.dxf, *.jpg, *.tif, *.tga i drugo) zbog kompatibilnosti s drugim programima.

3D Sudio 4.0 već je pomalo stara verzija koju nasljeđuju novi 3D-programi s puno većim i zanimljivijim mogućnostima i poboljšanim sučeljem. Ta je verzija napravljena samo za MS-DOS operativni sustav. Nova je inačica toga programa 3D Studio MAX koji radi pod Microsoftovim sustavom Windows 95, ali najbolje rezultate pokazuje u Windowsima NT 3.51. i 4.0.

Tibor Szirovicza
učenik V. gimnazije

Pročelje i interijer V. gimnazije u Zagrebu izveli su (96/97) učenici Hrvoje Šolman i Tihomir Jauk • AutoCAD 12, SoftDesk, Ver.7.0

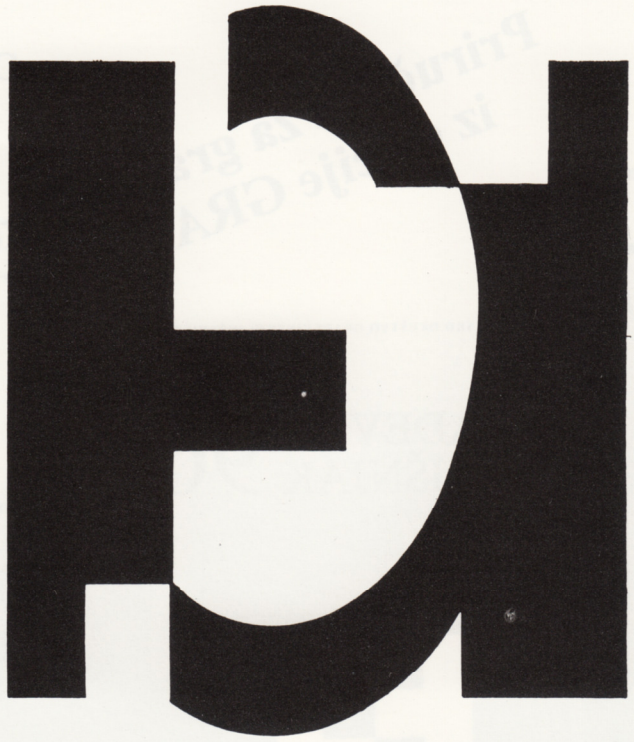

INSTITUT GRAĐEVINARSTVA HRVATSKE

Civil Engineering Institute of Croatia

10000 Zagreb, Janke Rakuša 1, pp 283

tel. 01/ 61 36 444, fax. 01/ 53 47 37. 01/ 53 38 89, telex 22275

POSLOVNI CENTAR 31000 OSIJEK, Drinska 18

fax/tel. 031/ 127-40

POSLOVNI CENTAR 51000 RIJEKA, Vukovarska 10a

tel. 051/ 330 744
fax. 051/ 211 310

POSLOVNI CENTAR 21000 SPLIT, Matice hrvatske 15

tel. 021/ 523 333
fax. 021/ 551 152

I G H d.o.o. 88000 MOSTAR, Dubrovačka bb

tel./fax. 99 387 88/ 314 529

HRVATSKO DRUŠTVO GRAĐEVINSKIH INŽENJERA

10000 ZAGREB, Berislavićeva 6, tel./fax: + 385 (01) 428 - 502, 422-937

Priručnici za graditeljske stručnjake iz edicije GRAĐEVNI GODIŠNJAK

Cijena po primjerku 280,00 kn

Do sada tiskane tri knjige iz edicije

GRAĐEVNI GODIŠNJAK mogu se naručiti

Narudžbe slati na fax 01/428-502 ili poštom na adresu HDGI-a Zagreb, Berislavićeva 6

✂.....✂

NARUDŽBENICA

Naručujemo **GRAĐEVNI GODIŠNJAK '95** primjeraka .....
GRAĐEVNI GODIŠNJAK '96 primjeraka .....
GRAĐEVNI GODIŠNJAK '97 primjeraka .....

Iznos od ..... kuna uplatili smo na žiro račun broj: 30102-678-4020 HDGI ,dana .....

Iznos od ..... kuna uplatit ćemo na temelju računa (predračuna)

Molimo da knjigu(e) pošaljete na adresu: .....

.....

Datum MP Potpis

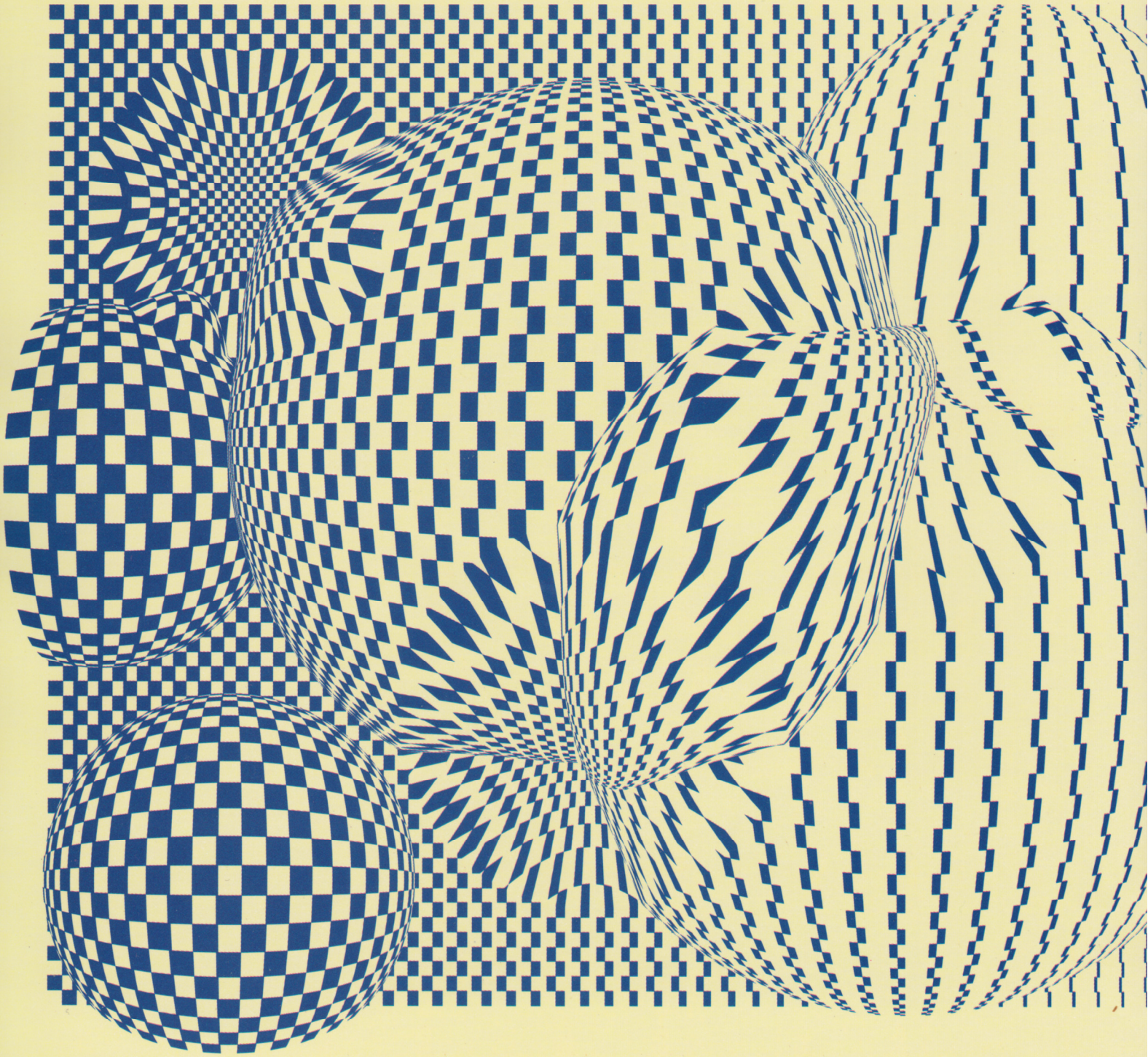

ISSN 1331-1611